

ABSTRACT

LIEBERMAN, DAVID VICTOR. Comparison of the Catalytic Activities of Ricin A-Chain, Maize rproRIP1, MaizeRIP1, and Two Maize rproRIP1 Deletion Mutants Interacting with an RNA 10-mer GAGA Tetraloop. (Under the direction of Charles C. Hardin.)

Ribosome-inactivating proteins (RIPs) catalytically depurinate a conserved adenine in the ribosomal α -sarcin domain, and it is believed that the local structure surrounding the target adenine is (at least transiently) an RNA GAGA tetraloop with the first A in the GAGA sequence being the target adenine. Studies of the catalytic activity of ricin A-chain interacting with ribosomes and with RNA GAGA tetraloops, as well as the catalytic activities of a set of related maize RIPs interacting with ribosomes have been reported in the literature. The purpose of this research project was to extend our understanding of maize RIP1 catalytic activity by measuring and comparing the catalytic activities of ricin A-chain and a set of related maize RIPs interacting with an RNA 10-mer GAGA tetraloop (denoted by A-10) over a range of pH values from pH 3.0 to 6.0.

Timecourse experiments of A-10/enzyme reactions were used to measure catalytic activity by quantitative HPLC detection of the adenine released during a succession of elapsed time intervals as the depurination reaction proceeded. The form of the timecourse data did not conform sufficiently to the integrated Michaelis-Menten equation to permit the use of nonlinear curve fitting to characterize the results in terms of the Michaelis-Menten parameters K_M and k_{cat} . Thus, the comparison of the activities of ricin A-chain and the

various maize RIP variants both among themselves and as a function of pH, although definitive, is semiquantitative. For one of the enzymes, maizeRIP1, initial velocity experiments at high substrate concentrations yielded an approximate V_{\max} directly, which was then used to treat V_{\max} as a constant rather than a variable in fitting the data to the integrated Michaelis-Menten equation, and corresponding values for K_M were obtained. However, these substrate concentrations were not sufficiently high to yield V_{\max} values for the other enzymes.

One unexpected result, with important ramifications concerning the conformation of the maize proRIP1, was evidence that maize rproRIP1, which is a zymogen (inactive precursor) with respect to ribosomes, may be catalytically active with respect to the small RNA tetraloop A-10.

**COMPARISON OF THE CATALYTIC ACTIVITIES OF RICIN A-
CHAIN, MAIZE RPRORIP1, MAIZERIP1, AND TWO MAIZE
RPRORIP1 DELETION MUTANTS INTERACTING WITH AN RNA
10-MER GAGA TETRALOOP**

by
DAVID VICTOR LIEBERMAN

A dissertation submitted to the Graduate Faculty of
North Carolina State University
in partial fulfillment of the
requirements for the Degree of
Doctor of Philosophy

DEPARTMENT OF STRUCTURAL AND MOLECULAR BIOCHEMISTRY

Raleigh, NC

2003

APPROVED BY:

DR. CHARLES C. HARDIN
Chair of Advisory Committee

DR. REBECCA S. BOSTON

DR. JAMES A. KNOPP

DR. PAUL L. WOLLENZIEN

BIOGRAPHY

David Lieberman was born and grew up in Brooklyn, New York. He graduated from Brooklyn Technical High School in 1944 and entered the City College of New York. After one year at City College he enlisted in the United States Navy, in which he served for one and one half years. After discharge from the Navy, he returned to City College and graduated in 1948 with a B.S. in Physics. This was followed by an M.S. in Physics from New York University in 1950 and a Ph.D. in Physics from the University of California at Los Angeles in 1958.

After graduation from UCLA, David became interested in the nascent field of computer science. He joined the Thomas J. Watson Research Center (IBM) where he worked in the areas of computational linguistics and interactive graphics. He then moved to academia, teaching Computer Science first at Queens College in New York, and then at Appalachian State University in North Carolina.

Upon retiring from Appalachian State University, David enrolled in the Ph.D. program in the Biochemistry Department at North Carolina State University and graduated with a Ph.D. in Biochemistry in 2003.

ACKNOWLEDGMENTS

I would like to thank Professor Charles C. Hardin for accepting me into his laboratory, for suggesting this area of research, and for providing mentorship, encouragement, and support during the course of the work.

My Graduate Advisory Committee, consisting of Professors Rebecca S. Boston, James A. Knopp, and Paul L. Wollenzein, in addition to its Chair, Professor Charles C. Hardin, provided helpful evaluation, advice, and guidance during our periodic Committee meetings.

Professor Rebecca S. Boston generously provided *E. coli* clones developed in her laboratory which enabled me to generate the enzymes used in my research.

Professor Paul F. Agris kindly granted me access to the equipment and reagents in his laboratory.

Professor Dennis T. Brown, Department Head, graciously provided necessary funds for purchase of equipment and materials during the terminal phase of my research.

The staff of the Departmental Office, especially Curtis P. Moore, Shoshana Serxner, and Aixa Morales-Diaz, by their good humor and spirits and their assistance in helping me satisfy the rules and regulations of the Department and the College, contributed significantly to my quality of life while at the University.

Finally, I would like to express very special thanks to Richard Guenther, who had no formal connection to my research, yet provided day-to-day help, interest and discussion in areas ranging from experimental design and technique to focusing on the science underlying my experimental investigations.

TABLE OF CONTENTS

LIST OF TABLES	vi
LIST OF FIGURES	vii
LIST OF ABBREVIATIONS	x
CHAPTER 1. INTRODUCTION TO RIBOSOME-INACTIVATING PROTEINS (RIPs)	1
The Enzymatic Reaction	1
History and Classification	1
Distribution	3
RIP Structure and Homology	4
Site of Action and Recognition Elements in Native Ribosomes	5
Substrate Specificity and Ribosomal Proteins	7
Cofactors	9
Product (Adenine) Inhibition	10
Other Substrates Subject to RIP N-Glycosylase Activity	12
Biological Function(s) of RIPs	15
Pharmaceutical Potentials of RIPs	16
Crystallographic Structures of RIPs Complexed with Substrate Analogs	16
Suggested Mechanisms of RIP N-Glycosidase Activity	17
CHAPTER 2. THE MAIZE PRORIP, MAIZERIP, AND THEIR DELETION MUTANTS ..	25
ProRIP	25
MaizeRIP	26
Deletion Mutants	26
CHAPTER 3. SYNTHETIC RNA SUBSTRATES REPORTED IN THE LITERATURE	29
α -Sarcin Domain Mimics	29
GAGA Tetraloops	30
CHAPTER 4. MEASURED VALUES IN THE LITERATURE OF THE PARAMETERS K_M AND K_{CAT} FOR RIBOSOME/RICIN A-CHAIN AND RNA OLIGORIBONUCLEOTIDE/RICIN A-CHAIN REACTIONS	33
CHAPTER 5. MATERIALS AND METHODS	35
Materials	35
Methods	43

CHAPTER 6. CONTROL EXPERIMENTS	49
CHAPTER 7. EXPERIMENTAL RESULTS	56
Michaelis-Menten Initial Velocity Experiments	56
Timecourse Experiments	60
CHAPTER 8. ANALYSIS, DISCUSSION, AND CONCLUSIONS	84
Comparison of enzyme activities [$\log(v_i/E_0)$ versus pH] at 30 °C using initial velocities from the timecourse experiments.	85
Estimates of pseudo k_{cat} and k_{cat}/K_M from initial velocity experiments with $S_0 \gg 10 \mu\text{M}$.	87
Requirements for obtaining credible Michaelis-Menten parameters from experimental data.	94
Conclusions	101
REFERENCES	110
APPENDICES	120
A1. Derivation of the Initial Velocity Equation When the Briggs and Haldane Assumption that the Substrate Concentration is Very Much Greater Than the Enzyme Concentration is Not Satisfied	121
A2. Derivation of the Integrated Form of the Michaelis-Menten Equation	126
A3. Calculation of the Difference Between the True and the Measured Initial Velocity as a Function of the Extent of Reaction	127

LIST OF TABLES

CHAPTER 1

- 1-1. Corresponding active site residue position numbers for ricin A-chain, trichosanthin, and gelonin. 19

CHAPTER 4

- 4-1. Some numerical values for ricin A-chain K_M and k_{cat} from the literature. 34

CHAPTER 7

- 7-1. Distribution of all timecourse and high substrate concentration experiments. 70

CHAPTER 8

- 8-1. Enzyme activities at 30 °C using initial velocities from timecourse experiments. 104
- 8-2. Estimates of pseudo k_{cat}/K_M for A-10/ricin A-chain at four pH values. 106
- 8-3. Estimates of pseudo k_{cat} for A-10/maizeRIP1 at four pH values. 106
- 8-4. Estimates of pseudo K_M for the A-10/maizeRIP1 reaction using nonlinear curve fitting with a constant V_{max} constraint. 106
- 8-5. Estimated pseudo K_M , k_{cat} , and k_{cat}/K_M values and bounds for A-10/ricin A-chain and A-10/maizeRIP1, including comparative values from the literature for ricin A-chain. 107

LIST OF FIGURES

CHAPTER 1

- 1-1. Ribbon drawing of the ricin A-chain backbone (from Katzin *et al.*, 1991, Fig. 2). 20
- 1-2. Multiple sequence alignment (using Clustal W) of six sequences - five ribosome-inactivating proteins with known structures determined by crystallography, and the maize proRIP mutant MOD1X. 21
- 1-3. Multiple sequence alignment (using Clustal W). Similar to Fig. 1-2, but without the MOD1X sequence. 22
- 1-4. Tertiary homology shown by backbone superpositions. 23
- 1-5. The RIP N-glycosidation reaction, and the active site structure of TADE, a complex of trichosanthin and a substrate analog. 24

CHAPTER 2

- 2-1. Schematic description of the sequence relations among the enzymes proRIP1, rproRIP1, maizeRIP1, and the deletion mutants MOD1 and MOD1X. 28

CHAPTER 5

- 5-1. SDS-PAGE gel of rproRIP1, maizeRIP1, MOD1, MOD1X, and ricin A-chain. 48

CHAPTER 6

- 6-1. A control experiment to investigate the stability of the RNA 10-mer oligoribonucleotide GAGA tetraloop (A-10) by UV-melting measurements of T_m versus pH. 52
- 6-2. A control experiment to investigate the effects of pH on the far UV (250-190 nm) CD spectra of ricin A-chain, maizeRIP1, MOD1, and MOD1X. 53
- 6-3. A control experiment to attempt to detect spontaneous release of adenine from A-10. 54
- 6-4. A control experiment to investigate the effect of the presence of ricin A-chain on the HPLC response to free adenine. 55

CHAPTER 7

7-1. Michaelis-Menten initial velocity experiments with A-10/ricin A-chain.	71
7-2. Six repetitions of an A-10/maizeRIP1 timecourse experiment showing the enzymatic release of adenine from the RNA hairpin A-10 catalyzed by maizeRIP1	72
7.3. Example of linear scaling of A-10/maizeRIP1 reactivity with respect to the enzyme concentration E_0	73
7-4. Effect of pH on A-10/maizeRIP1 activity.	74
7-5. Four repetitions of an A-10/MOD1 timecourse experiment showing the enzymatic release of adenine from the RNA hairpin A-10 catalyzed by MOD1.	75
7-6. Effect of pH on A-10/MOD1 activity.	76
7-7. Timecourses, statistical means and SEMs for the interaction of A-10 and ricin A-chain at pH 4.0 and 4.5.	77
7-8. A-10/MOD1X timecourses for pH 4.7 and 4.9.	78
7-9. Effect of pH on A-10/maize rproRIP1 activity.	79
7-10. Effect of pH on A-10/MOD1 activity at 20 °C.	80
7.11. Linear fitting to high A-10 concentration A-10/ricin A-chain initial velocity experiments.	81
7-12. The results of high A-10 concentration A-10/maizeRIP1 initial velocity experiments at pH 4.0, 4.3, 4.9, and 5.4.	82
7-13. The results of high A-10 concentration A-10/MOD1 initial velocity experiments at pH 4.0, 4.3, 4.8, and 5.2	83

CHAPTER 8

8-1. A line plot comparison of ricin A-chain, maizeRIP1, MOD1, MOD1X, and rproRIP1 reactivities with A-10 as a function of pH, based on initial velocities.	108
8-2. Results obtained from nonlinear curve fitting of the integrated	

Michaelis-Menten equation to A-10/maizeRIP1 reaction timecourses with V_{\max} held constant at values given by the high substrate concentration experiments and with K_M and S_0 as fitting variables.	109
8-3. A line plot comparison of MOD1 reactivity with A-10 at 20 °C and 30 °C as a function of pH, based on initial velocities.	110

APPENDICES

A1-1. The percent error in the initial velocity, as a function of the substrate/enzyme ratio E_0/S_0 , incurred by using the Michaelis-Menten equation rather than the equation for v_i derived using the conservation of substrate condition $S_0 = S + C_{ES}$	129
A3-1. The percent error in measurements of the Michaelis-Menten initial velocity as a function of the extent of reaction.	130

LIST OF ABBREVIATIONS

The typographic convention that substances are represented by unbracketed symbols (*e.g.*, S for substrate), and that the same symbol in square brackets represents the concentration of the substance (*e.g.*, [S] represents the concentration of the substance S) is generally followed herein. However, in a few specific contexts, particularly in mathematical expressions and derivations where there is very little chance of confusion, for convenience and readability the brackets are omitted around symbols representing concentrations.

<u>Symbol</u>	<u>Meaning</u>
α	K_M/S_0
β	E_0/S_0
ξ_f	fractional extent of reaction: $(S_0 - S)/S_0$
$\xi_{\%}$	percent extent of reaction: $100(S_0 - S)/S_0 = 100(1 - S/S_0)$
A-10	RNA 10-mer hairpin GAGA tetraloop
A-32	RNA 32-mer hairpin mimic of the ribosome alpha-sarcin loop
amp	ampicillin
C_{ES}	the substrate-enzyme complex (usually denoted by E•S)
CAEB	citric acid, EDTA buffer (pKa's: 3.13, 4.76, and 6.40)
carb	carbenicillin
cap	chloramphenicol
E	free enzyme concentration
E_0	total enzyme concentration
h	hour
k_2	rate constant used interchangeably with k_{cat}
k_{cat}	catalytic constant in the Michaelis-Menten model
K_M	Michaelis constant in the Michaelis-Menten equation
LB	Luria broth
m	minute
maize proRIP1	inactive precursor form of maizeRIP1
maize rproRIP1	recombinant maize proRIP1
maizeRIP1	active RIP derived from maize rproRIP1
MAP	mirabilis antiviral protein
MOD1	an active maize rproRIP1 mutant similar to maizeRIP1
MOD1X	an active maize rproRIP1 mutant closer than MOD1 to maizeRIP1
P	reaction product

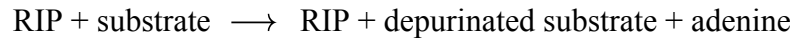
List of abbreviations, con'd.

<u>Symbol</u>	<u>Meaning</u>
PAP	pokeweed antiviral protein
RA	ricin A-chain
RB	Rich broth
RIP	ribosome-inactivating protein
RTA	ricin toxin A-chain (equivalent to RA)
S	substrate concentration
SEM	statistical error of the mean
S_0	initial substrate concentration
t-dep form	integrated Michaelis-Menten equation with time as the dependent variable
TB	Terrific Broth
v	reaction velocity ($-dS/dt$ or dP/dt) when $S_0 \gg E_0$
v_i	initial reaction velocity when $S_0 \gg E_0$
v_{im}	measured initial reaction velocity
v_{isc}	initial reaction velocity when $S_0 \approx E_0$ (taking substrate conservation into account)
v_{it}	true initial reaction velocity
V	equivalent to V_{max} . Used when quoting or paraphrasing literature which uses the symbol V rather than V_{max} .
V_{max}	Michaelis-Menten parameter ($V_{max} = E_0 k_{cat}$).

CHAPTER 1. INTRODUCTION TO RIBOSOME-INACTIVATING PROTEINS (RIPs)

The Enzymatic Reaction

The stoichiometric form of the enzymatic reaction is:



A schematic of the chemical reaction is shown in Fig. 1-5A, on p. 24. The proposed mechanism is described on p 17. Note that Figures and Tables are grouped at the end of the Chapter in which they are first referenced.

History and Classification

Ribosome-inactivating proteins (RIPs) are a large group of cytotoxic plant proteins that inactivate the protein synthesis elongation machinery by cleaving the N-glycosidic bond of a specific conserved adenine base in the α -sarcin loop region of most eukaryotic and some prokaryotic ribosomes. However, there is great variation in the overall toxicity among the RIPs, and also, in the relative toxicity of different RIPs to different ribosomes. Most of the known RIPs have been isolated only during the last three decades, but a few members of this group have been a part of the human pharmacopia for hundreds of years. For example, the RIP trichosanthin from the plant *Trichosanthes kirilowii* was used in ancient China to induce abortion (Gu *et al.*, 2000), and the famous (or infamous) RIP ricin from castor beans (the seeds of *Ricinus communis*) was purified and named in 1820 (referenced in Barbieri *et al.*, 1993).

That the ribosome is the target of ricin's toxicity was first deduced experimentally by Olsnes and Pihl (1972) who concluded that, “. . . ricin interferes with the completion of already initiated peptide chains.” The expression “ribosome inactivation” was introduced

by Olsnes *et al.* (1975). The specific manner in which RIPs inactivate ribosomes -- by depurination of a specific conserved adenine base in the α -sarcin loop region of the ribosome -- was first demonstrated by Endo in 1987 (Endo *et al.*, 1987).

In 1970 Lin *et al.* (1970) observed that the RIPs ricin and abrin were more toxic to tumor cells than to healthy cells, which resulted in more widespread interest in the structure, function, and catalytic mechanism of these and other known RIPs, as well as in a wide search among plants for other RIPs.

RIPs are currently classified into three types: *Type 1* RIPs, the most common type by far, are typically highly basic ($\text{pI} \geq 9$) 30-32 kDa single-chain catalytically active proteins. Primary sequence homology among members of this class of RIPs ranges from extensive to relatively sparse, except for a very highly conserved set of ~13 residues, five of which come together in the folded tertiary structure to form a conserved catalytic active site. *Type 2* RIPs are heterodimers consisting of one subunit similar to *Type 1* RIPs, called the A-chain, bound by a disulfide bond to a second subunit consisting of a galactose-specific lectin, also ~30-32 kDa, called the B-chain. The B-chain is not catalytically active, but binds to cell-surface galactosides, thereby facilitating the entry of the catalytically active A-chain into cells by endocytosis. As a result, *Type 2* RIPs are generally much more toxic in vivo to mammals than *Type 1* RIPs (which are usually unable to enter healthy cells). *Type 3* RIPs are rare. They are similar to *Type 1* RIPs in that they consist of a single peptide chain, but differ in that the initially translated form of the protein is a catalytically inactive proenzyme requiring post-translational proteolytic processing of an internal segment (in addition to N and C terminal segments and signal peptide removal required by

many *Type 1* and *2* RIPs) to become enzymatically active.

The active site in ricin was initially proposed by Ready's group (Montfort *et al.*, 1987) based on X-ray crystallographic observation of a cleft in the ricin A-chain tertiary structure, and later confirmed by Ready *et al.* (1991) and others using site-directed mutagenesis of ricin A-chain and by modeling of RIPs bound to substrate analogs.

The maize proRIP1, which along with its derivatives is the subject of this thesis, is a *Type 3* RIP. It was originally purified by Di Fonzo *et al.* (1986), when it was known as b-32, but its function was unknown. The ribosome-inactivating properties of naturally activated maize proRIP1 (extracted from corn kernels during maturation and germination) were discovered independently by Bass *et al.* (1992) and by Walsh *et al.* (1991).

Distribution

RIPs are not just a specialized product of a few plants, but are very widely distributed. They have been isolated and characterized from more than 60 plant species covering 13 families (Krawetz and Boston, 2000; Hartley *et al.*, 1996). RIPs occur not only in a wide variety of plants, but also in a wide variety of plant organs and tissues. They have been extracted from seeds, leaves, roots, bark, and latex (Barbieri *et al.*, 1993; Hartley *et al.*, 1996; Stirpe *et al.*, 1992). Many plants have RIPs in more than one tissue and in a few cases there are multiple RIPs produced in the same tissue (Barbieri *et al.*, 1993). The amounts of RIP produced vary from barely detectable to surprisingly large. For example, the group of saporin RIPs in the seeds of *Saponaria officinalis* comprise 10% of the total seed protein (referenced in Stirpe *et al.*, 1992), and RIPs comprise up to 20% of the soluble proteins in the storage roots of the Andean root crop *Mirabilis expansa* (referenced in

Nielsen and Boston, 2001). At present, there are close to 200 *Type 1* RIPs, 8 *Type 2* RIPs, and 3 *Type 3* RIPs known. RIPs may be even more widespread because the search for RIPs has (i) focused on finding sources of large quantities of RIPs, (ii) concentrated on finding new RIPs rather than studying the distribution of known RIPs, and (iii) used only a very limited set of testing ribosomes (mostly from rabbit reticulocytes) which may be insensitive to some RIPs (Stirpe *et al.*, 1992; Barbieri *et al.*, 1993; Hartley *et al.*, 1996). In fact, Hartley speculates that “. . . all plants may contain RIP genes, and our inability to detect RIP activity may be caused by the resistance of the ribosomes used for screening, and the possibility that their expression had not been induced in the tissue being investigated.”

RIP Structure and Homology

Structure of ricin A-chain: After many years of effort, Robertus and co-workers obtained an X-ray crystallographic structure of ricin (the heterodimer) at 2.8 Å resolution (Montfort *et al.*, 1987). This was the first molecular model of a RIP based on X-ray diffraction. The A-chain subunit was refined further to 2.5 Å by Katzin *et al.* (1991). A ribbon drawing of the ricin A-chain backbone from that paper (Fig. 2 therein) is shown here as Fig. 1-1. Three domains are distinguished: *domain 1*, residues 1-117, consists of a six-stranded β -sheet and two helices; *domain 2*, residues 118-210, contains five helices; and *domain 3*, residues 211-267, has one helix but mostly random coil. A deep cleft formed by the intersection of the three domains and containing the conserved residues Tyr180, Tyr123, Glu177, Arg180, and Trp211 appears to be a plausible active site.

Primary (sequence) homology: The overall sequence homology among RIPs is quite weak, although there are some pairs and groups with extensive similarity. A multiple

sequence alignment using Clustal W (Thompson *et al.*, 1994) of six sequences -- five ribosome-inactivating proteins with known structures determined by X-ray crystallography, and MOD1X (a deletion mutant of maize rproRIP1, described below in Chapter 2) -- is shown in Fig. 1-2. The specific RIPs are identified in the Figure. There are 16 conserved positions with identical residues for all six of the sequences.

A multiple sequence alignment similar to Fig. 1-2, but without the MOD1X sequence is shown in Fig. 1-3. Comparison of Figs. 1-2 and 1-3 illustrates the extent to which MOD1X does not share sequence similarity with the other five ribosome-inactivating proteins. The omission of MOD1X increases the number of identical residue positions from 16 to 35, and also permits the appearance of one location at which a subsequence of four contiguous residues is conserved among the other five ribosome-inactivating proteins

Tertiary (structural) homology: In contrast to the weak overall primary sequence homology among RIPs, the tertiary structures are highly conserved, as seen in the α -carbon backbone superpositions of models of ricin A-chain and several other RIPs, shown in Fig. 1-4. This Figure shows superpositions of (A) ricin A-chain and abrin-A, (B) of ricin A-chain and trichosanthin (TCS), (C) of ricin A-chain and pokeweed antiviral protein (PAP), and (D) of ricin A-chain, gelonin, and α -momorcharin.

Site of action and recognition elements in native ribosomes

The site of action of RIPs was first discovered by Endo *et al.* (1987). They established that ricin A-chain (as well as abrin and modeccin) inactivates rat liver ribosomes by modifying either G₄₃₂₃ and/or A₄₃₂₄ in 28S rRNA and suggested that the actual modification

was the removal of the base of the latter. They observed similar activity of ricin A-chain when deproteinized 28S rRNA was used as a substrate, indicating that the toxin acts directly on the RNA. Subsequently, Endo and Tsurugi (1988a) established definitively that the mechanism of inactivation of intact rat liver ribosomes was cleavage of the N-glycosidic bond at A₄₃₂₄ in 28S rRNA, and that the same N-glycosidic bond was cleaved by ricin A-chain in deproteinized 28S rRNA but at a greatly reduced rate. They also observed that ricin A-chain has no effect on 23S rRNA in *E. coli* ribosomes, but that in deproteinized 23S rRNA, ricin A-chain cleaved the N-glycosidic bond at A₂₆₀₀. This nucleotide is in the *E. coli* ribosomal α -sarcin domain at a position which corresponds to the A₄₃₂₄ ricin target position in eukaryotic 28S rRNA. They also found that in addition to the A₂₆₀₀ site in deproteinized *E. coli* rRNA, ricin A-chain cleaved the N-glycosidic bond of A₁₀₁₄ in 16S rRNA. Comparison of the nucleotide sequences in the neighborhoods of the site of base cleavage observed in eukaryotic 28S and prokaryotic 23S and 16S rRNA led to the proposal that, "...ricin A-chain acts on the first adenosine residue in the sequence of GAGA in a loop with a stem of 6 or more base pairs." Note that the apparent loop sizes of the 28S, 23S, and 16S rRNA are 17, 15, and 4, respectively.

Endo *et al.* (1988b) answered the question of whether single chain (*Type 1*) ribosome-inactivating proteins inactivated ribosomes by a similar mechanism to that of ricin A-chain, which is the catalytically active part of a *Type 2* ribosome-inactivating protein. They demonstrated that the site of action of six *Type 1* ribosome-inactivating proteins: gelonin from the seeds of *Gelonium multiflorum*, saporin from the seeds of *Saponaria officinalis* (soapwort), momordin from the seeds of *Momordica charantia* (bitter pear melon), and the

pokeweed antiviral proteins PAP and PAP-II from the leaves and PAP-S from the seeds of *Phytolacca americana*, was the same as that of ricin A-chain in a cell-free system (rabbit reticulocyte).

Endo *et al.* (1988b) first proposed that the recognition element is a GAGA tetraloop (an RNA hairpin with a loop consisting of the four-base sequence GAGA). They were motivated by the discovery that ricin A-chain cleaves an N-glycosidic bond at position A₁₀₁₄ in deproteinized 16S *E. coli* rRNA, which is not within the ribosomal α -sarcin domain, but rather, in a local environment consisting of a GAGA tetraloop on a 7-base stem. It was subsequently proposed by Heus and Pardi (1991), based on NMR studies, that RNA hairpins containing GNRA loops have unusual stability, arising from i) an unusual G-A base pair between the first and last residue in the loop, ii) a hydrogen bond between a G base and a phosphate, iii) extensive base stacking, and iv) a hydrogen bond between a sugar 2'-hydroxyl and a base.

Substrate specificity and ribosomal proteins

The site of action of RIPs in intact ribosomes is a very highly conserved GAGA sequence within the ribosomal α -sarcin domain, and the result of the enzymatic action is a universally conserved N-glycosidase depurination of the first A in the conserved GAGA sequence. The tertiary conformations of the RIP active site and the active site residues are also highly conserved even though the overall primary sequences of RIPs are far from conserved. And yet, the substrate specificities among RIPs are widely divergent. Ricin A-chain, which is the most toxic of the RIPs with respect to mammalian ribosomes, is

completely inactive with respect to intact *E. coli* ribosomes (Barbieri *et al.*, 1993). Pokeweed antiviral protein (PAP) is less toxic to eukaryotic ribosomes than ricin, but in contrast to ricin, PAP is also toxic to prokaryotic ribosomes (specifically, *E. coli*). Habuka *et al.* (1990) compared the inhibitory effects of mirabilis antiviral protein (MAP) from *Mirabilis jalapa* L. and ricin A-chain on protein synthesis in *E. coli* and *in vitro* protein synthesis in rabbit reticulocyte lysate and wheat germ extract. They found that ricin A-chain was much more active with respect to rabbit reticulocyte ribosomes than MAP. They also found that MAP was much more active with respect to wheat germ ribosomes than ricin A-chain, and that MAP was active with respect to *E. coli* ribosomes whereas ricin A-chain showed no measurable inhibitory effect. These and other examples of divergent substrate specificity suggest that not only substrate and enzyme structure but also the presence of ribosomal proteins must have a substantial effect on RIP activity.

Krawetz and Boston (2000) developed a quantitative kinetics-based assay to measure RIP activity *in vitro*. They measured the activity of maizeRIP1, a papain-activated form of maize rproRIP1, with respect to ribosomes from diverse taxa: rabbit reticulocyte lysate, *Aspergillus flavus* (a corn pathogen), *N. tabacum*, and *Z. mays*. The measured rate constants varied over a very wide range from 303.1 m⁻¹ for the rabbit system to 0.071 m⁻¹ for *Z. mays*.

Chaddock *et al.* (1996) investigated whether the differing ribosome specificities of ricin A-chain and PAP derived from small structural differences. They noted that both RTA (ricin A-chain) and PAP depurinate eukaryotic ribosomes, but only PAP depurinates intact prokaryotic ribosomes (RTA weakly depurinates deproteinized *E. coli* ribosomes). The

authors used information from X-ray structures of RTA and PAP to delineate regions of possibly significantly different tertiary structure, and designed a series of PAP/RTA hybrids using both gross polypeptide recombination switches and specific peptide insertions to try to ascertain which regions of the RIPs were important for ribosome recognition and inactivation. Their results were not definitive. In summary, they hypothesized that since the active site residues and their positions in the active site of all RIPs studied are highly conserved, as are the target ribosomal RNA sequences, and removal of prokaryotic ribosomal proteins permits ribosome-inactivating activity by RTA, "... the deciding factor for depurination *in vivo* is the presence of ribosomal proteins and their relative ability to interact with RIPs."

Cofactors

There has been no exhaustive study of the effects of cofactors on RIP activity, but there are many specific observations of cofactors required for certain substrate/RIP reactions, as well as substrate/RIP reactions in which cofactors have enhancing or inhibiting effects.

Sperti *et al.* (1991) found that inactivation of *Artemia salina* and rabbit ribosomes by the RIP gelonin requires ATP and high molecular weight factors present in the rabbit reticulocyte lysate post-ribosomal supernatant. The measured kinetic constants for the gelonin-catalyzed release of adenine from *A. salina* ribosomes were $K_M = 4.35 \mu\text{M}$ and $k_{\text{cat}} = 0.1 \text{ m}^{-1}$ in the absence of cofactors, and $K_M = 1.15 \mu\text{M}$ and $k_{\text{cat}} = 108 \text{ m}^{-1}$ in their presence.

Carnicelli *et al.* (1992) preincubated *A. salina* ribosomes with eight RIPs in the absence and the presence of ATP and high molecular weight fractions of rabbit reticulocyte lysate

post-ribosomal supernatant, and then tested the ability of the ribosomes to carry out poly(U) directed translation. Measurements of IC_{50} values were made at 28 °C and pH 7.6. They found that the addition of ATP and gel-filtered rabbit reticulocyte post-ribosomal supernatant (gel-filtered 'S-140') had no substantial effect on the ribosome-inactivating activities of the RIPs byrodin-R, lychnin, momordin, momorcochin-S, and saporin 6, but for the RIPs tritin, PAP-S, and barley RIP, the IC_{50} values were lowered by factors of 220, 1,254, and 77,538, respectively.

Gluck and Wool (1996a) found that the simultaneous presence of divalent cations and chelating agents (magnesium and EDTA or calcium and EGTA) had a large enhancing effect on the depurination by ricin A-chain of the first adenine in a GAGA sequence in a 35-mer synthetic oligoribonucleotide mimic of the eukaryotic ribosomal α -sarcin domain, but had no effect on ricin A-chain depurination activity with respect to intact ribosomes. However, the activity of PAP (pokeweed antiviral protein) on the same synthetic oligoribonucleotide was not affected by the presence of calcium and EGTA.

Product (adenine) inhibition

Watanabe *et al.* (1992) noted that, "Since adenine is a product of the N-glycosidase action of RTA, it is expected that adenine interacts with the active site". They found evidence, using fluorescence spectroscopy, that binding of adenine to RTA resulted in an enhancement of fluorescence from Trp-211, one of the conserved residues in the RTA active site. They also measured the inhibitory effect of the presence of adenine on the ribosome-inactivating activity of RTA on polyphenylalanine synthesis by rat liver 80S

ribosomes after incubation with RTA. They found that the presence of 9 mM adenine increased by a factor of four the concentration of RTA required to give 50% inhibition of polyphenylalanine synthesis, but that similar concentrations of cytosine or uracil had no effect. However, it should be noted that the ribosome concentration in the experiments was 0.17 μ M (3.4 pmol in 20 μ l), which means that the maximum possible concentration of adenine released by the N-glycosidase action of RTA in these experiments would be 0.17 μ M. The use of 9 mM adenine to test for inhibitory effects on RTA represents a molar concentration of adenine which is 52,000 times the maximum concentration of adenine that could be present during the reaction without the addition of 9 mM adenine. Thus, although these results are relevant to understanding the mechanism of the N-glycosidase action of ricin A-chain and other RIPs, they indicate that effects of product inhibition are negligible under the typical conditions used in Michaelis-Menten initial velocity experiments and in the timecourse measurements of substrate/enzyme reactions described in this thesis.

Pallanca *et al.* (1998) found that preincubation of ricin A-chain and momordin with adenine protected *A. salina* ribosomes to various degrees from inactivation by these RIPs. However, as in the case of the experiments by Watanabe *et al.* (1992), the concentrations of the added inhibitory adenine were one to two orders of magnitude greater than the maximum concentration of released adenine potentially available as a normal product of the N-glycosidase action of the RIPs.

Other Substrates Subject to RIP N-Glycosylase Activity

DNA, genomic and poly(A) RNA, and tetraloop mutants: One of the distinctive characteristics of RIPs as a class is that the recognition element for its N-glycosidase activity is an RNA GAGA tetraloop with a short (4-7 base pair) stem. It is believed that the universally conserved GAGA sequence targets in the α -sarcin domains of eukaryotic 28S rRNA and prokaryotic 23S rRNA are probably in the form of local GAGA tetraloops with short stems. As discussed above, there is a wide divergence in the specificity of different RIPs toward different eukaryotic ribosomes, and most RIPs have only little or no activity with respect to prokaryotic ribosomes. These differences are widely thought to be due to differences in ribosomal proteins rather than active site structural differences. However, in a paper questioning the universality of the generally accepted GAGA sequence as the RIP target, Marchant and Hartley (1995) compared the action of PAP and ricin A-chain on mutants in the α -sarcin loop of *E. coli* 23S rRNA and concluded that the recognition elements for PAP and RTA differ, and that the difference might be involved in the fact that PAP but not ricin A-chain is active with respect to *E. coli* ribosomes.

There is also some evidence of RIPs showing N-glycosidase activity with respect to other substrates, such as dsDNA, ssDNA, genomic RNA, RNA poly(A), and tetraloop mutants. Orita *et al.* (1996) found that the N-glycosidase activity of ricin A-chain was 26 times higher with respect to a GdAGA tetraloop than with respect to a GAGA tetraloop. Barbieri *et al.* (1996) found that saporin-L1 (a RIP from the leaves of *Saponaria officinalis*) catalyzed the release of adenine from several substrates other than ribosomes, including herring sperm DNA (hsDNA), genomic RNA from bacteriophage MS 2, and poly(A) RNA,

and proposed that saporin-L1 be characterized as a polynucleotide:adenosine glycosidase. Unlike the action of RIPs with respect to ribosome substrates, in some of these experiments the ratios of moles of released adenine to moles of substrate were much greater than one. Up to 80% of the adenine residues were removed in experiments with saporin-L1 acting on poly(A) RNA. This paper was followed by an extensive set of screening experiments (Barbieri *et al.*, 1997) in which 52 *Type 1* and *Type 2* RIPs were observed to be active with respect to bacteriophage MS 2 genomic RNA, and 32 *Type 1* and *Type 2* RIPs were observed to be active with respect to hsDNA, rRNA from *E. coli*, and poly(A).

Nicolas *et al.* (1998, 2000) found that the RIP gelonin showed DNA glycosidase activity with respect to single-stranded and duplex DNA as well as single-stranded and double-stranded oligonucleotides. When the oligonucleotides had multiple adenines, gelonin activity produced strand breakage in the case of single-stranded oligonucleotides and duplex melting in the case of double-stranded oligonucleotides, suggesting that gelonin has an apurinic or apyrimidinic (AP) lyase activity (which leaves a sugar with no attached base) as well as its DNA glycosidase activity. Gelonin's DNA glycosidase activity was damaging to the DNA in that it removed normal, non-mispaired bases, unlike other DNA glycosidases which have a protective effect by removing only damaged or mispaired bases.

RIP antiviral and anti-tumor activity: Antiviral activity is common among RIPs (Barbieri *et al.*, 1993). In fact, the antiviral activities of some RIPs were known before their RIP activity was demonstrated. For example, PAP (pokeweed antiviral protein) was named for antiviral activity observed in leaf extracts of *Phytolacca americana* (pokeweed), and only later, after purification of the antiviral protein, was it recognized that the same protein

was the source of the extract's RIP activity.

The full mechanism (or mechanisms) of RIP antiviral activity is not clear at present. One model of antiviral RIP activity offers several reasons which suggest that the RIP may not act directly on the virus, but rather, on the host. Firstly, viral RNAs do not have the conserved GAGA tetraloop structure recognized by RIPs, secondly, there are many observations in which a mixture of a RIP and virus was not infective to a plant, but when the RIP was removed, the virus regained its ability to infect the plant, and thirdly, RIPs which do not have ribosome-inactivating activity with respect to a particular host do not provide antiviral protection to that host. This suggests a model for RIP antiviral activity in which the virus, in entering a cell, disrupts the cell membrane which then permits the RIP to penetrate the membrane and enter the cytosol of the cell. The RIP then kills the cell by inactivating its ribosomes, thereby preventing viral replication. This model is compatible with some observations of RIP antiviral activity, but there are also experiments in which it appears that the RIP acts directly on the virus. Tumer *et al.* (1997) constructed a C-terminal deletion mutant of pokeweed antiviral protein which was found to inhibit viral infection but did not depurinate host ribosomes. Another example is the work on MAP30 from *Momordica charantia* (bitter melon) by Wang *et al.* (1999, 2000). They suggest that the anti-tumor and anti-HIV activities of MAP30 derive directly from its DNA glycosylase/apurinic or apyrimidinic (AP) lyase properties rather than its RIP activity.

Biological function(s) of RIPs

Many biological functions of RIPs have been proposed to help explain their presence in plants (reviewed in Barbieri *et al.*, 1993; Hartley *et al.*, 1996; Mehta and Boston, 1998; Nielsen and Boston, 2001). Most of these proposed biological functions are based on plausibility considerations given the known *in vitro* and *in vivo* catalytic activities of RIPs. However, it has proven difficult to design experiments to definitively test hypotheses concerning RIP biological functions, and to account for the widespread evolutionarily conserved occurrence of RIPs as well as the energy required to produce the occasionally large proportion of the RIP protein in some plant tissues. For example, it would be very informative if experiments could be carried out to observe the consequences of suppression of RIP expression in a plant.

One group of plausible RIP functions consists of protective or defensive actions with respect to insects, fungi, viruses and possibly bacteria. There are many *in vitro* as well as feeding studies which lend credibility to these hypotheses. One current gap in the argument (except for antiviral activities) is a mechanism for *Type I* RIPs, which are the most common type of RIP, to gain access to the interior of target cells. Another possible RIP function could be participation in cell apoptosis (reviewed in Mehta and Boston, 1998). It is possible that the diversity in RIP quantities, specificities and levels of activity might be associated with corresponding diversity of biological functions.

Pharmaceutical potentials of RIPs

Some experiments have shown direct selective action of certain RIPs with respect to tumor cells and HIV. Lin *et al.* (1970, 1971) found that abrin and ricin (Type 2 RIPs) had a greater inhibitory effect on protein synthesis in Ehrlich ascites tumor and Yoshida ascites hepatoma cells than on rat liver cells. More recently, Wang *et al.* (1999, 2000) found that the *Type 1* RIP MAP30 exhibited anti-HIV and anti-tumor activity (reviewed in Putnam and Tainer, 2000). However, most work on the therapeutic use of RIPs is based on conjugates in order to combine the highly toxic properties of RIPs with greater target selectivity than is achievable with RIPs acting alone (reviewed in Stirpe *et al.*, 1992; Barbieri *et al.*, 1993; Hartley *et al.*, 1996). Immunotoxin conjugates are constructed by binding a RIP as the cytotoxic moiety and an antibody as the targeting moiety. Lectins, hormones, and growth factors have also been used as the targeting moiety. Conjugates are also obtained by constructing chimeric genes to express fusion proteins with the desired cytotoxic and targeting subunits.

Crystallographic structures of RIPs complexed with substrate analogs

Knowledge of the positions and orientation of the substrate target adenosine and the conserved active site residues when bound in the substrate/RIP complex can suggest and validate proposed catalytic mechanisms. Some insight into the active site geometry of a substrate/RIP complex can be gained by studying substrate analogs bound to the RIP active site, and a number of X-ray crystallographic studies of substrate/RIP analog complexes have been reported. Monzingo *et al.* (1992) obtained the structure of a complex of FMP

(formycin 5'-monophosphate)/PAP. Note that FMP does not have an N-glycosidic bond. Monzingo and Robertus (1993) carried out an X-ray analysis of a FMP/ricin A-chain complex. Huang *et al.* (1995) studied complexes of both trichosanthin and α -mormorcharin with ATP and formycin. Gu and Xia (2000) obtained crystal structures of complexes of trichosanthin with four substrate analogs, including ApG and GpA. A schematic of the active center structure common to all four of the analogs is shown in Fig. 1-5B (from Gu and Xia, 2000, Fig. 4). The active site geometries found in all of the above-referenced studies are consistent with the main features of the geometry shown in Fig. 1-5B.

Suggested mechanisms of RIP N-glycosidase activity

Although a set of universally conserved residues characterize the active sites of all RIPs, the actual residue numbers vary from RIP to RIP as may be seen in the alignments shown in Figs. 1-2 and 1-3. A useful convention in discussing mechanisms of RIP N-glycosidase activity is to refer to universally conserved active site residues by the corresponding residue number in ricin A-chain. For example, a list of corresponding residue numbers for ricin A-chain, trichosanthin, and gelonin is shown in Table 1-1.

Mechanisms of RIP N-glycosidase activity have been proposed by several researchers (Ready *et al.*, 1991; Monzingo and Robertus, 1992; Ago *et al.*, 1994; Hosur *et al.*, 1995; Huang *et al.*, 1995; Day *et al.*, 1996; Gu and Xia, 2000). These proposed mechanisms differ in some details, but agree on the essential features of the reaction. A schematic of the chemical reaction is shown in Fig. 1-5A. The substrate adenine ring is bound between Tyr80 and Tyr123 in an energetically favorable stacking conformation, as shown in Fig. 1-

5B. The positively charged guanidinium group of Arg180 protonates N₃ of the substrate adenine ring thereby inducing an anionic charge on the adenine ring, which through delocalization weakens the C_{1'}-N₉ bond. The negatively charged side chain of Glu177 stabilizes a corresponding cationic charge on the ribose which results in the formation of a ribooxycarbenium-like transition state. The glycosidic bond is then cleaved by a nucleophilic attack by a water molecule (preassociated or free) at C_{1'}.

This proposed mechanism is consistent with observations of ribosome/RIP reactions at pH ~7. However, Chen *et al.*, (1998) in experiments on the pH dependence of the activity of ricin A-chain with small RNA oligoribonucleotide mimics of the ribosome target domain found that the reaction was optimal pH at ~4.0, and that the activity fell off rapidly for values of pH above and below pH 4.0, decreasing by an order of magnitude at pH 3.0 and 5.0. Similar results were obtained in the research reported here. The pK_a of arginine (12.5) is far too basic to account for the loss of activity at pH ~5.0. Thus, the above mechanism does not fully account for the pH dependence of the activity of RIPs interacting with small RNA oligoribonucleotide substrates.

Table 1-1. Corresponding active site residue position numbers for ricin A-chain, trichosanthin, and gelonin.

Ricin A-chain	Trichosanthin	Gelonin
Tyr80	Tyr70	Tyr74
Gly121	Gly109	Gly111
Tyr123	Tyr111	Tyr113
Glu177	Glu160	Glu166
Arg180	Arg163	Arg169
Trp211	Trp192	Trp198

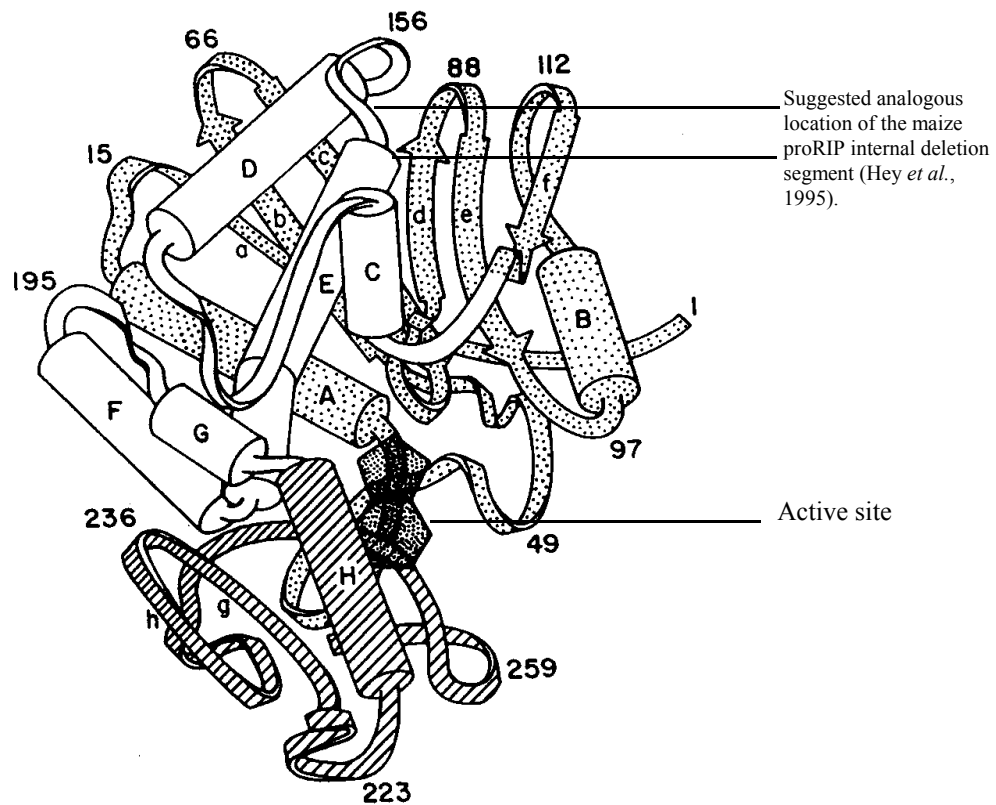


Figure 1-1. Ribbon drawing of the ricin A-chain backbone, from Katzin *et al.*, (1991). The helices (cylinders) are labeled A-H along the chain. β -sheets (arrows) are labeled a-h. The active site, and binding site for adenine, is indicated by the stippled purine symbol. Domain 1, residues 1-117, is dotted, domain 2 (118-210) is open, and domain 3 (211-267) is striped.

```

1MOM_      -----DVSFRLSGADPRS YGMFINDLRNALPF---REKVYNIPLLLP--SVSGAGRY
RLTZT      -----DVSFRLSGATSSSYGVFISNLRKALPN---ERKLYDIPLLRS--SLPGSQRY
1RTC_      MIFPKQYPIINFTTAGATVQSYTNFIRAVRGRLTTG--ADVRHEIPVLPNVRGLPINQRF
tr|Q9S9E4  -----GLDTVSFSTKGATYITYVNFVFLNELRVKLKP---EGNSHGIPLLRK--GDDPGKCF
1PAF       -----VNTIIYVVGSTTISKYATFLMDLRNEAKDP---SLKCYGIPMLPN---TNTNPKY
MOD1X_     -KRIVPKFTEIFPVEDANYP-YSAFIASVRKDVVKHCTDHKGIFQPVLPP--EKKVPELW
           :   :   *   *   :   *   :   *   :
           21 24   29               43 45

1MOM_      LLMHLFNYDGKTTITVALDVTVNYIMGYLADTTS-----YFFN--EPAAELASQYVFRDAR
RLTZT      ALIHLTNYADETISVAIDVTNVIIMGYRAGDTS-----YFFN--EASATEAAKYVFKDAM
1RTC_      ILVELSNHAELSVTLALDVTVNAYVVGVRAGNSA-----YFFHPDNQEDAEATHLFTDVQ
tr|Q9S9E4  VLVALSNDNGQLAEIAIDVTSVYVVGQVVRNRS-----YFFK--D-APDAAYEGLFKNTI
1PAF       VLVELQGSNKKTTITLMLRRNNLYVMGYSDPFETNCRYHIFNDISGTERQDVETTLCPNA
MOD1X_     FYTELKTRTS-SITLAIRMDNLYLVGFRTPGGV-----WWEFG-----KGDTHLLGDNP
           *       :   :   .   *   *   :   *       :
           62               80 83               93

1MOM_      R-----KITLPYSGNYERLQIAAG-KPREKIPIGLPALDSAISTLLHYDST-----AA
RLTZT      R-----KVTLPYSGNYERLQTAAG-KIRENIPGLPALDSAITTLFYNNAN-----SA
1RTC_      N-----RYTFAFGGNYDRLEQLAG-NLRENIELGNGPLEEAISALYYYSTGGTQLPTL
tr|Q9S9E4  KNPILLFGGKTRLHFSGSYPSLEGEK--AYRETTDLGIEPLRIGIKKLDENAIIDNYKPTEI
1PAF       N----SRVSKNINFDSDRYPTLESKAGVKSRSQVQLGIQILDSNIGKISGVMSFTEK--TE
MOD1X_     R-----WLGFGGRYQDLIGNKG---LETVTMGRAEMTRAVNDLAKKKAADPQADT
           :   :   .   *   *   :   :   :   :   :
           123 126               140

1MOM_      AGALLVLIQTTAEAAARFKYIEQQIQERA--YRDEVPSLATISLENSWSGLSKQIQLAQGN
RLTZT      ASALMVLIQSTSEAARYKFFIEQQIGKRV--DKTFLPSLAIISLENSWSALSQKIQIASTN
1RTC_      ARSFIICIQMISEAARFYIEGEMRTRIRYNRRSAPDPSVITLENSWGRLLSTAIQES--N
tr|Q9S9E4  ASSLLVVIQMVSEAAARFTFIENQIRNNF--QQRIRPANNTISLENKWKGLSFQIRTSG-A
1PAF       AEFLLVAIQMVSEAAARFKYIENQVKTNFN--RAFNPNPVKVLNLQETWGGKISTAIHDA--K
MOD1X_     KSKLVKLVVMVCEGLRFNTVSRVTDAGFNSQHGVTLTVTQCKQVQKWDRIKAAFEW---
           :   :   .   *   *   :   :   :   :   :   :   :
           177 180               211 215

1MOM_      NGIFRTPIVLVDNKGNRVQITNVTSKVVTSNIQLELLNTRNI----
RLTZT      NGQFESPVVLINAQNRVTITNVDAVVTSNIALLLNRNMA---
1RTC_      QGAFASPIQLQRRNGSKFSVDVSIPIPIALMVYRCAPPPSSQF
tr|Q9S9E4  NGMFSEAVELERANGKYYVTAVDQVKPKIALLLKFVDKDFE----
1PAF       NGVLPKPLELVDASGAKWIVLRVDEIKPDVALLNYVGGSCQTT--
MOD1X_     -A---DHPTAVIPDMQLGIDKNEAARIVALVKNQTTAAA----
           :   :   :   :   :

```

Figure 1-2. Multiple sequence alignment (using Clustal W) of six sequences - five ribosome-inactivating proteins with known structures determined by crystallography, and the maize proRIP1 mutant MOD1X. 1MOM: momordin, from the seeds of *Momordica charantia*; RLTZT: trichosanthin (*Trichosanthes kililowii maxim*), from P09989, residues 24-270; 1RTC: ricin A chain from castor (*Ricinus communis*) bean; tr|Q9S9E4: Gelonium multiflorum (*Euphorbiaceae himalaya*); 1PAF: pokeweed antiviral protein from pokeweed (*Phytolacca americana*) leaves; MOD1X: represented by Genbank M83926 (deposited by Bass *et al*, 1992) minus residues 1-16, 162-186, and 289-300. The sequence numbering is relative to 1RTC, the ricin A-chain. The BLOSUM matrix was used. The alignment parameters were the clustal W defaults: gap open penalty: 10; gap extension penalty: 0.05; gap distance: 8.

The symbols “*”, “:”, and “.” appearing in a row beneath the alignment blocks denote the degree of conservation observed in each column:

“*” means that the residues or nucleotides in that column are identical in all sequences in the alignment.

“:” means that conserved substitutions have been observed, according to the COLOUR table: Red: AVFPMILW; Blue: DE; Magenta: RHK; Green: STYHCNGQ.

(Note: colors are not visible in this black-and-white Figure)

“.” means that semi-conserved substitutions are observed.

[illegible]

Figure 1-3. Multiple sequence alignment (using Clustal W). Similar to Fig. 1-2, but without the MOD1X sequence. Comparison of Figures 1-2 and 1-3 illustrates the extent to which MOD1X does not share sequence similarity with the other five ribosome-inactivating proteins. The omission of MOD1X increases the number of positions at which there are identical residues from 16 to 35, and also, permits the appearance of one location at which a subsequence of four contiguous residues is conserved among the five ribosome-inactivating proteins.

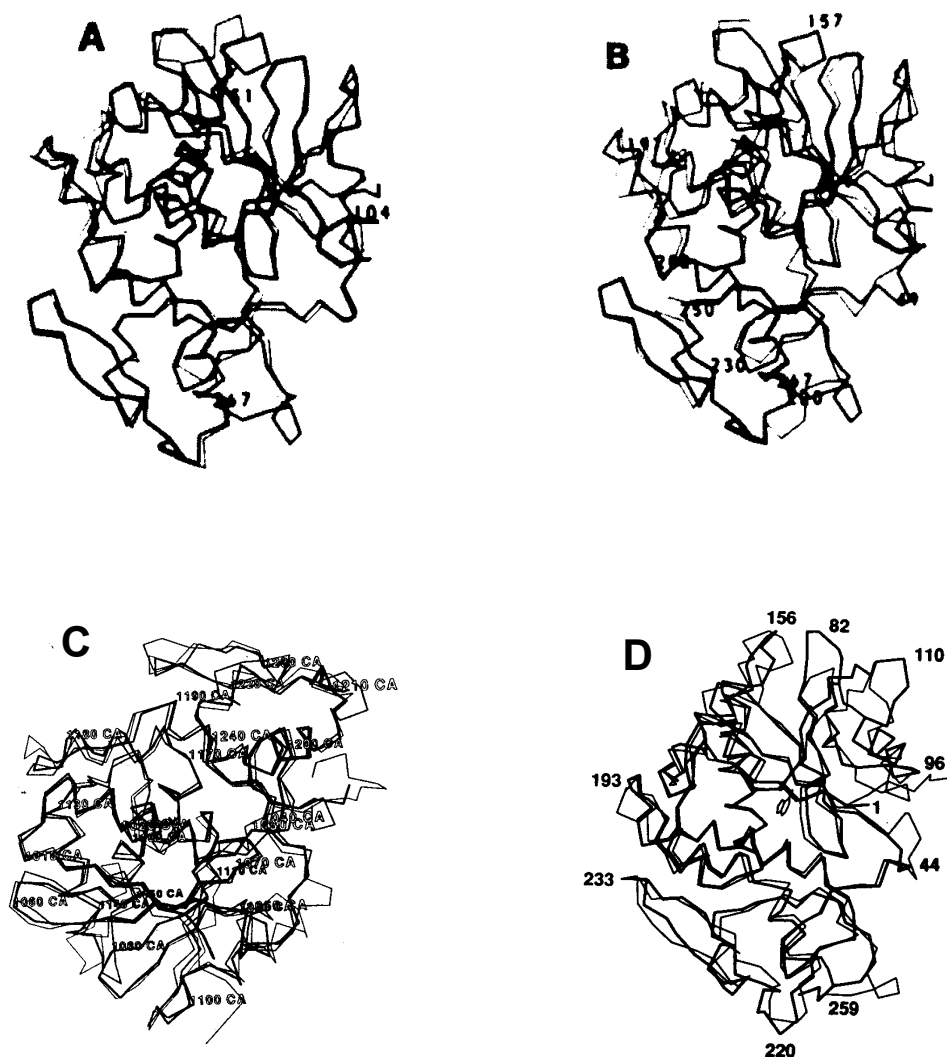


Figure 1-4. Tertiary homology shown by α -carbon backbone superpositions.

(A) Ricin A-chain and abrin A-chain (from Collins *et al.*, 1990). (B) Ricin A-chain and TCS (trichosanthin) (from Collins *et al.*, 1990). (C) Ricin A-chain and PAP (pokeweed antiviral protein) (from Monzingo *et al.*, 1993). (D) Ricin A-chain, gelonin, and α -momorcharin (from Hosur *et al.*, 1995).

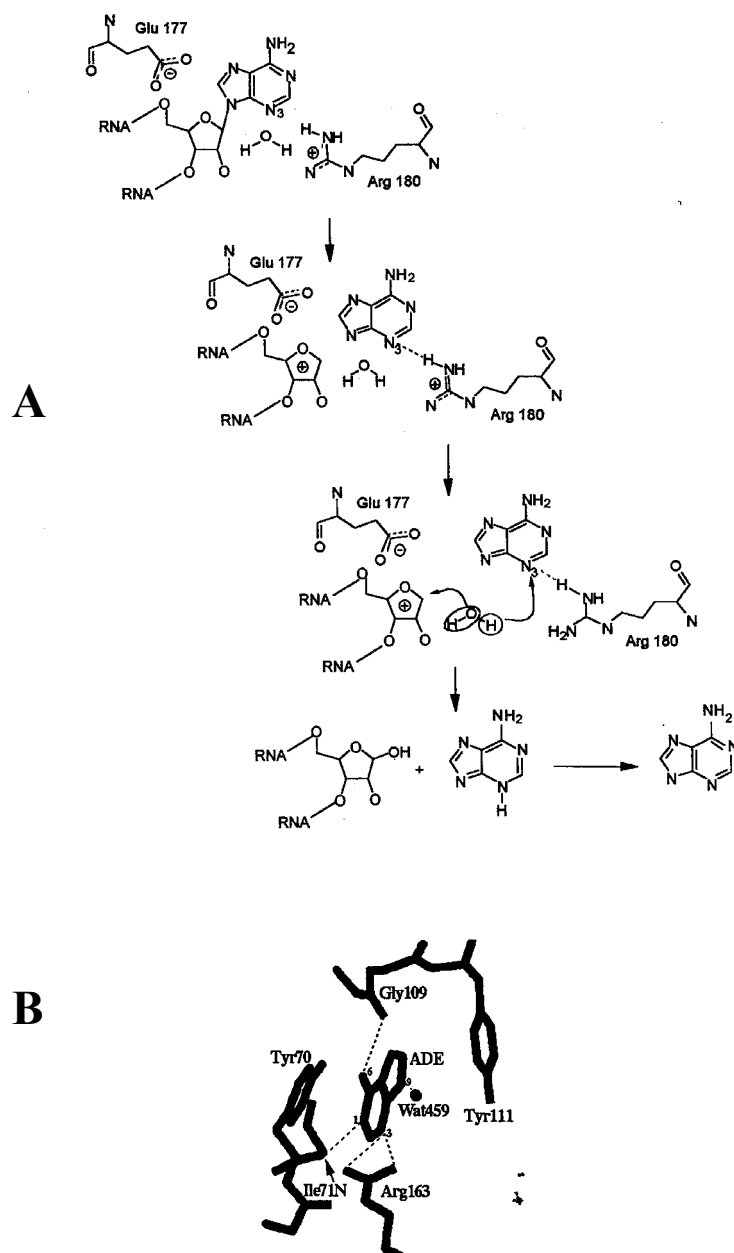


Figure 1-5. The RIP N-glycosidation reaction, and the active site structure of TADE, a complex of trichosanthin and adenine. **(A)** The RIP N-glycosidation reaction (from Krawetz, 1998). **(B)** The active site structure of TADE, a complex of trichosanthin and adenine (from Gu and Xia, 2000).

CHAPTER 2. THE MAIZE PRORIP, MAIZERIP, AND DELETION MUTANTS

proRIP

Di Fonzo *et al.* (1986) purified a maize endosperm protein, which had earlier been named b-32 by Soave *et al.* (1981), associated with the *Opaque-2* and *Opaque-6* genes. The cDNA encoding the b-32 protein was cloned by Di Fonzo *et al.* (1988) and by Hartings *et al.* (1990), and the amino acid sequence(s) of the protein was deduced. The function of b-32 was unknown, but it was believed to function as a regulatory factor for the synthesis of zeins, storage proteins of corn. That the protein b-32 is a zymogen which can be proteolytically converted into an active RIP was discovered by Bass *et al.* (1992), and independently by Walsh *et al.* (1991). It is now referred to as maize proRIP because it is synthesized as a zymogen, and since its proteolytic activation involves deletion of an internal segment, it is a member of the very small class of *Type 3* RIPs. The sequence of the Boston clone, used in the research herein, is deposited in the GenBank with accession number M83926. The sequence of the Walsh clone is in the GenBank with accession number M77122. There are two small differences between the two deposited sequences: i) the residue at position 171 is K in the Boston clone and Q in the Walsh clone, and ii) the sequence of A's following position 285 is of length six in the Boston clone and four in the Walsh clone.

The characterization of the maize proRIP as a zymogen implies that it is an inactive precursor to an active enzyme. However, this characterization may require some qualification. Hey *et al.* (1995) found that the activity of the proRIP with respect to rabbit reticulocyte ribosomes was not strictly zero, but was about 1/5000 of the activity of the

activated maize RIP. Krawetz (1998), on the basis of results from several methods for assaying RIP activity, suggested that the maize proRIP was strictly inactive with respect to rabbit reticulocyte ribosomes, and speculated that the proRIP activity observed by Hey *et al.* (1995) may have resulted from a very low level of proRIP activation by components in their translational inhibition assay. Although the maize proRIP may be a zymogen with respect to ribosomes, the research herein shows that it may have significant catalytic activity with respect to a small synthetic RNA oligoribonucleotide, described and discussed in detail below.

maizeRIP1

The enzymatically active maizeRIP1 is obtained by proteolytic processing of the maize proRIP1. Full activation consists of the removal of the first 16 residues (residues 1-16) at the amino terminus, the final 12 residues (residues 289-300) at the carboxy terminus, and an internal segment of 25 residues (residues 162-186) (Hey *et al.* 1995; “Krawetz, 1998). Removal of the internal section of the proRIP1 results in two subunits, one 16.5 kDa and one 8.5 kDa, which associate noncovalently to form a heterodimeric enzymatically active RIP.

Deletion mutants

A schematic description of the sequence relationships among the enzymes proRIP1, rproRIP1, maizeRIP1, and the deletion mutants MOD1 and MOD1X is shown in Fig. 2-1. The blocks “a+b”, “d”, and “f” represent the 16-residue amino terminal, the 25-residue

internal linker, and the 12-residue carboxy terminal segments, respectively, removed during proteolytic activation of the zymogen proRIP1 into the catalytically active maizeRIP1. The block “a”, alone, represents the initial five residues (MAEIT) of native proRIP1 that were not included in the cloned version, rproRIP1. The block “ α ” represents 38 residues, including a 6-residue His-tag, prefixed to the amino terminus during cloning. The sizes of the various blocks are not drawn to scale. Note that for the maizeRIP1, the blocks “c” and “e” are shown separated to indicate that they form a heterodimer but are not bound covalently. In both MOD1 and MOD1X the blocks “c” and “e” are bound covalently. Also, note that the “ α ” block is a component of MOD1 but not of MOD1X.

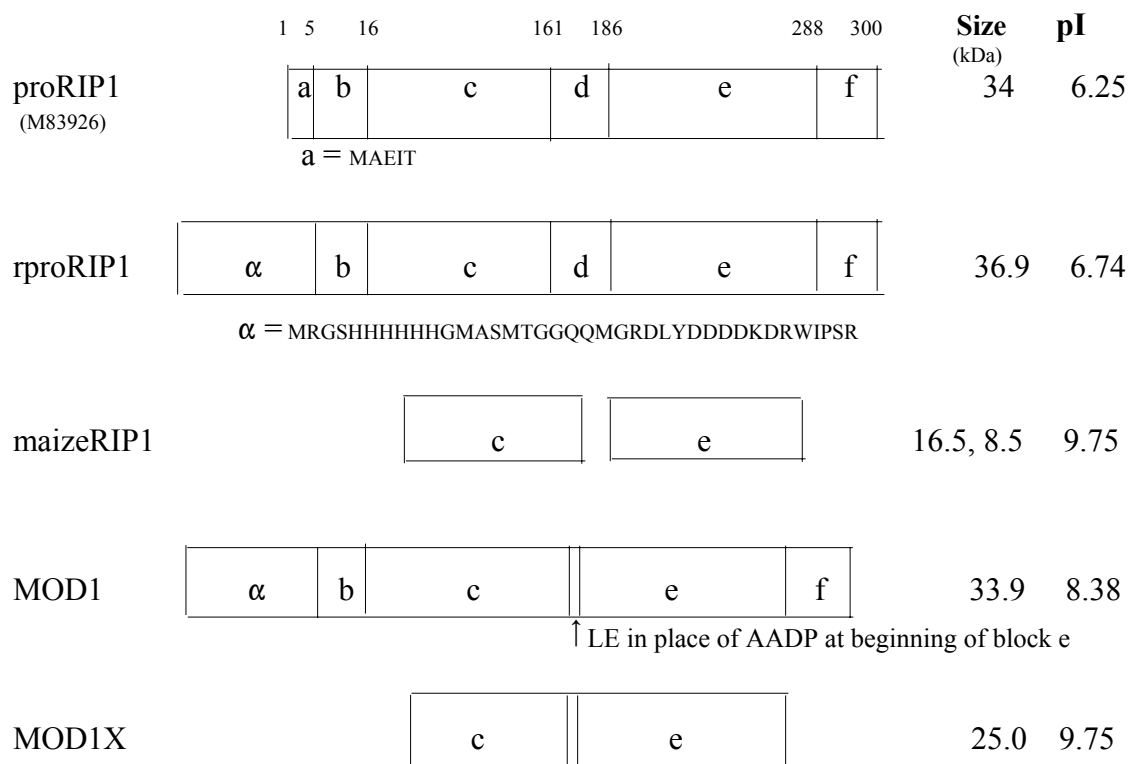


Figure 2-1. Schematic description of the sequence relations among the enzymes proRIP1, rproRIP1, maizeRIP1, and the deletion mutants MOD1 and MOD1X.

The blocks “a+b”, “d”, and “f” represent the 16-residue amino terminal, the 25-residue internal linker, and the 12-residue carboxy terminal segments, respectively, removed during proteolytic activation of the zymogen proRIP1 into the catalytically active maizeRIP1. The block “a”, alone, represents the initial five residues (MAEIT) of native proRIP1 that were not included in the cloned version, rproRIP1. The block “α” represents 38 residues, including a 6-residue His-tag, prefixed to the amino terminus during cloning. The sizes of the various blocks are not drawn to scale. Note that for the maizeRIP1, the blocks “c” and “e” are shown separated to indicate that they form a heterodimer but are not bound covalently. In both MOD1 and MOD1X the blocks “c” and “e” are bound covalently. Also, note that the “α” block is a component of MOD1 but not of MOD1X.

CHAPTER 3. SYNTHETIC RNA SUBSTRATES REPORTED IN THE LITERATURE

α -Sarcin domain mimics

Endo *et al.* (1987) were the first to establish that the specific action of ricin on eukaryotic ribosomes (rat liver ribosomes) was the depurination of the adenosine residue A₄₃₂₄ in the α -sarcin domain of 28S rRNA. After determining the location of the ricin target in the ribosome, experiments were conducted on synthetic models of the α -sarcin domain of 28S rRNA. Endo *et al.* (1988c) studied the specificity of ricin A-chain with respect to a synthetic RNA 35-mer oligonucleotide mimic of the α -sarcin domain. They found that ricin hydrolyzes an adenosine glycosidic bond in the model substrate at a position corresponding to A₄₃₂₄ in 28S rRNA, the site where ricin acts on intact ribosomes. The ricin A-chain/35-mer RNA oligonucleotide glycohydrolase reaction was carried out at 37 °C and pH 7.6. The ricin A-chain concentration required for depurination of the 35-mer mimic at the position corresponding to A₄₃₂₄ in 28S rRNA was 10,000 times greater than was required to depurinate A₄₃₂₄ in intact 28S rRNA. This requirement for very much greater concentration of ricin A-chain is similar to that found earlier by Endo *et al.* (1987) in experiments with deproteinized 28S rRNA. However, in view of more recent experimental results with ricin A-chain activity with respect to synthetic RNA tetraloops, discussed below, in which it was found that optimal activity occurred around pH 4.0, it would be interesting to observe ricin A-chain activity with respect to the 35-mer RNA α -sarcin loop mimic at pH values below 7.6.

Endo *et al.* (1991) continued experiments with the 35-mer RNA synthetic oligonucleotide mimic of the α -sarcin loop, and established that a stem was necessary for

recognition of the RNA by ricin A-chain, but the stem length could vary from seven (as in 28S rRNA) to three without loss of identity, although the oligonucleotide mimic with a stem of length three was less sensitive to ricin. They observed that the sequence required for recognition is a GAGA tetranucleotide, where the first adenosine is the ricin target, and that the position of the GAGA tetranucleotide in the loop could not be varied without losing recognition. They also found that the bulged nucleotide U at position 6 in the substrate (position 4310 in 28S rRNA) is not necessary for ricin A-chain action, and noted that it is not present in *E. coli* 23S rRNA.

GAGA tetraloops

As noted above, Endo and Tsurugi (1988a) observed N-glycosidase activity by ricin A-chain on the first adenosine (A₁₀₁₄) in a GAGA tetraloop on a 7-base stem in deproteinized 16S *E. coli* rRNA, and proposed that the general recognition element for ricin is a GAGA tetraloop. Since the structure of the ricin-sensitive region in 16S rRNA is definitely a GAGA tetraloop, and it appeared likely that the GAGA segment in both the ribosomal α -sarcin domain and the synthetic α -sarcin loop mimics was in the form of a (perhaps transient) tetraloop, it was of interest to study directly the interaction of ricin A-chain and synthetic GAGA tetraloops.

The first study of synthetic tetraloops was conducted by Gluck *et al.* (1992). They constructed a 19-mer GAGA tetraloop approximation of the sensitive site in 16S rRNA. In addition to the GAGA tetranucleotide and a 6-base stem, the construct contained a GGG segment at the 5' end which was a vestige from the T7 promoter utilized during the phage

T7 RNA polymerase synthesis procedure used to obtain the 19-mer construct. This 19-mer construct was treated as a “wild type” tetraloop, and was subjected to a very thorough set of mutations in which the bases surrounding the adenosine corresponding to 16S rRNA A₁₀₁₄ were systematically varied, as was the length of the stem and the composition of the base-pairs (G-C or A-U) comprising the stem. They found that the GAGA sequence in the loop was an absolute requirement, but that neither the stem length (from seven to three base-pairs) nor the composition of the stem base-pairs had a significant effect on the sensitivity of the mutant to depurination by ricin A-chain. They also found that recognition was lost when the loop was opened to form a GAGA-containing hexaloop, and suggested that a GAGA tetraloop either exists in the 17-member single-stranded region of the ricin domain (the α -sarcin loop) in 28S rRNA or is formed during the elongation cycle.

Gluck *et al.* (1994) working with a 35-mer RNA mimic of the 28S rRNA α -sarcin domain studied the effect of mutations in the 5' C and 3' G that bracket the GAGA segment. They found that sensitivity of the 35-mer substrate to ricin requires that the bracketing bases be a Watson-Crick pair, which supports the suggestion that the conserved GAGA segment exists, at least transiently, in the form of a tetraloop. Additional support for the probability that the GAGA segment in both the ribosomal and the synthetic α -sarcin domains is a tetraloop comes from NMR studies by Szewczak *et al.* (1993), Kajava and Ruterjans (1993), and Orita *et al.* (1993).

Link *et al.* (1996) studied the reactivity of ricin A-chain with respect to a 10-mer RNA GAGA tetraloop. They reported that, they “were not able to achieve catalytic turnover”. However, they were able to measure product formation, but at a much lower rate than

observed by Gluck *et al.* (1992) for a 10-mer RNA GAGA tetraloop. A hypothesis to explain these results was proposed involving competing rates of catalysis and enzyme denaturation under their assay conditions. A simpler explanation could be that their experiments were run at pH 7.5, which is very far from pH 4.0 to 4.5, later found by Chen *et al.* (1998) and herein (Chap. 7) to be the optimum range of pH for ricin A-chain depurination of 10-mer RNA GAGA tetraloops.

Chen *et al.* (1998) obtained the kinetic parameters K_M and k_{cat} as a function of pH for ricin A-chain catalyzed depurination of RNA GAGA tetraloops with stem lengths ranging from three to seven (10-mers to 18-mers). They found that the optimum pH was close to 4.0 for all stem lengths, but unlike the results of Gluck *et al.* (1992) which were obtained at pH 7.5, they found that at pH 4.0 the stem length had a significant effect on the ricin A-chain activity. The most sensitive stem length was five (14-mer), at which k_{cat} was 50 times greater than that of stem length three (10-mer). The measured values are listed in Chap. 4, below.

CHAPTER 4. MEASURED VALUES IN THE LITERATURE OF THE PARAMETERS K_M AND k_{cat} FOR RIBOSOME/RICIN A-CHAIN AND RNA OLIGORIBONUCLEOTIDE/RICIN A-CHAIN REACTIONS

Some numerical values for ricin A-chain K_M and k_{cat} are listed in Table 4-1 to show the wide range of measured values not only between different substrates, but also, between different measurements with the same substrate. This illustrates the tremendous dependence of measured parameter values on assay conditions. References listed beneath the Table provide further details about the enzyme, substrate, reaction conditions, and assay.

The lack of repeatability, even to an order of magnitude, of kinetic parameter measurements is illustrated by the following two commentaries from researchers in the area: Kim *et al.* (1992) write that, “Depending on the source of ribosomes and assay conditions, RTA has a $k_{cat} = 300\text{-}1500 \text{ min}^{-1}$ and a $K_M = 0.1\text{-}1.3 \mu\text{M}$ ”. Gluck and Wool (1996b) [using oligoribonucleotides] note that, “A new procedure has been adopted for the assay of ricin A-chain activity because it markedly improves the apparent activity of the toxin. k_{cat} is increased from 0.06 to 3.8 min^{-1} despite a concurrent increase in K_M from 17 to $130 \mu\text{M}$ The details of the characterization of the new reaction conditions will be reported elsewhere.”

Table 4-1. Some numerical values for ricin A-chain K_M and k_{cat} from the literature.

Substrate	Assay	pH	Temp (°C)	K_M (μM)	k_{cat} (m^{-1})	Ref.
Ribosomes	Aniline	7.6	37	2.6	1777	1
35-mer “wild type”	Adenine	7.5	35	13.55	0.23	2
Ribosomes	Adenine	7.4		2.02	317	3
19-mer “wild type”	Adenine	7.5	35	5.7	0.01	4
10-mer tetraloop	Adenine	7.5	37	6.2	1.7	5
10-mer tetraloop	Adenine	7.5	37		0.00033	6
10-mer tetraloop	Adenine	4.0	37	4.1	4.1	7
12-mer tetraloop	Adenine	4.0	37	2.7	101	7
14-mer tetraloop	Adenine	4.0	37	8.1	219	7
16-mer tetraloop	Adenine	4.0	37	6	54	7
18-mer tetraloop	Adenine	4.0	37	6.1	16	7

- (1) Endo, Yaeto and Tsurugi, Kunio (1988).
- (2) Endo, Yaeto, Gluck, Anton, and Wool, Ira G. (1991).
- (3) Sperti *et al.* (1991): Ricin reacting with *A. Salina* ribosomes without cofactors.
- (4) Gluck, Anton, Endo, Yaeto, and Wool, Ira G. (1992).
- (5) Chen *et al.* (1996).
- (6) Link *et al.* (1996). With 10-mer, no catalytic turnover, but measured product formation rate of up to 0.02 hr^{-1} .
- (7) Chen *et al.* (1998).

Note: For the two ribosome values (Refs 1 and 3), $K_M = 2.3 \pm 0.4 \mu M$
For the five tetraloop values (Ref. 7), $K_M = 5.4 \pm 2.0 \mu M$

CHAPTER 5. MATERIALS AND METHODS

Materials

Adenine was purchased from Sigma. Stock concentrations were determined by absorption measurements at 260 nm using Beer's Law and the extinction coefficient $\epsilon = 13,400 \text{ M}^{-1}\text{cm}^{-1}$ from Fasman, 1975.

A-10, the 10-mer oligoribonucleotide CGCGAGAGCG, was purchased from Dharmacon. After deprotection and lyophilization, the oligonucleotide was dissolved in citric acid, EDTA buffer (CAEB, see Buffers) pH 4.0, or water. Stock concentrations were determined by absorption measurements at 260 nm using Beer's Law and the extinction coefficient $\epsilon = 0.0973 \text{ }\mu\text{M}^{-1}\text{cm}^{-1}$ obtained by adjusting the denatured extinction coefficient supplied by Dharmacon (by 18%) to take into account the change in hypochromicity upon folding observed during UV melting experiments. The molecular weight, specified by Dharmacon, was 3239.1 g/mole.

Ricin A-chain was purchased from Sigma (Product Number L 9514). Stocks were prepared by dialysis in CAEB pH 4.0 at 4 °C. Stock concentrations were determined by absorption measurement at 280 nm using Beer's Law and the extinction coefficient $\epsilon = 23670 \text{ M}^{-1}\text{cm}^{-1}$ from ExPASy (<http://us.expasy.org>): RICI_RICCO, SWISS-PROT: P02879. Stock purity was estimated from SDS-PAGE gels by inspection, for example, see Fig. 5-1, lane 7. According to Sigma, the double band visible in the Figure is "normal" for this product and does not affect its activity.

Maize rproRIP1 was obtained by overexpression of *E. coli* clones provided by Prof. Rebecca Boston. Two variations of expression clones were used: one was an *E. coli* strain

BL21(DE3)pLysS clone containing the pRSET vector constructed by Krawetz (1998), and the other was an *E. coli* strain BL21(DE3) clone containing the pRSET vector constructed by Nielsen (Nielsen and Boston, 2001). In both clone variations, the gene in the pRSET vector was based on the native maize proRIP1 sequence (Bass *et al.*, 1991; GenBank Accession Number M83926), but was modified to replace five N-terminal amino acids with a five-residue histidine tag to permit purification of the expressed protein by nickel-affinity chromatography, and an enterokinase cleavage site to allow removal of the tag after purification. Krawetz (1998, Appendix C) verified experimentally that the N-terminal histidine tag did not affect proRIP1 activation or maizeRIP1 activity with ribosomes. Actually, since one of the results of proRIP1 activation is the removal of 16 N-terminal residues from the native maize proRIP1, the five-residue histidine tag and enterokinase cleavage site should no longer be present in the maizeRIP1.

The expression protocols used here were essentially those developed in Prof. Boston's lab, with some minor modifications designed to enhance the protein yield. In the initial stage of this research, maize rproRIP1 was obtained by overexpression of the clone provided by Krawetz, following her expression protocol. However, in the final stages of the research, the clone and expression protocol provided by Nielsen were used. Since all of the data on maize rproRIP1 and maizeRIP1 presented herein were obtained using enzymes derived from the Nielsen clone and protocol, only the details of the Nielsen protocol will be given here, with a summary at the end of this section of places where there were appreciable differences between the Krawetz and Nielsen procedures. No clear differences were noted between the enzyme yields and purities obtained from the different

clones and expression protocols.

The *E. coli* clones were provided by Kirsten Nielsen (of the Boston lab) in the form of a streaked plate. Freezer stocks were prepared by selecting one isolated colony from the plate and inoculating a 25 mL culture of Terrific Broth (TB, see Buffers) containing 200 µg/mL carb (100 µL of 50 mg/mL carb stock) and 35 µg/mL cap (25 µL of 35 mg/mL cap stock). The culture was incubated at 37 °C with shaking at 250 rpm overnight, then separated into 1 mL aliquots of freezer stock consisting of 850 µL of the overnight culture and 150 µL of glycerol, and stored at -70 °C.

Expression protocol: An LB/carb/cap/glucose plate (see Buffers) was streaked using freezer stock and incubated overnight at 37 °C. One small colony was picked from the plate to inoculate a 25 mL TB culture containing 200 µg/mL carb and 35 µg/mL cap in a 250 mL flask, and shaken at 37 °C and 250 rpm until the absorbance at the wavelength of 600 nm, $A_{600} = 0.4-0.6$, then refrigerated overnight. The 25 mL culture was centrifuged at 1000 x g for 5 minutes. The cells were then resuspended in 25 mL of fresh TB. Six mL of the resuspended cells were used to inoculate each 500 mL TB culture containing 500 µg/mL carb (5 mL of 50 mg/mL carb stock) and 35 µg/mL cap (500 µL of 35 mg/mL cap stock) in a 2000 mL flask, and shaken at 37 °C and 250 rpm until $A_{600} = 0.4-0.6$. Protein expression was induced by adding fresh IPTG (isopropylthiogalactoside) to make each culture 1 mM IPTG (500 µL of 1 M IPTG stock) and the cultures were grown at 30 °C for two hours. Each 500 mL culture was transferred to two centrifuge tubes and centrifuged at 4066 x g for 10 minutes at 4 °C. The supernatants were discarded, and the pellets were stored at -70 °C overnight.

Lysate preparation: The specific reagent quantities described here are for one liter of culture, resulting in pellets in four centrifuge tubes. The cells were lysed by adding 15 mL of BugBuster (from Novagen) to each centrifuge tube and vortexing the tubes to resuspend the pellet. The contents of the centrifuge tubes were transferred to 50 mL conical tubes (two centrifuge tubes per conical tube). The nucleic acid was degraded by adding 30 μ L of Benzonase (from Novagen) to each conical tube, and then shaking the tube at room temperature on a horizontal shaker table at 70 rpm for 30 minutes. The contents of each conical tube were transferred to a Corex tube and centrifuged at 16000 x g for 20 minutes.

Column purification: Six mL of ProBond Resin slurry (from Invitrogen) were added to the column and allowed to flow through by gravity. The column was equilibrated by adding 6 mL of NBB (see Buffers) and allowing it to flow through by gravity. Binding of the protein to the resin was accomplished by adding the lysate to the column and pumping it through with air. The column was washed with NBB (see Buffers) until A_{280} was less than 0.01. This step required about thirty to fifty 2 mL fractions. The column was then washed with NWB#2 (see Buffers) until A_{280} was less than 0.01. This step required about twenty 2 mL fractions. The column was then washed with IWB40 (40 mM imidazole wash buffer, see Buffers) until A_{280} was less than 0.01. This step required about twenty to forty 2 mL fractions. Finally, the protein was eluted with IEB250 (250 mM imidazole elution buffer, see Buffers). Fractions with A_{280} greater than 0.2 (typically from about fraction 4 to 14) were pooled.

Dialysis, concentrating, and concentration determination: The pooled fractions

were dialyzed against AB (activation buffer, see Buffers) in preparation for activation. The protein concentration after dialysis was usually in the range of 0.4-0.7 mg/mL. The protein was further concentrated to 4-6 mg/mL by centrifugation using YM-10 Centricon tubes. The concentration of the purified protein was determined by absorption measurements at 280 nm using Beer's Law and the extinction coefficient $\epsilon = 40780 \text{ M}^{-1}\text{cm}^{-1}$ calculated by the method of Gill and von Hippel (1989) (see also, ExPASy, RIP3_MAIZE, P25891). Purity was estimated from SDS-PAGE gels by inspection, for example, see Fig. 5-1, lanes 2 and 3.

Summary of Krawetz/Nielsen protocol differences: Cell lysis was carried out by repeated freeze-thaw cycles and sonication in the Krawetz protocol, but in the Nielsen protocol, cell lysis and also nucleic acid degradation were carried out by chemical means (BugBuster and Benzonaze). Induction was carried out at 37 °C for 3-4 hours in the Krawetz protocol, but at 30 °C for 2 hours in the Nielsen protocol.

maizeRIP1 (activation of maize rproRIP1)

MaizeRIP1 was obtained by papain-bead based partial proteolysis of maize rproRIP1 using the protocol developed in Prof. Boston's lab. The reagent quantities described here are for activation of ~ 500 μL of 4-6 mg/mL rproRIP1 dialyzed in AB (activation buffer).

Activation Protocol: The beads were prepared by adding 100 μL of 50% papain bead slurry (Pierce, # 20341) to 1 mL of digestion buffer (DB). The preparation was mixed by inverting the tube several times, and then centrifuged at 13,500 x g for 2 minutes. The supernatant was discarded, 1 mL of DB was added to the tube, and the mixture was

centrifuged for 2 minutes. The papain beads were resuspended in 100 μL of DB. 500 μL of rproRIP1 stock were diluted with 500 μL of DB, and the mixture was added to the tube containing the papain beads, which was then incubated at 37 °C with shaking for 3-4 hours. After adding 500 μL of AB and centrifuging for 2 minutes, the supernatant was transferred to a 1.9 mL centrifuge tube. 500 μL of AB was added to the bead pellet, mixed by inverting several times, centrifuged for 2 minutes, and the supernatant was added to the digest in the 1.9 mL centrifuge tube. The contents of the 1.9 mL centrifuge tube were dialyzed in CAEB60 (citric acid/EDTA buffer, pH 6.0, see Buffers) using a BioRad Microdialysis apparatus. The concentration of the dialyzed protein was determined by absorption measurements at 280 nm using Beer's Law and the same extinction coefficient ($\epsilon = 40780 \text{ M}^{-1}\text{cm}^{-1}$) as for the maize proRIP since the segments deleted during activation contain no Tyr, Trp, or Cys residues. Purity was estimated from SDS-PAGE gels by inspection, for example, see Fig. 5-1, lane 4. Note that maizeRIP1 is a heterodimer which separates into its constituent parts (16.5 and 8.5 kDa) in the denaturing gel. The dialyzed protein was separated into 100 μL aliquots and stored at -70 °C.

MOD1 (described in fig. 2-1, p. 27) was obtained by overexpression in *E. coli* clones provided by Julie Krawetz (of the Boston lab). These clones were similar in construction to those designed by Krawetz for maize rproRIP1 expression, the only difference being the insertion of a DNA sequence for MOD1 rather than for maize proRIP1 in the plasmid. The expression and purification protocol were the same as those for maize rproRIP1, described above.

MOD1 concentration was determined by first using the Pierce Coomassie Plus-200

Protein Assay Reagent and their ‘Standard Protocol: Test Tube Version’ to determine the concentration of MOD1 relative to BSA, and then using the calibration provided by Sigma for BSA: $A_{279} = 0.667$ per mg/mL. Purity was estimated from SDS-PAGE gels by inspection, for example, see Fig. 5-1, lane 5.

MODIX was obtained by papain-bead based partial proteolysis of MOD1 following the protocol, described above, for obtaining maizeRIP1 by activation of maize rproRIP1. MOD1X concentration was determined by using the Pierce Coomassie Plus-200 Protocol for comparison with the previously determined concentration of MOD1. Purity was estimated from SDS-PAGE gels by inspection, for example, see Fig. 5-1, lane 6.

Buffers

AB (activation buffer)

NaPi 20 mM (see below for definition of NaPi)
EDTA 10 mM
Adjust to pH 7.0 with NaOH.

DB (digestion buffer)

NaPi 20 mM
EDTA 10 mM
Cysteine-HCl 20 mM
Adjust to pH 7.0 with NaOH.

CAMP600 (citric acid mobile phase)

Citric acid 100 mM
Adjust to pH 3.6 with NaOH.

CAEB40 (citric acid/EDTA buffer, pH 4.0)

Citric acid 10 mM
EDTA 1 mM
Adjust to pH 4.0 using KOH.

CAEB60 (citric acid/EDTA buffer, pH 6.0)

Citric acid 10 mM
EDTA 1 mM
Adjust to pH 6.0 using KOH.

IEB250 (250 mM imidazole elution buffer)

Imidazole	250 mM
NaPi	20 mM
NaCl	500 mM

Adjust to pH 6.0 with acetic acid, then filter sterilize.

IWB40 (40 mM imidazole wash buffer)

Imidazole	40 mM
NaPi	20 mM
NaCl	500 mM

Adjust to pH 6.0 with acetic acid, then filter sterilize.

LB (Luria-Bertani Medium)

Per liter:

bacto-tryptone	10 g
bacto-yeast extract	5 g
NaCl	10 g

Adjust to pH 7.0 using NaOH.

Autoclave at 15 lbs/sq. in. for 20 min.

LB/carb/cap/glucose plate

LB	20 mL (autoclaved)
glucose	1% w/v
carb	50 µg/mL
added when cooled	
cap	35 µg/mL
added just prior to streaking	

NaPi

50% NaH₂PO₄ (monobasic)

50% Na₂HPO₄ (dibasic)

NBB (Native Binding Buffer)

NaPi	20 mM
NaCl	500 mM

Adjust to pH 8.0 with acetic acid, then filter sterilize

NWB#2 (Native Wash Buffer #2)

NaPi	20 mM
NaCl	500 mM

Adjust to pH 6.0 with acetic acid, then filter sterilize

TB - Terrific Broth (Sambrook *et al.*, p. A.1)

Per liter:

i) To 900 mL of deionized H₂O, add

bacto-tryptone	12 g
bacto-yeast extract	24 g
glycerol	4 mL

Autoclave for 20 min at 15 lb/sq. in.

ii) Prepare 100 mL of a sterile solution of 0.17 M KH_2PO_4 , 0.72 M K_2HPO_4 by dissolving 2.31 g of KH_2PO_4 and 12.54 g of K_2HPO_4 in 90 mL of deionized H_2O , adjusting the volume to 100 mL, and autoclaving for 20 min at 15 lb/sq.in.

iii) After solution (i) has cooled to 60 °C or less, add solution (ii) to solution (i).

Methods

Released adenine measurement: The concentration of adenine released during a substrate-enzyme reaction was measured by injecting a 100 μL aliquot of the reaction mixture into an HPLC (High-Performance Liquid Chromatography) system. All measurements were made with a Hamilton Co. PRP-1 reversed phase column (Product Number: 79444). The column dimensions were 150 x 4.1 mm (volume: 1.98 mL), with particle size of 5 μm . The mobile phase was 100 mM citric acid adjusted to pH 3.6 using NaOH solution (CAMP600). Between the injector and the main column was a guard column (Hamilton Co. Part # 79445) which trapped the protein, thereby extinguishing the reaction within a few seconds after the injection.

The detector was a two-channel Waters Co. model. Both channels were set to 254 nm and were typically set to different sensitivities so that if the more sensitive channel went off-scale during a measurement, the less sensitive channel would provide a valid data value at that point. The detector output was measured as peak height on a chart reader with 200 mm full scale. The detector sensitivity settings were labeled 0.005, 0.02, 0.05, 0.2, 0.5, and 1.0 Absorbance Units Full Scale (AUFS). The detector was calibrated for adenine

concentration using a 100 μL injection of a 5 μM adenine standard at a sensitivity setting of 0.02. Over the entire period during which the data presented herein was obtained, the peak height of the 5 μM adenine standard ranged from ~ 70 to ~ 130 mm, depending on the age and condition of the column and the line voltage level in the lab. However, during a typical 180 minute timecourse, the calibration varied less than 5%. A calibration was usually obtained just before the first data point was measured, another after 90 minutes had elapsed, and a final one immediately after the last data point was obtained. Then, an average value of the three calibrations was used for analysis of all of the data obtained during the run.

For a typical calibration peak of 90 mm for a 100 μL injection of a 5 μM adenine standard measured at a detector setting 0.02 AUFS, for example, the released adenine concentration in a 100 μL injection would be given by

$$[\text{Adenine}]_{\mu\text{M}} = [2.78 (\mu\text{M}/\text{mm-AUFS})] (\text{peak height in mm}) (\text{AUFS})$$

At the most sensitive detector setting of 0.005 AUFS, the noise magnitude on the chart trace was ~ 2 mm. A signal/noise ratio of at least ten would therefore require a peak of at least ~ 20 mm when using detector setting 0.005 AUFS. Using the above calibration, the smallest effectively measureable concentration of released adenine would be

$$[\text{Adenine}]_{\mu\text{M}} = (2.78 \mu\text{M}/(\text{mm-AUFS})) (20 \text{ mm}) (.005 \text{ AUFS}) \cong 0.3 \mu\text{M}$$

Constraints on choice of experimental conditions:

Time scale constraints: The retention time for the adenine peak (using CAMP600 as the mobile phase) is ~ 230 - 270 secs (~ 4.25 minutes). After the peak, about 2.5-3

minutes are required to reestablish the base line. This brings the total to about 7-8 minutes. Adding time required for setting and marking the chart recorder, adjusting the detector sensitivity, and resetting the chart recorder for drift, the minimum time between injections is about 10 minutes.

Note the assumption that the reaction continues normally in the syringe and in the injection loop during the approximately one minute it takes to fill the syringe with a 100 μL aliquot from the reaction mixture, empty the syringe contents into the injection loop, and actuate injection into the HPLC stream. To keep the variations due to the above uncertainties within a reasonable range, 10 minutes should be adopted as a minimum initial duration for initial velocity experiments, and 15 minutes as a practical interval between sample measurements during timecourse experiments.

Substrate concentration constraints: For Michaelis-Menten initial velocity experiments, as can be seen from Eq. A1-10 (Appendix A1), if the initial substrate concentration S_0 is very much greater than K_M , the reaction becomes essentially zero-order. The initial velocity v_i approaches V_{\max} and is no longer dependent on either K_M or S_0 . On the other hand, if the initial substrate concentration S_0 is very much less than K_M , the reaction becomes essentially first-order. The initial velocity v_i approaches $v_i = V_{\max} S_0 / K_M$, and is dependent only on the ratio of the two parameters K_M and S_0 rather than on each of the parameters independently. Thus, for a plot of v_i as a function of S_0 to show the effects of both K_M and S_0 and thereby permit the determination of the values of the two Michaelis-Menten parameters K_M and k_{cat} , the initial substrate concentration S_0 should be of the order of K_M . Allison and Purich (1979, p. 11) state, “Since the greatest velocity change occurs

in the region of the K_M , it is frequently satisfactory to vary the concentration from about 0.2 to 5.0 times this constant. This changes the fractional attainment of maximal velocity from 0.14 to 0.83, and reasonable estimates of K_M can be made.” Segel (1975) recommends that S_0 be of the order of K_M (~ 0.3 to 2.0 times K_M) for Michaelis-Menten initial velocity experiments.

Another constraint on the initial substrate concentration S_0 in Michaelis-Menten initial velocity experiments is imposed by the detector sensitivity. The initial velocity should be measured before the extent of reaction exceeds $\sim 10\%$. Thus, the initial substrate concentration must be at least ten times the smallest effectively measureable concentration of free adenine. This may conflict with the requirement that S_0 be of the order of K_M .

For timecourse experiments, Duggleby and Clarke (1991) recommend that for optimum data analysis, the initial substrate concentration be ~ 2 to 3 times K_M , and that the data be collected until the extent of reaction reaches 90% . Vandenberg *et al.* (1986) believe that data collected beyond an extent of reaction of 80% is superfluous, and that timecourse experiments should be carried out until the extent of reaction reaches 60 - 80% .

Enzyme concentration constraints: Once an initial substrate concentration compatible, as far as possible, with the above constraints has been chosen, the corresponding enzyme concentration is subject to two constraints. First, the assumptions underlying the Michaelis-Menten equation require that the [substrate]/[enzyme] ratio be very large. The quantitative interpretation of “very large” is discussed in Appendix A1. Second, the enzyme concentration must provide for a reaction rate which results in an experimental time scale appropriate to the time/extent-of-reaction constraints described

above. These two constraints may be in conflict with each other if the range of enzyme concentrations which satisfy the first constraint does not overlap the range of enzyme concentrations satisfying the second constraint.

pH determination: For each timecourse experiment, a 700 μL reaction mixture was prepared to permit six 100 μL aliquots to be withdrawn during the course of the experiment. The enzyme component of the mixture was taken from stocks that were all at pH 4.0. The substrate component was taken from stocks that were almost all at pH 4.0, but in a few cases were at pH 7.0. The buffer component was taken from a set of buffer stocks at pH between pH 3.0 and 7.0 in 0.5 pH increments. Although the buffer volume was usually predominant in the reaction mixture, the pH of the mixture was not exactly that of the buffer component. The actual pH of each timecourse reaction mixture was determined by measuring the pH of a solution in which the substrate and enzyme components were represented by buffers of the appropriate pH and the substrate, enzyme, and buffer volumes were proportional to those in the reaction mixture.

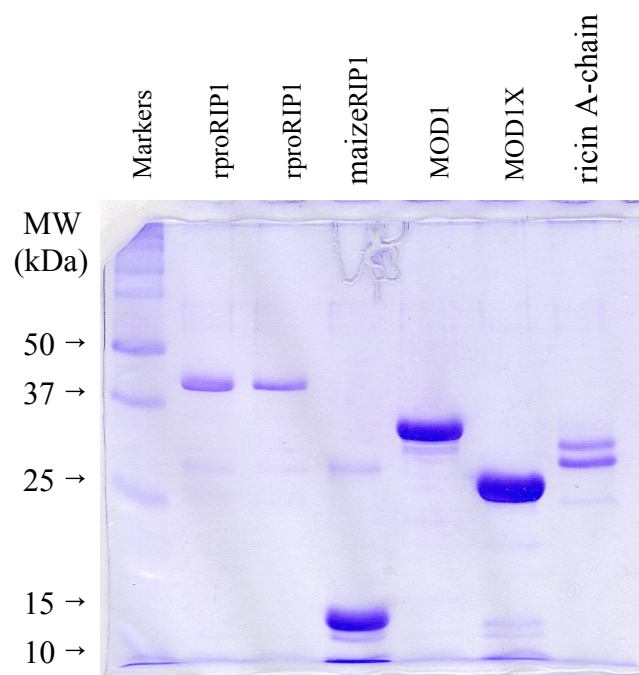


Figure 5-1. SDS-PAGE gel of maize rproRIP1, maizeRIP1, MOD1, MOD1X, and ricin A-chain. The markers in Lane 1 were BIO-RAD Prestained Precision Protein Standards, Catalog # 161-0372, representing molecular weights of 10, 15, 25, 37, 50, 75, 100, 150, and 250 kDa. As mentioned in Materials and Methods, it is asserted by Sigma, from whom the ricin A-chain was purchased, that the double band in the ricin A-chain lane is “normal” for the product (L 9514) and does not affect its activity. The amounts of protein in the lanes were: lane 2, 0.15 nmole; lane 3, 0.10 nmole; lane 4, 0.20 nmole; lane 5, 0.14 nmole; lane 6, 0.20 nmole; lane 7, 0.14 nmole. The gel was 12% acrylamide, and was stained with Coomassie blue.

CHAPTER 6. CONTROL EXPERIMENTS

Three types of control experiments were carried out: i) to estimate the possible effects of pH-dependent substrate or enzyme structural instabilities over the range of pH used in the initial velocity and timecourse reactivity experiments, ii) to determine whether there was any tendency for the substrate A-10 to release adenine spontaneously when not reacting with a RIP, and iii) to detect whether the enzymes were not effectively captured by the guard column (see Materials and Methods), and might possibly have direct effects on the HPLC response to free adenine.

Substrate stability: T_m versus pH for A-10 from UV-melts. The T_m is defined as the temperature at which half of the RNA molecules in a sample are in hairpin form, and half are in one or another denatured form. Values of T_m were measured as a function of pH for A-10 using UV thermal denaturation experiments. The temperature range was 5.0 to 90 °C at 1 °C/min. Seven up and return ramps were measured. Results, based on the third up-ramp, are shown in Fig. 6-1. All of the initial velocity and timecourse experiments were carried out at 30 °C. For pH values above ~4.5, which turned out to be the optimum pH for all the A-10/enzyme activities studied here, this experimental temperature was well below the T_m of A-10, so that the measured effects of pH on the catalytic reactions were clearly much greater than the effects of substrate instability. In fact, in the range of pH above ~4.5, as the pH increases from ~4.5 to ~6.0 the effects of substrate instability and pH on the A-10-enzyme reactivity are in opposite directions, with the pH effect being clearly dominant. But below pH ~4.5, the effects of substrate instability and pH on the A-10-enzyme reactivity are in the same direction. In order to separate the two effects, a set

of A-10/MOD1 timecourse experiments was carried out at 20 °C and compared with the corresponding experiments at 30 °C to distinguish between the temperature and pH effects. The results of these experiments are presented in Chap. 7 and discussed in Chap. 8.

Enzyme structural stability: CD as a function of pH. The effects of pH on the far UV (250-190 nm) CD spectra of ricin A-chain, maizeRIP1, MOD1, and MOD1X are shown in Fig. 6-2. Each trace is the mean of three scans. The pH range tested was from pH 3.0 to 7.0 for maizeRIP1 and MOD1, and pH 4.0 to 6.0 for ricin A-chain and MOD1X. It is clear from the consistent shapes of the CD spectra that to the extent that far UV CD measurements are indicative of macromolecular stability, none of the enzymes showed significant instability over the pH range tested.

HPLC of substrate alone. The results of an experiment to attempt to detect spontaneous release of adenine by A-10 is shown in Fig. 6-3. Panel A shows the HPLC trace of a 100 μ L injection of 5.0 μ M adenine at pH 4.0 for reference. Panel B shows the HPLC trace of a 100 μ L injection of 5.0 μ M A-10 at pH 4.0 using the same HPLC settings and mobile phase. Note that the small blip at \sim 100 sec in Panel B does not correspond to the retention time of adenine, which as seen from Panel A is \sim 235 sec. There is no discernable response in Panel B at \sim 235 sec. Thus, there is no evidence for spontaneous release of adenine by A-10.

HPLC of adenine + enzyme. An experiment was performed to determine whether the presence of ricin A-chain in the reaction mixture might have an effect on the HPLC response to free adenine. The results are shown in Fig. 6-4. Panel A shows the HPLC trace of 5.0 μ M adenine, pH 4.0. Panel B shows the HPLC trace after a five minute

incubation of 5.0 μ M adenine and 5.0 μ M ricin A-chain at pH 4.0 and 30 °C. The adenine peak occurs at a retention time of \sim 250 sec. Note that the differences in peak magnitudes and retention times between Figs. 6-3 and 6-4 are due to a difference in mobile phases and perhaps to some of the other experimental variations discussed above in Methods.

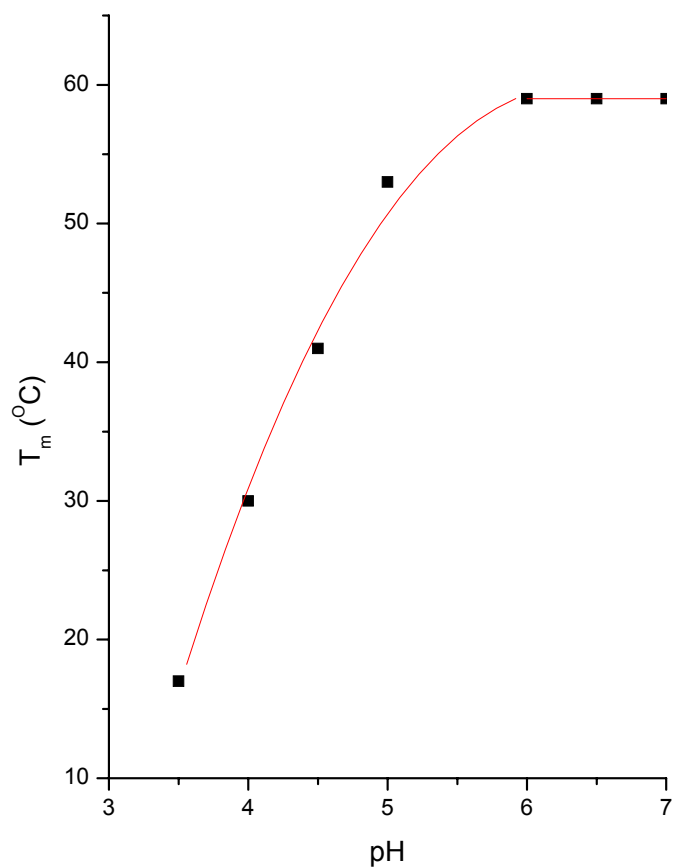


Figure 6-1. A control experiment to investigate the stability of the RNA 10-mer oligoribonucleotide GAGA tetraloop (A-10) by UV-melt measurements of T_m versus pH. The curved portion of the solid trend line is a second order polynomial fit to the data.

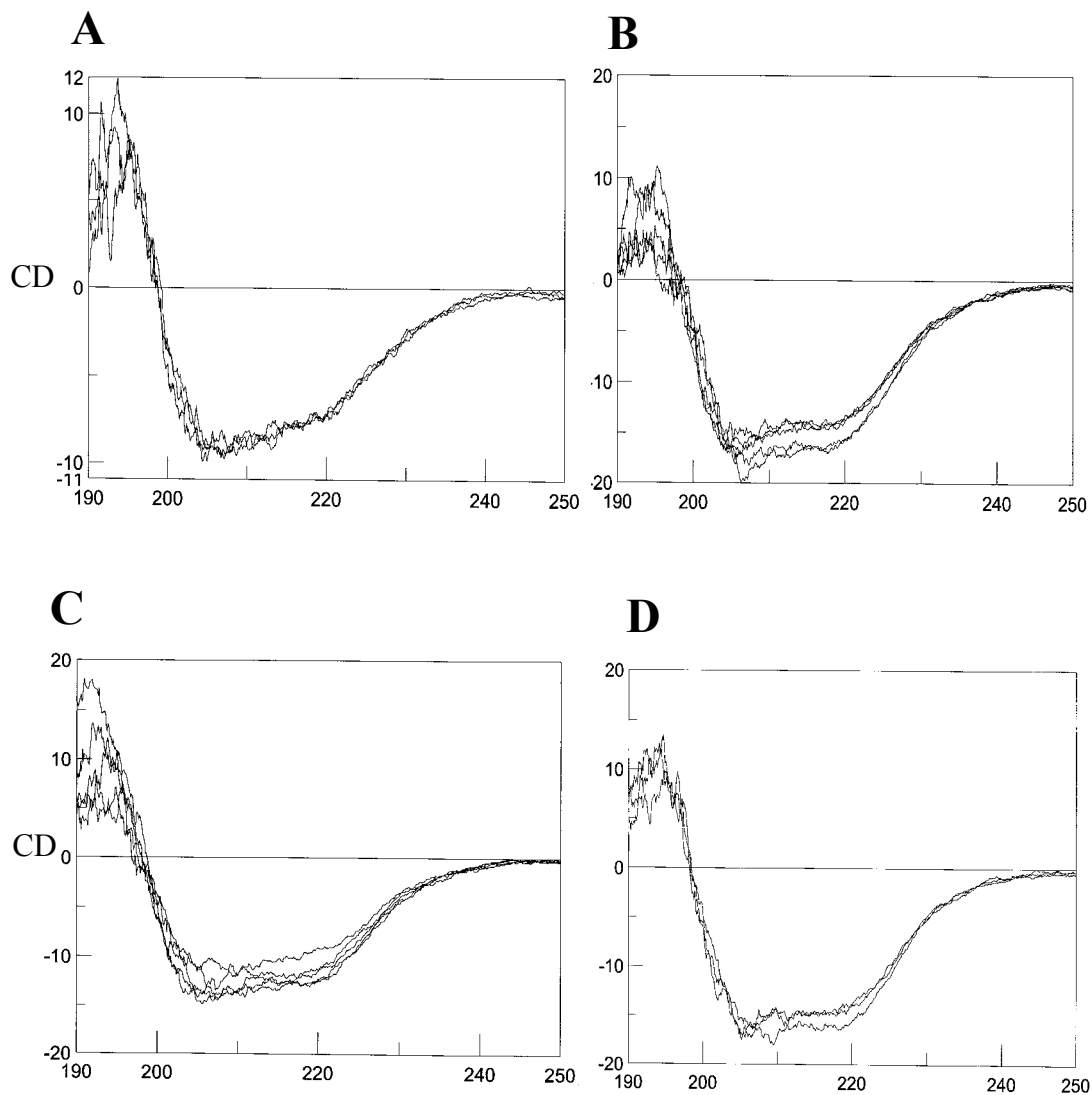


Figure 6-2. A control experiment to investigate the effects of pH on the far UV (250-190 nm) CD spectra of ricin A-chain, maizeRIP1, MOD1, and MOD1X as an indicator of protein structural stability. **(A)** ricin A-chain: pH 4.0, 5.0, and 6.0. **(B)** maizeRIP1: pH 3.0, 4.0, 5.0, 6.0, and 7.0. **(C)** MOD1: pH 3.0, 4.0, 5.0, 6.0, and 7.0. **(D)** MOD1X: pH 4.0, 5.0, and 6.0

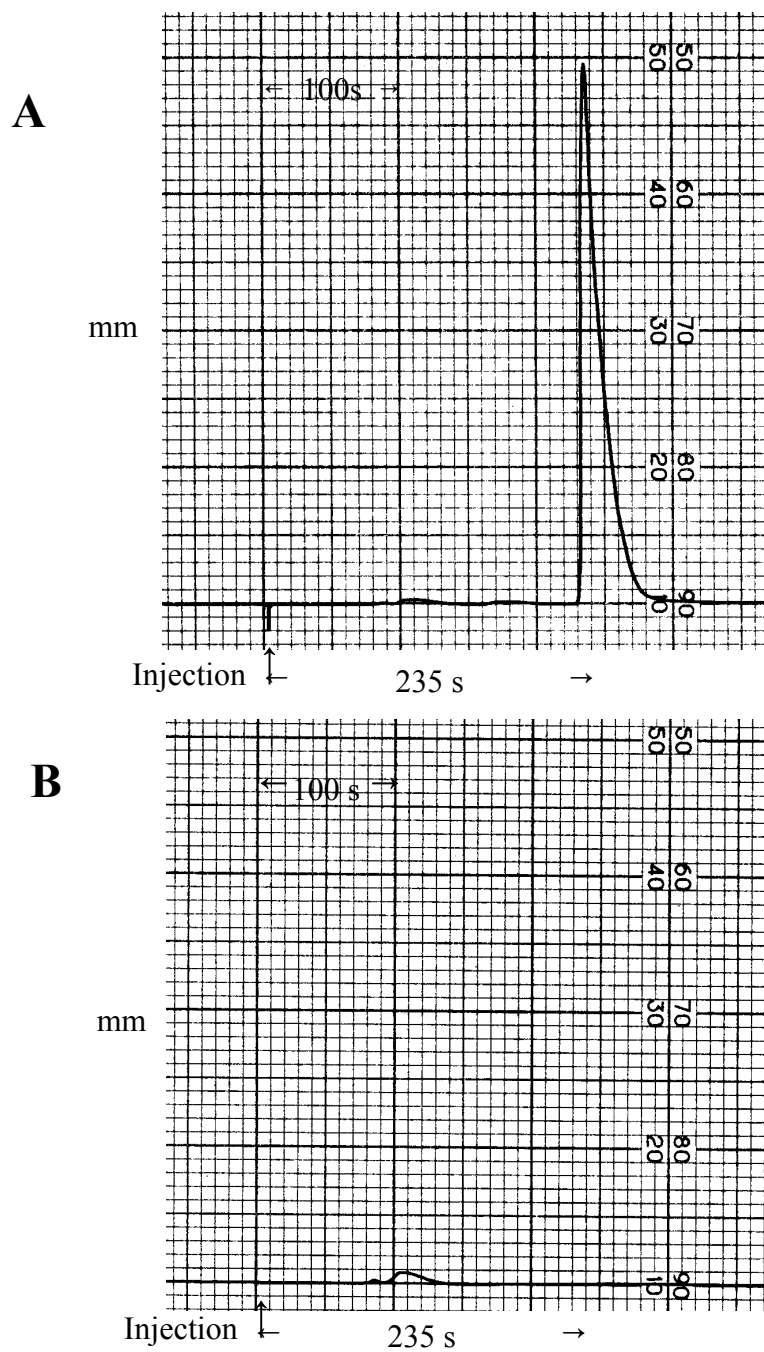


Figure 6-3. A control experiment to attempt to detect spontaneous release of adenine from A-10. **(A)** 0.5 nmole of adenine, pH 4.0. **(B)** 0.5 nmole of A-10, pH 4.0.

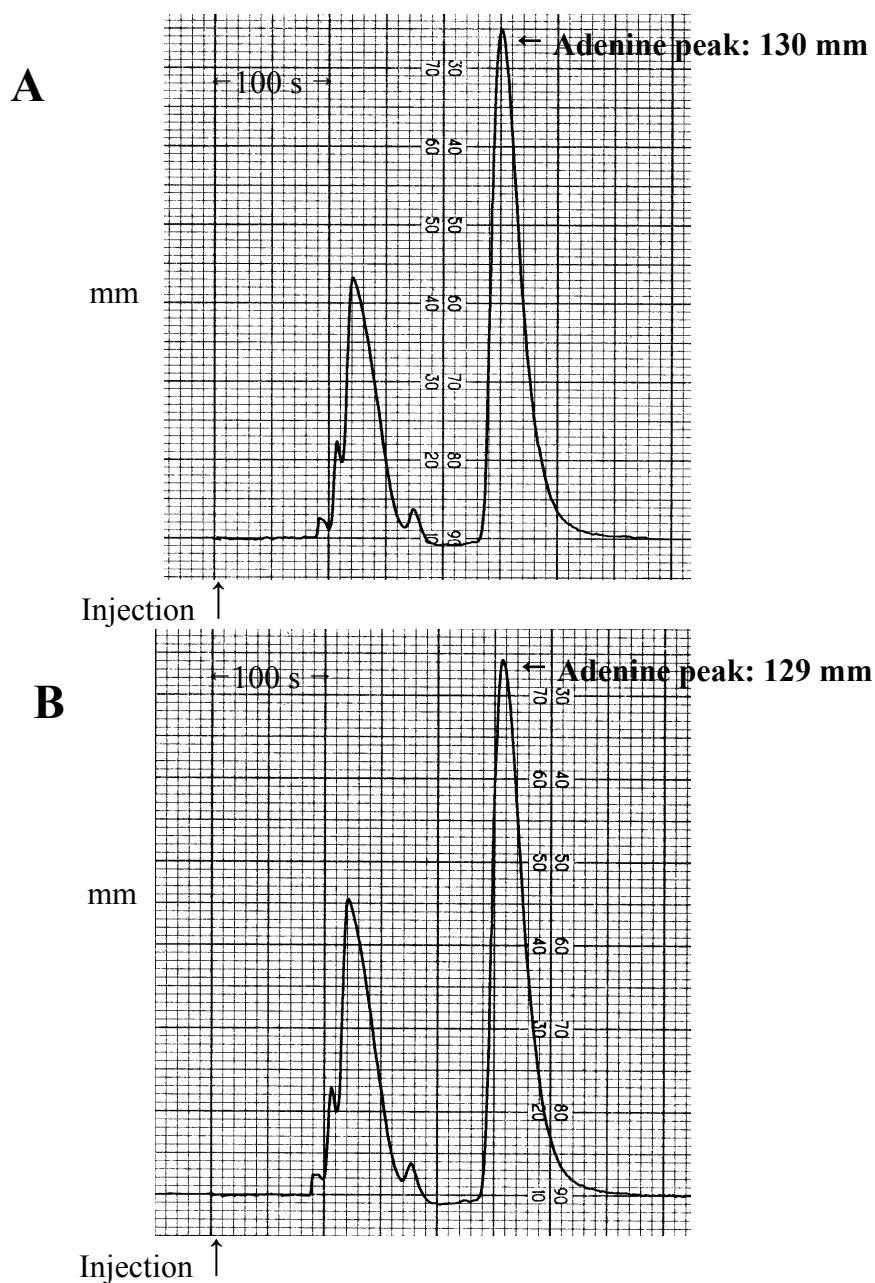


Figure 6-4. A control experiment to investigate the effect of the presence of ricin A-chain on the HPLC response to free adenine. **(A)** HPLC response to 5.0 μM adenine, pH 4.0. **(B)** HPLC response after a five minute incubation of 5.0 μM adenine, pH 4.0 and 5.0 μM ricin A-chain, pH 4.0. Note that the retention time of the adenine peak is 255 sec. The peak at 120 sec is an artifact of the HPLC system. It is highly variable in size and shape, ranging from almost nothing, as in Figure 6-3, to several times the magnitude seen in Figure 6-4. The retention time of the adenine peak is controlled by the pH of the mobile phase, which is adjusted so as to place the adenine peak away from distortion by the HPLC artifact at 120 sec.

CHAPTER 7. EXPERIMENTAL RESULTS

Michaelis-Menten initial velocity experiments

Attempts to obtain Michaelis-Menten parameters K_M and k_{cat} for ricin A-chain when reacting with an RNA 10-mer GAGA tetraloop. The initial research objective was the development of a quantitative assay, based on measurement of the Michaelis-Menten parameters K_M and k_{cat} , of the specific catalytic activities of ricin A-chain and maizeRIP1 when reacting with a 35-mer RNA mimic of the mammalian ribosomal α -sarcin loop. As a preliminary test of the experimental design, some Michaelis-Menten initial velocity experiments were carried out with ricin A-chain reacting with an RNA 10-mer GAGA tetraloop (A-10) to compare with results obtained by Chen *et al.* (1998). These experiments were carried out at pH 4.0 because Chen *et al.* had found in measurements of K_M and k_{cat} as a function of pH, that the optimum pH for the A-10/ricin A-chain reaction was 4.0, and that by pH 5.0 the value for k_{cat} was an order of magnitude lower than its value at the optimum pH. Their steady-state kinetics experiments used reactions containing 0.5-50 μM substrate and 1.0 nM to 0.25 μM ricin A-chain buffered in 10 mM potassium citrate and 1 mM EDTA (pH 4.0), and were incubated at 37 °C for 10 min.

Appropriate experimental conditions for A-10/ricin A-chain initial velocity experiments were sought over a substrate (A-10) range from 1.5 to 18.8 μM and an enzyme range of 0.03 to 0.25 μM . It was very difficult to find manageable reaction durations, at either the lower end of the substrate concentration range or the upper end of the enzyme concentration range, at which the released adenine concentration was measurable and at the same time, the extent of reaction remained below $\sim 15\%$. Experiments with A-10

concentrations of 3.5, 6.1, 10.1, and 18.8 μM and a ricin A-chain concentration of 0.04 μM yielded credible values of initial velocities (the measured values of adenine released by cleavage were well above noise level, and the extent of reaction was $\leq 15\%$). These results are shown in Fig. 7-1 (A) in which the mean and SEM (Standard Error of the Mean) of all the corresponding data points are plotted as a function of substrate concentration. The number of experimental points at each substrate concentration is shown in the Figure. Note that the initial velocity versus substrate concentration relation has a sigmoidal rather than the hyperbolic shape expected from a reaction following the simple Michaelis-Menten model and satisfying the Briggs and Haldane hypotheses. The Lineweaver-Burk double reciprocal plot of the data in Fig. 7-1(A) is shown in Fig. 7-1 (B). The fact that the values of the parameters V_{max} and K_{m} determined from Fig. 7-1 are negative indicates that the experimental conditions of these experiments are not conducive to obtaining credible values of the Michaelis-Menten parameters, or that the reaction does not conform to the simple Michaelis-Menten model.

In the context of the relevant literature, the lack of specific repeatability was disappointing, but not surprising. Chen *et al.* (1998) did not report sufficient experimental details to permit determination of the source of the lack of specific repeatability. Experiments with ricin A-chain reacting with a 10-mer RNA GAGA tetraloop were first reported by Gluck *et al.* (1992). They experimented with this construct because it is a mimic of a GAGA tetraloop at a ricin A-chain-sensitive site in deproteinized *E. coli* 16S rRNA. (Recall that ricin A-chain is not toxic to intact *E. coli* ribosomes). The value for k_{cat} obtained by them was less by a factor of 400 than that obtained by Chen *et al.* (1998).

Further, in an earlier paper published by the Schramm laboratory (Link *et al.*, 1996) it was reported that in experiments with ricin A-chain reacting with a 10-mer RNA GAGA tetraloop, they were unable to measure catalytic turnover, and their observed product formation rate was four orders of magnitude less than that later reported in Chen *et al.* (1998). This was noted in Chen *et al.* (1998) with the comment that, “With small stem-loop RNA substrates, the reported catalytic rate is decreased by as much as 6 orders of magnitude [relative to native substrates] under the same conditions, and is highly dependent on assay conditions”. The differences in activities could, at least in part, arise from the fact that both Gluck *et al.* (1992) and Link *et al.* (1996) carried out their experiments at pH 7.5 rather than at the optimum pH 4.0 found later by Chen *et al.* for the A-10/ricin A-chain reaction.

The reaction conditions used in our exploratory initial velocity experiments were close to those used by Chen *et al.* (1998). However, since they reported only the overall ranges of the substrate and enzyme concentrations used in their experiments, but did not give any information on specific data points obtained from reactions with specified substrate and enzyme concentrations at a specified pH and for a specified reaction duration, it was not possible to duplicate their experiments in sufficient detail to isolate replication discrepancies.

To evaluate the likelihood of obtaining credible Michaelis-Menten parameters for the A-10/ricin A-chain catalytic reaction by trying other reaction conditions, it must be kept in mind that in Michaelis-Menten initial velocity experiments the choice of substrate and enzyme concentrations can not be made solely on the basis of experimental or financial

convenience. For successful analysis of the experimental data there are obligatory constraints, discussed above (see Methods), on the choice of substrate concentrations and substrate/enzyme concentration ratios. The experiments must be carried out under conditions in which the effects of binding and catalytic turnover on the overall substrate-to-product rate are about equal, and the range of substrate concentrations should cover a factor of ~ 10 (Reiner, 1969; Segel, 1988). At very high substrate concentrations, the overall substrate-to-product rate will be determined essentially by the rate of the catalytic mechanism, which means that the effects of binding parameters will be relatively small and difficult to discern experimentally. Similarly, at very low substrate concentrations, the overall substrate-to-product rate will be determined essentially by binding parameters and the effects of the catalytic mechanism will be obscured. Quantitatively, from the point of view of the Michaelis-Menten equation, these considerations translate into the requirement that S_0 be close to K_M . Thus, the set of substrate concentrations used in a Michaelis-Menten experiment should be designed to cover the range from ~ 0.3 to 3 times K_M . However, the available range of initial substrate concentrations was limited to $\sim 2 \mu\text{M}$ at the low end by the sensitivity threshold of the HPLC detector, and at the high end, to $\sim 20 \mu\text{M}$ by the cost of the A-10 substrate. This meant that Michaelis-Menten experiments might be successful only under conditions in which it turned out that $K_M \sim 6 \mu\text{M}$. The corresponding enzyme concentrations, which, as shown above, should satisfy the condition $S_0/E_0 > 10$, were also limited by constraints on the acceptable duration of the experiments being no more than ~ 3 hours to avoid or minimize possible problems with enzyme inactivation and other side effects. This left little room to experiment with other reaction

conditions, and effectively ruled out the advisability of searching for conditions conducive to obtaining credible Michaelis-Menten parameters for the A-10/ricin A-chain reaction with the available equipment. Moreover, even if such conditions were found for the A-10/ricin A-chain reaction, they could not be expected to be appropriate for experiments with maize-related enzymes which (as turned out to be the case) would probably be an order of magnitude less reactive than ricin A-chain. One consequence of a much lower reactivity of the maize-related enzymes would be that greater enzyme concentrations for given substrate concentrations would be required, and would result in experimental conditions in which the errors due to departures from the condition $S_0/E_0 > 10$ would no longer be negligible.

Thus, it became clear that the initial objective of developing a quantitative assay based on determination of the Michaelis-Menten parameters K_M and k_{cat} for ricin A-chain and maizeRIP1 reacting with RNA oligoribonucleotides using initial velocity experiments was not feasible with the available equipment and resources. Therefore, the initial research goals were redirected.

Timecourse experiments

An alternative to initial velocity experiments for studies of enzyme kinetics is the use of timecourse experiments, which involve measuring the substrate diminution or product accumulation as a function of time during an enzyme-substrate reaction, usually through a time period in which the extent of reaction reaches ~ 60 -80%. Data from timecourse experiments can be used in conjunction with an integrated form of the Michaelis-Menten

equation, either through double reciprocal forms of the integrated equation (Orsi and Tipton, 1979) or through direct curve fitting, to attempt to obtain the Michaelis-Menten parameters K_M and k_{cat} . It must be kept in mind, however, that the use of the integrated form to obtain Michaelis-Menten parameters is meaningful only to the extent that the assumptions essential to the derivation of the underlying Michaelis-Menten equation are satisfied. If the timecourse experiments do not yield quantitative Michaelis-Menten parameters K_M and k_{cat} , the timecourse data can still be used to carry out semiquantitative analyses to characterize and compare enzymatic activities of different enzyme/substrate reactions.

Therefore, our research goals were modified to include comparisons of the magnitudes and pH dependencies of the RNA glycosidase activities of ricin A-chain, maizeRIP1, MOD1, and MOD1X (see Fig. 2-1) reacting with the RNA oligoribonucleotide GAGA tetraloop A-10. Later, when it was discovered, unexpectedly, that maize rproRIP1 may be catalytically active with respect to A-10, it was included among the enzymes whose activities were being compared.

Timecourse (also called “progress curve”) experiments are not as widely used as Michaelis-Menten initial velocity experiments for kinetic studies of enzyme reactions. There is a much smaller, but still sizeable, literature on the design and analysis of timecourse experiments and the advantages and disadvantages of their use as an alternative (or complement) to initial velocity experiments. Orsi and Tipton (1979) derived integrated forms of the Michaelis-Menten equation for reactions involving competitive inhibition, uncompetitive inhibition, mixed and noncompetitive inhibition, substrate inhibition and

competitive and uncompetitive product inhibition. Among the advantages of timecourses, Stayton and Fromm (1979) note that there is more information on a reaction over its entire time course as compared with its initial velocity. Thus, a reduced number of experiments are necessary to determine kinetic constants. Timecourse experiments are especially advantageous when the concentration of the product can be continuously monitored, because kinetic parameters could then be determined from a single experiment (Atkins and Nimmo, 1973). Some disadvantages of timecourse experiments are: i) data analysis is more complex (Duggleby, 1995), ii) because of the relatively long duration of experiments, instrument drift and enzyme inactivation are more possible (Orsi and Tipton, 1979), iii) there is more possibility of significant effects of product inhibition as product concentration increases, and iv) substrates and products have more of a chance to undergo uncatalyzed side reactions (Duggleby, 1995). Cornish-Bowden (1975) noted that small errors in assumed values of experimental parameters, especially the assumption that the product concentration asymptotically approaches the initial substrate concentration, may lead to large errors in the estimated values of K_M and V_{max} . He recommended that integrated rate equations should not be used for direct evaluation of enzyme kinetic parameters, but should be used to obtain more accurate values of the initial velocity than are available from simple methods.

Atkins and Nimmo (1973) simulated progress curves for a reaction obeying Michaelis-Menten kinetics. Values for K_M and V_{max} were estimated by fitting the simulated progress curves to the integrated Michaelis-Menten equation. They could not obtain fits with non-linear least-squares methods, but found that a transformed form of the equation could be

fitted by a linear method. When S_0 was greater than K_M , the estimates using the timecourse methods were as good as those derived from initial velocity experiments, and were based on fewer experiments, but when S_0 was not greater than K_M , the estimates were too low. This is consistent with an analytic and simulation study by Duggleby and Clarke (1991) on error minimization in which they found that for timecourse experiments, the starting substrate concentration S_0 should be 2-3 times K_M .

Bartha (1980) showed that in timecourse analyses, the effect of errors due to the steady-state approximation (the assumption that the concentration of the substrate-enzyme complex remains constant during the course of the experiment) were minimal when the enzyme concentration was one or two orders of magnitude lower than the lowest substrate concentration detected.

In summary, timecourse experiments, as compared to Michaelis-Menten initial velocity experiments, are more economical in that they can yield more information from a given amount of reaction materials. However, analysis of the data to get reactivity parameters involves more complex and indirect calculations, and the resulting parameter values are more sensitive to variations in initial conditions.

Summary of all the timecourse and high S_0 experiments reported herein: Overall, the experiments reported here consisted mostly of measurements of the concentrations of adenine released as a function of time during A-10/enzyme reactions over a range of pH values for five enzymes (ricin A-chain, maizeRIP1, MOD1, MOD1X, and rproRIP1), and also, some initial velocity experiments with high substrate concentrations to attempt to get direct estimates of k_{cat} . To facilitate the use of the timecourse results for semiquantitative

comparisons of the reactivities of the various enzymes, reaction conditions were kept as uniform as possible over the range of experiments. All the timecourse experiments used for comparison of the reactivities of the different enzymes were done with A-10 concentration of 10 μ M and at 30 °C. One set of experiments was carried out at 20 °C to investigate the possible relevance of A-10 hairpin instability at low pH. Experiments were carried out over a pH range from 3.0 to 6.0, although not all of the enzymes were measured over the entire pH range. A comprehensive tabulation of the experimental conditions, both timecourse and high S_0 , is presented in Table 7-1.

Repeatability statistics for reactions with maize-derived enzymes were determined for maizeRIP1 through six timecourse experiments with [maizeRIP1] = 0.5 μ M at pH 4.0, and for MOD1 through four experiments with [MOD1] = 1.0 μ M, also at pH 4.0. These repeatability statistics were assumed to be typical for all the maize-derived enzymes over the experimental range of pH values, so that at most other enzyme/pH combinations, it was considered sufficient to perform only one timecourse experiment. This assumption was supplemented by looking at the internal consistency of all trends.

Timecourse experiments for five enzymes over a range of pH at 30 °C. In this Section, the direct experimental results will be presented. The analysis, discussion, and conclusions will be given in Chap. 8.

Six repetitions of an A-10/maizeRIP1 timecourse experiment are shown in Fig. 7-2(A). The experimental conditions were: [A-10] = 10.0 μ M, [maizeRIP1] = 0.5 μ M, at pH 4.0. This group of repeated experiments is one of two such groups used to establish typical statistics for reactions of maize-derived enzymes with the RNA oligo tetraloop A-10. The

statistical mean and SEM (Standard Error of the Mean) for these six A-10/maizeRIP1 timecourse experiments are shown in Fig. 7-2(B).

To determine the extent to which enzyme reactivities are proportional to enzyme concentration within the range of enzyme concentrations used in our experiments, two repetitions of an A-10/maizeRIP1 timecourse experiment similar to those shown in Fig. 7-2(A), except with $[\text{maizeRIP1}] = 1.0 \mu\text{M}$ rather than $0.5 \mu\text{M}$ were performed, all other conditions being the same. Fig. 7-3(A) is a superposition of the two A-10/maizeRIP1 timecourse experiments with $[\text{maizeRIP1}] = 1.0 \mu\text{M}$ and of the statistical mean of the six A-10/maizeRIP1 timecourse experiments with $[\text{maizeRIP1}] = 0.5 \mu\text{M}$ (shown in Fig. 7-2(B)). Note that the ordinate in Fig. 7-3(A) is the ratio $[\text{ade}]/E_0$ rather than $[\text{ade}]$. These results confirm that the enzyme reactivities scale linearly with respect to the enzyme concentration. Therefore, results of experiments at different enzyme concentrations can be compared by using the ratio of released adenine divided by enzyme concentration as the measure of enzyme activity. The statistical mean and SEM with respect to the ratio $[\text{ade}]/E_0$ for the combined eight timecourse experiments with $[\text{maizeRIP1}] = 0.5$ and 1.0 are shown in Figure 7-3(B).

The foregoing timecourse experiments (Figs. 7-2 and 7-3) were all concerned with A-10/maizeRIP1 activity at one pH (pH 4.0), and were carried out repetitively to measure repeatability (SEM) and scalability with respect to enzyme concentration. The effect of pH on A-10/maizeRIP1 activity is shown in Fig. 7-4.

Fig. 7-5 shows four repetitions of an A-10/MOD1 (for a description of MOD1, see Chapter 2, Deletion mutants, and Fig. 2-1) timecourse experiment at pH 4.0 to establish

repeatability statistics analogous to those obtained above for the A-10/maizeRIP1 reaction. The four repetitions are shown in Fig. 7-5(A), and the statistical mean and SEM for these four experiments are shown in Fig. 7-5(B). The effect of pH on A-10/MOD1 activity is shown in Fig. 7-6. At pH values for which there were repeated experiments, the means and SEMs are shown. Note that the enzyme concentration was the same ($[\text{MOD1}] = 1.0 \mu\text{M}$) in all of these experiments. As a result, there was no need to take scaling into account, and the ordinate in the plots is free adenine concentration rather than the $[\text{ade}]/E_0$ concentration ratio.

The results of timecourse experiments with the A-10/ricin A-chain reaction at two pH values are shown in Fig. 7-7. The results of three experiments at pH 4.0 and two experiments at pH 4.5, and the corresponding statistics are shown. The experimental conditions were $[\text{A-10}] = 10.0 \mu\text{M}$ and $[\text{ricin A-chain}] = 0.05 \mu\text{M}$. These experiments were carried out for comparison with the results of Chen *et al.* (1998) in the neighborhood of the optimum pH reported by them. Note that the ricin A-chain concentration required to yield an extent of reaction ~60-80% during a 3 hr experiment is much less than that required for maizeRIP1 and MOD1.

The timecourse experiments with MOD1X (for a description of MOD1X, see Chapter 2, Deletion mutants, and Fig. 2-1) were not designed to cover a broad range of pH values as with the other enzymes, but rather, were intended to provide a comparison with maizeRIP1 limited to the neighborhood of the optimal pH for the A-10/maizeRIP1 reaction. Fig. 7-8 shows the results of two A-10/MOD1X timecourses, at pH 4.7 and pH 4.9. The experimental conditions were: $[\text{A-10}] = 10.0 \mu\text{M}$ and $[\text{MOD1X}] = 0.1 \mu\text{M}$ for

both timecourses.

Timecourse experiments with the A-10/rproRIP1 reaction were initially carried out only to “confirm” that there was essentially no A-10/rproRIP1 catalytic activity. Significant catalytic activity was not expected, since mammalian ribosome/proRIP interactions reported in the literature have resulted in only very little or no catalytic activity (Walsh *et al.*, 1991; Hey *et al.*, 1995; Krawetz, 1998). Unexpectedly, exploratory experiments at pH 4.0 showed significant A-10/rproRIP1 catalytic activity, which could not be definitely attributed to some low level of autonomously generated maizeRIP1 being present in the proRIP1 stock. In Fig. 5-1, lanes 2 and 3, there is no indication of the presence of the maizeRIP1 dimer, which dissociates in the denaturing SDS-PAGE gel into 16.5 and 8.5 kDa components as seen in the maizeRIP1 lane 4. There is a faint band visible in both rproRIP1 lanes at a position with a molecular weight somewhat lower than MOD1 and higher than MOD1X. However, it was considered very unlikely that a covalently bound species similar to MOD1 or MOD1X could be formed autonomously during rproRIP1 expression, purification, or storage. Therefore, a set of timecourse experiments to measure the A-10/rproRIP1 activity was carried out over the same range of pH values used with maizeRIP1 and MOD1. The results are shown in Fig. 7-9. The experimental conditions were: [A-10] = 10.0 μ M and [maize rproRIP1] = 1.0 μ M for all timecourses. The possibility that there may be significant A-10/rproRIP1 catalytic activity is one of the most interesting results of this study.

Timecourse experiments with one enzyme over a range of pH at 20 °C. The observed decrease in enzyme activity at low pH for all of the enzymes studied here might be due, at

least in part, to A-10 substrate instability at low pH at the experimental temperature of 30 °C. As seen in the T_m versus pH UV-melting experiments (Fig. 6-1), the T_m at pH 4.0 is equal to the experimental temperature of 30 °C, and at pH values less than 4.0, the T_m is less than the experimental temperature. The possible effect of A-10 substrate instability at low pH at 30 °C can be evaluated by carrying out timecourse experiments at 20 °C to compare with those at 30 °C. Fig. 7-10 shows the adenine released as a function of time for A-10/MOD1 timecourse experiments at 20 °C and at pH values of 3.4, 3.8, 4.4, 4.6, 4.8, 5.3, and 5.8. The experimental substrate and enzyme concentrations were the same as were used in the experiments at 30 °C: $[A-10] = 10.0 \mu\text{M}$ and $[MOD1] = 1.0 \mu\text{M}$. These results are analyzed and discussed in Chap. 8, p. 91, “Comparison of A-10/MOD1 activity at 20 °C and 30 °C”.

Initial velocity experiments with high S_0 . Plots of initial velocity experiments in which the substrate concentration is much higher or much lower than K_M can be used directly to obtain estimates of k_{cat} or k_{cat}/K_M , respectively (see Chap. 8). Not knowing in advance what the values of K_M might be for the maizeRIP1 related enzymes, but keeping in mind that for ricin A-chain, Chen *et al.* (1998) found that K_M was in the range 0.2 to 50 μM over the range of pH from 3.0 to 5.0 (Fig. 2 therein), initial velocity experiments were carried out over a pH range from 4.0 to 5.5 at the highest affordable A-10 concentrations, namely, $[A-10] = 30$ and $60 \mu\text{M}$, with the enzymes ricin A-chain, maizeRIP1, and MOD1. It turned out that at these values of S_0 , for ricin A-chain, $S_0 \ll K_M$; for maizeRIP1, $S_0 \gg K_M$; and for MOD1, $S_0 \approx K_M$ at all values of pH in the sets of experiments.

Fig. 7-11 shows the results of high A-10 concentration A-10/ricin A-chain initial

velocity experiments at pH 4.0, 4.3, 4.9, and 5.5. The experimental conditions were $[A-10] = 30$ and $60 \mu\text{M}$, and $[\text{ricin A-chain}] = 0.2 \mu\text{M}$. Also shown in this Figure are linear fits to the data at each of the experimental values of pH indicating that $S_0 \ll K_M$ at each pH. These results are used in Chap. 8 to obtain direct estimates of k_{cat}/K_M for ricin A-chain.

Fig. 7-12 shows the results of high A-10 concentration A-10/maizeRIP1 initial velocity experiments at pH 4.0, 4.3, 4.9, and 5.4. The experimental conditions were: at pH 4.0, $[A-10] = 30$ and $60 \mu\text{M}$, and $[\text{maizeRIP1}] = 1.0 \mu\text{M}$; at pH 4.3, $[A-10] = 30$ and $60 \mu\text{M}$, and $[\text{maizeRIP1}] = 1.0 \mu\text{M}$; at pH 4.9, $[A-10] = 30$ and $60 \mu\text{M}$, and $[\text{maizeRIP1}] = 0.8 \mu\text{M}$; at pH 5.4, $[A-10] = 30$ and $60 \mu\text{M}$, and $[\text{maizeRIP1}] = 0.8 \mu\text{M}$, and also $[A-10] = 36 \mu\text{M}$, and $[\text{maizeRIP1}] = 0.98 \mu\text{M}$. In this case (maizeRIP1), the data can be fit at each pH by a line of constant v_i/E_0 , indicating that $S_0 \gg K_M$ at each pH. These results are used in Chap. 8 to obtain direct estimates of k_{cat} for maizeRIP1.

Fig. 7-13 shows the results of high A-10 concentration A-10/MOD1 initial velocity experiments at pH 4.0, 4.3, 4.8, and 5.2. The experimental conditions were $[A-10] = 30$ and $60 \mu\text{M}$, and $[\text{MOD1}] = 2.0 \mu\text{M}$. The data can not be approximated either by linear fits or by constants, indicating that $S_0 \approx K_M$ at each pH.

Table 7-1. Distribution of All Timecourse and High Substrate Concentration Experiments^a

Timecourse Experiments

Enzyme		[A-10] (μM)	Temp (°C)	Nominal pH							
Type	E ₀ (μM)			3.0	3.5	4.0	4.5	4.75	5.0	5.5	6.0
ricin A-chain	0.05	10.0	30.0			3	2				
maizeRIP1	0.1	10.0	30.0				1		2	1	
	0.5	10.0	30.0			6					
	1.0	10.0	30.0	1	1	2					
MOD1	1.0	10.0	30.0	1	1	4	1		1	2	2
	1.0	10.0	20.0		1	1	1	1	1	1	1
MOD1X	0.1	10.0	30.0					1	1		
rproRIP1	1.0	10.0	30.0			1	1		1	1	1

High Substrate Concentration Experiments

ricin A-chain	0.2	30.0	30.0			1	1		1	1	
maizeRIP1	1.0	30.0	30.0			1	1				
	1.0	60.0	30.0			1	1				
	1.0	36.6	30.0							1	
	0.8	30.0	30.0						1	1	
	0.8	60.0	30.0						1	1	
MOD1	2.0	30.0	30.0			1	1		1	1	
	2.0	60.0	30.0			1	1		1	1	

^a The table shows, for each enzyme, the set of concentrations, pHs, and incubation temperatures at which experiments were performed, and the number of repeated experiments at each concentration-pH combination. The pH values are labeled “Nominal pH” because they serve as group headings. The actual pH values in most of the experiments differ slightly from the nominal values. The true pH values are given in the Figures and Tables in which experimental results are presented.

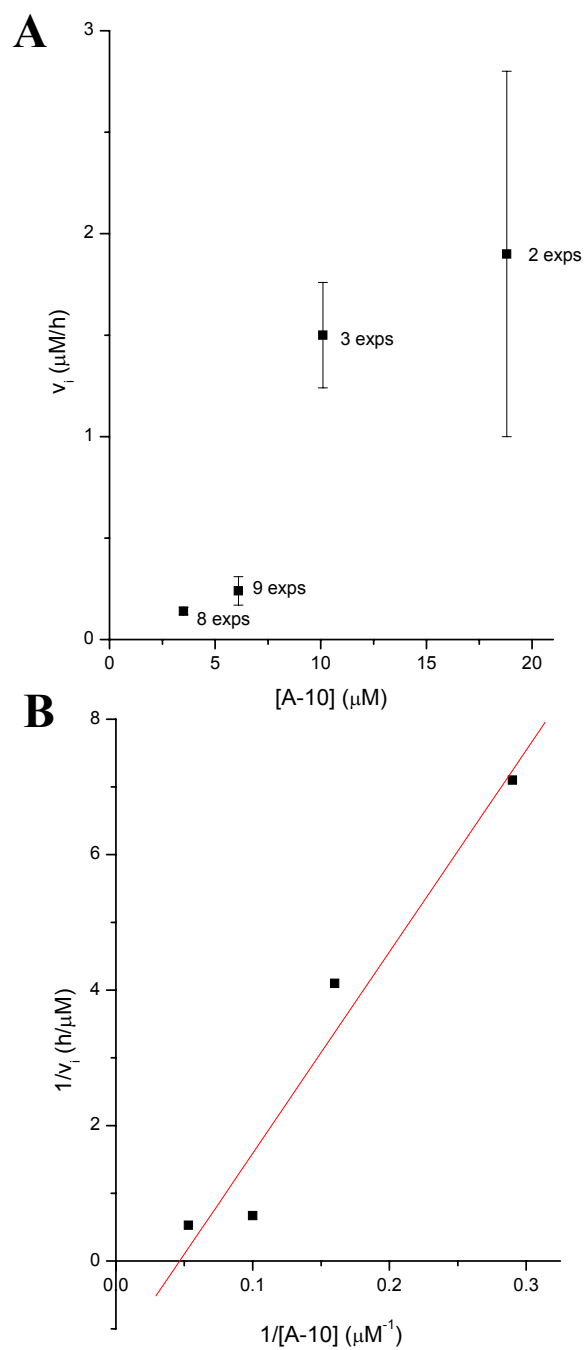


Figure 7-1. Michaelis-Menten initial velocity experiments with A-10/ricin A-chain. **(A)** Initial velocity of product (adenine) formation versus initial substrate (A-10) concentration. **(B)** Double-reciprocal Lineweaver-Burk plot for determination of the parameters K_M and k_{cat} .

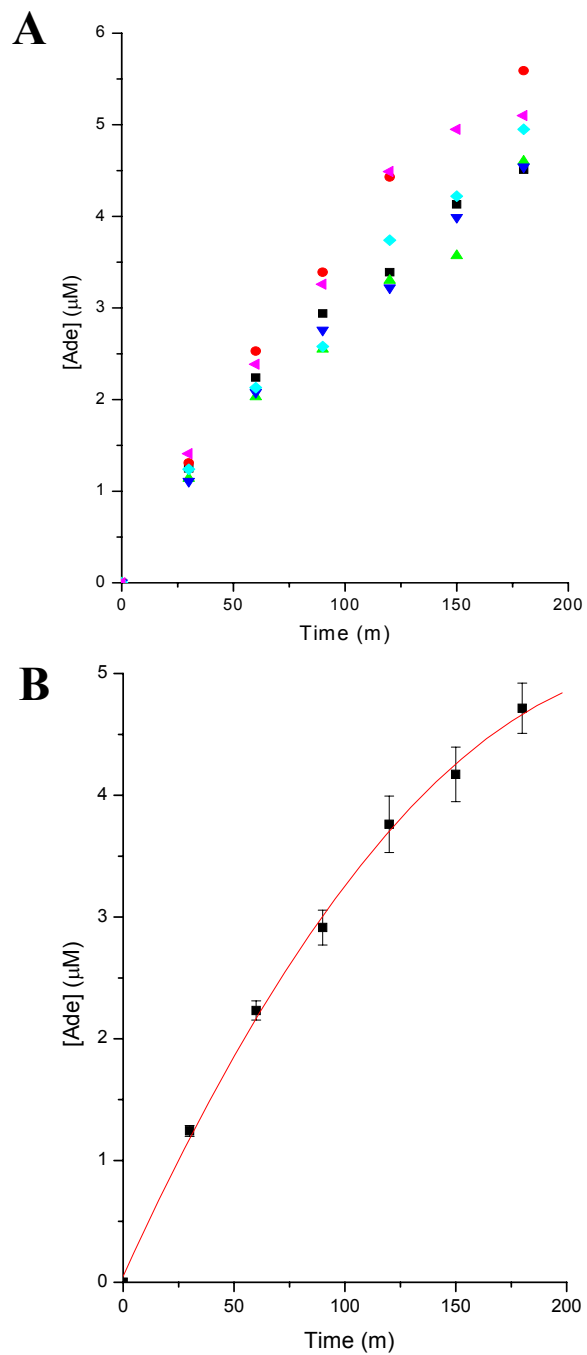


Figure 7-2. Six repetitions of an A-10/maizeRIP1 timecourse experiment showing the enzymatic release of adenine from the RNA hairpin A-10 catalyzed by maizeRIP1. The experimental conditions were: [A-10] = 10.0 μM , [maizeRIP1] = 0.5 μM , at pH 4.0. **(A)** Timecourse data for the six repetitions. **(B)** Statistical means and SEMs for the six repetitions. The trend line in **(B)** is a second order polynomial fit.

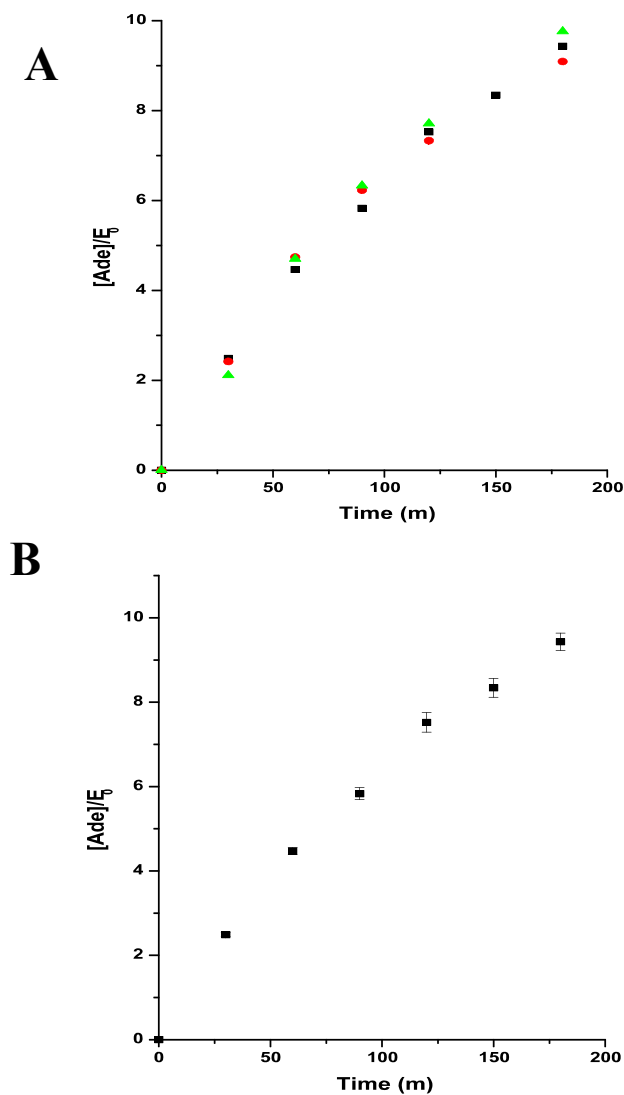


Figure 7-3. Example of linear scaling of A-10/maizeRIP1 reactivity with respect to the enzyme concentration E_0 . **(A)** The ratio $[Ade]/E_0$ for the mean of the six $[A-10] = 10.0 \mu\text{M}$, $[\text{maizeRIP1}] = 0.5 \mu\text{M}$, pH 4.0 timecourses shown in Fig. 7-2B (■), and for two timecourse experiments with $[A-10] = 10.0 \mu\text{M}$, $[\text{maizeRIP1}] = 1.0 \mu\text{M}$, pH 4.0 (●, ▲). **(B)** The statistical mean and SEM with respect to the ratio $[Ade]/E_0$ for the combined six timecourses at $[\text{maizeRIP1}] = 0.5 \mu\text{M}$ and two timecourses at $[\text{maizeRIP1}] = 1.0 \mu\text{M}$.

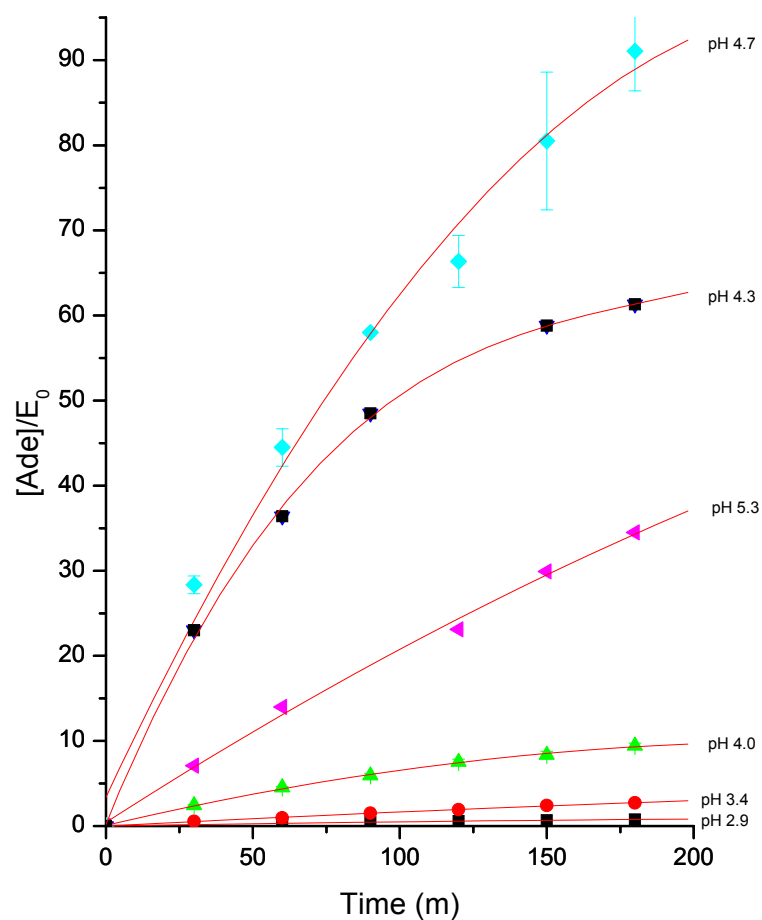


Figure 7-4. Effect of pH on A-10/maizeRIP1 activity. The experimental conditions were: [A-10] = 10.0 μ M for all timecourses; for pH 2.9 (■) and pH 3.4 (●), [maizeRIP1] = 1.0 μ M; for pH 4.0 (▲) the mean and SEM from Fig. 7-2B is shown; for pH 4.3 (▼), pH 4.7 (◆), and pH 5.3 (◄), [maizeRIP1] = 0.1 μ M. Note that for pH 4.7, the mean and SEM of two timecourses are shown. The trend lines are second order polynomial fits except for pH 4.3 where it is a third order polynomial fit.

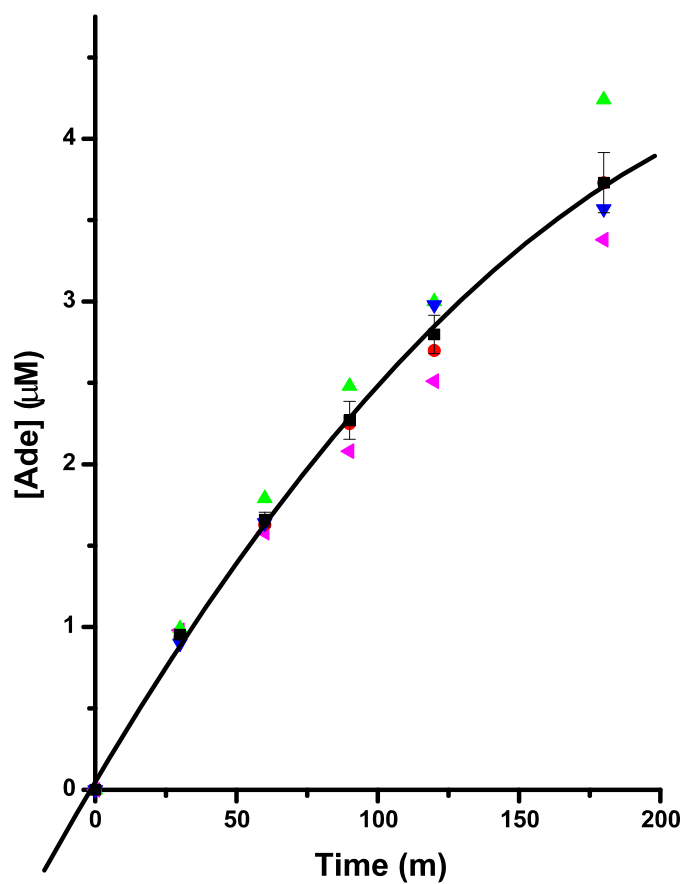


Figure 7-5. Four repetitions and its statistical mean and SEM of an A-10/MOD1 timecourse experiment showing the enzymatic release of adenine from the RNA hairpin A-10 catalyzed by MOD1. The experimental conditions were: $[A-10] = 10.0 \mu\text{M}$, $[MOD1] = 1.0 \mu\text{M}$, and pH 4.0. The mean is indicated by the symbol (■). The trend line is a second order polynomial fit to the mean.

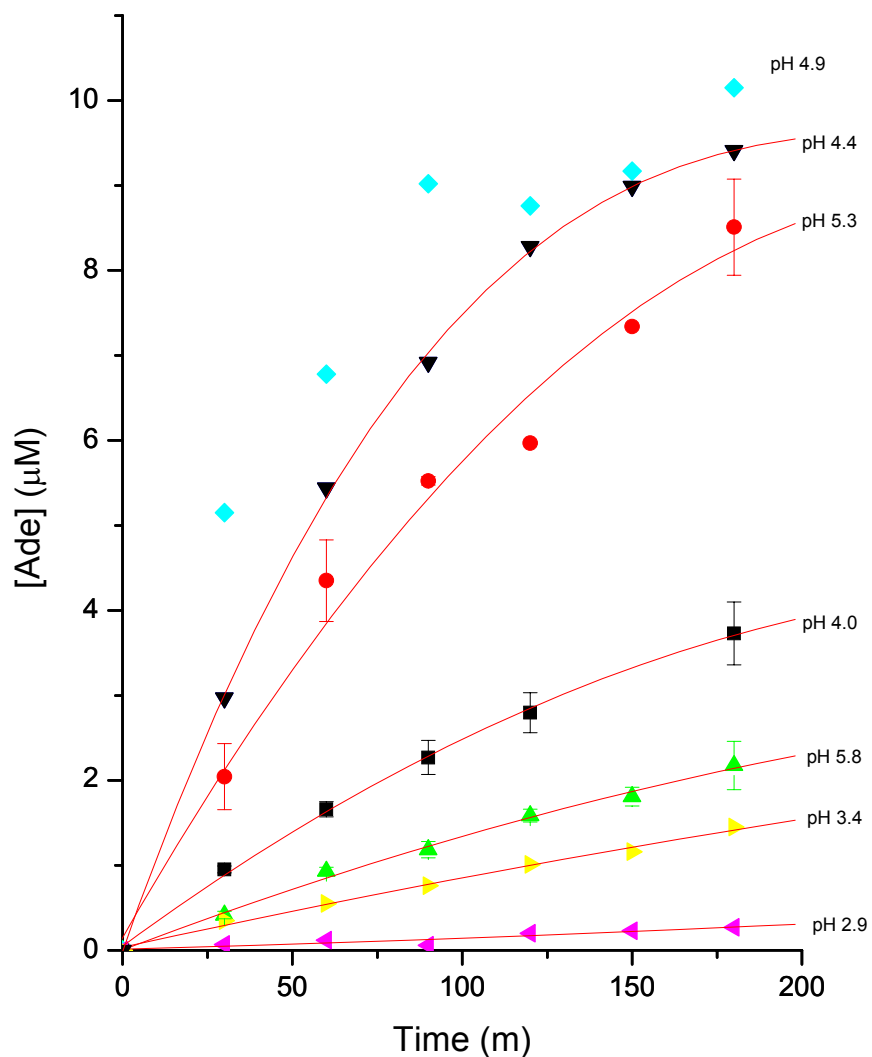


Figure 7-6. Effect of pH on A-10/MOD1 activity. The experimental conditions were: $[A-10] = 10.0 \mu\text{M}$ and $[MOD1] = 1.0 \mu\text{M}$ for all timecourses. Results are shown for pH 2.9 (\blacktriangleleft), pH 3.4 (\blacktriangleright), the mean and SEM of four experiments at pH 4.0 (\blacksquare), pH 4.4 (\blacktriangledown), pH 4.9 (\blacklozenge), the mean and SEM of two experiments at pH 5.3 (\bullet), and the mean and SEM of two experiments pH 5.8 (\blacktriangle). The trend lines are second order polynomial fits except for pH 4.4 where it is a third order polynomial fit. An appropriate trend line using polynomial fits could not be obtained for pH 4.9.

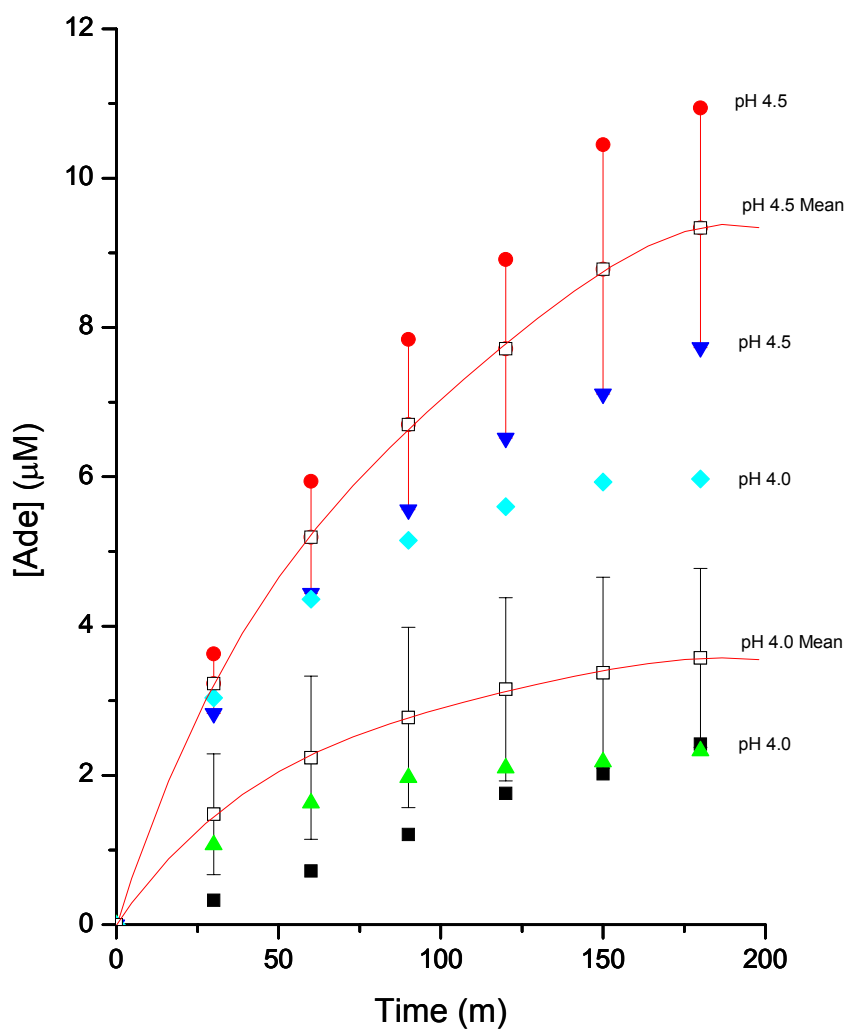


Figure 7-7. Timecourses, statistical means and SEMs for the A-10/ ricin A-chain reaction at pH 4.0 (■, ▲, ◆) and 4.5 (●, ▼). The experimental conditions were [A-10] = 10.0 μM and [ricin A-chain] = 0.05 μM. The trend lines for the means (□) are second order polynomial fits.

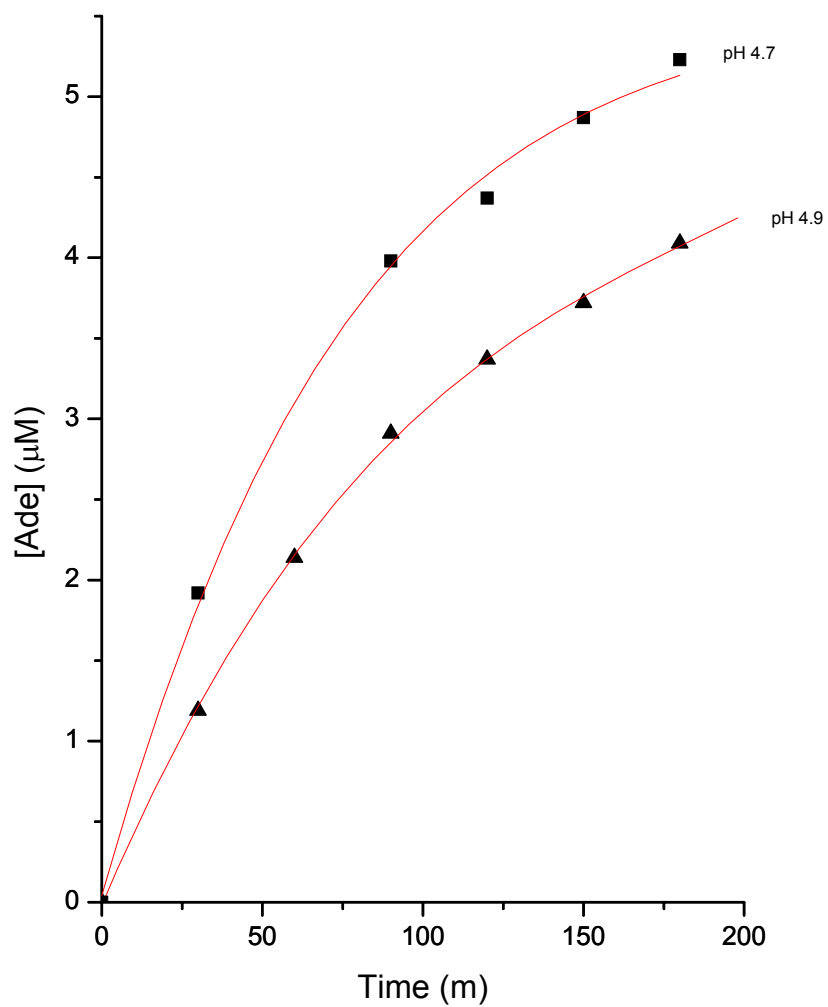


Figure 7-8. A-10/MOD1X reaction timecourses for pH 4.7 (■) and pH 4.9 (▲). The experimental conditions were $[A-10] = 10.0 \mu\text{M}$ and $[\text{MOD1X}] = 0.1 \mu\text{M}$. The trend lines for pH 4.9 and pH 4.7 are a third order polynomial fit and a sigmoidal fit, respectively.

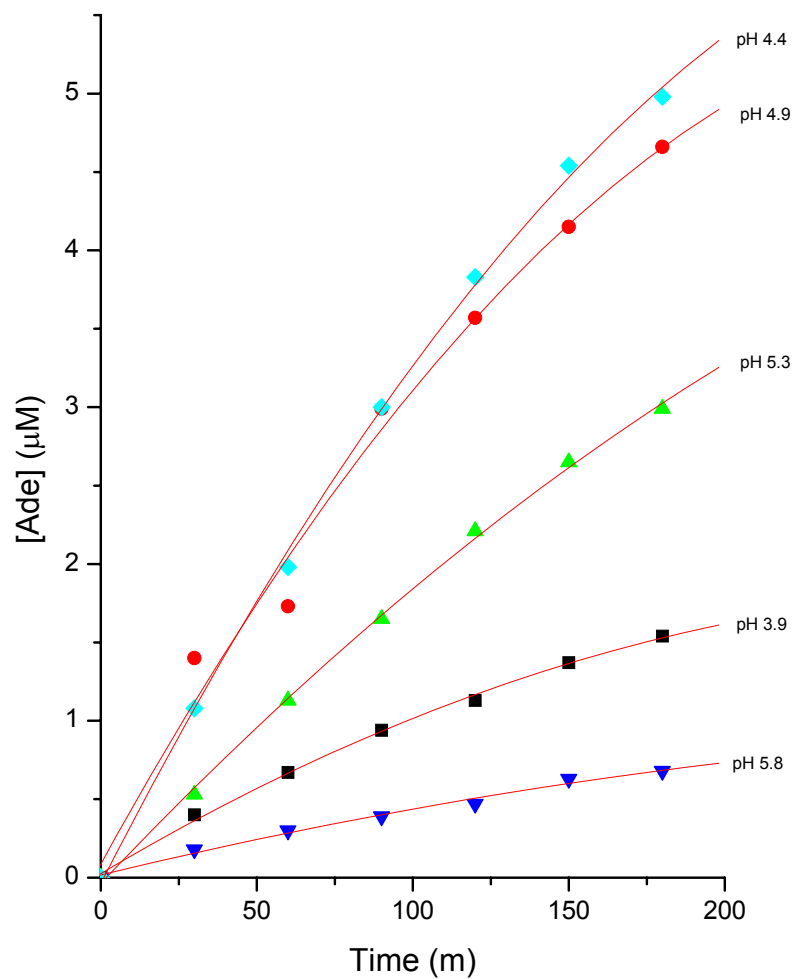


Figure 7-9. Effect of pH on A-10/maize rproRIP1 activity. The experimental conditions were: [A-10] = 10.0 μ M and [maize-rproRIP1] = 1.0 μ M for all timecourses. Results are shown for pH 3.9 (■), pH 4.4 (◆), pH 4.9 (●), pH 5.3 (▲), and pH 5.8 (▼). All the trend lines are second order polynomial fits.

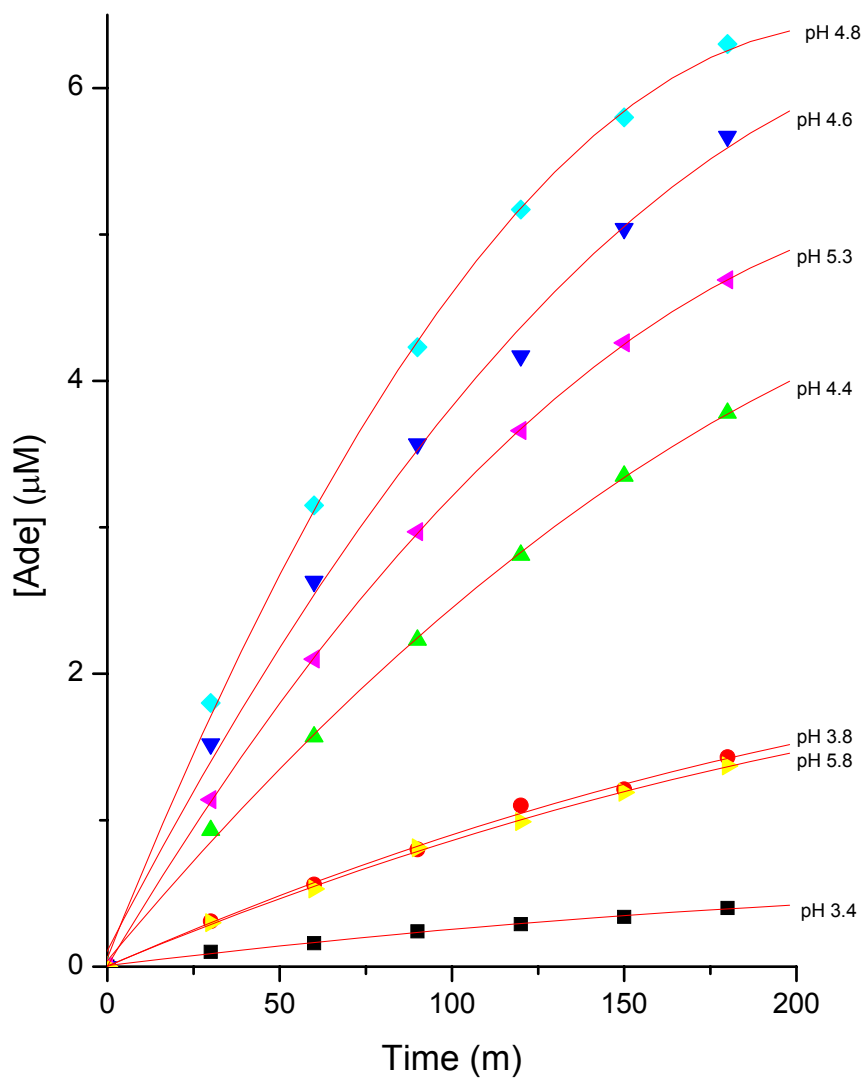


Figure 7-10. Effect of pH on A-10/MOD1 activity at 20 °C. The experimental conditions were: [A-10] = 10.0 μ M and [MOD1] = 1.0 μ M for all timecourses. Results are shown for pH 3.4 (■), pH 3.8 (●), pH 4.4 (▲), pH 4.6 (▼), pH 4.8 (◆), pH 5.3 (◄), and pH 5.8 (►). All the trend lines are second order polynomial fits.

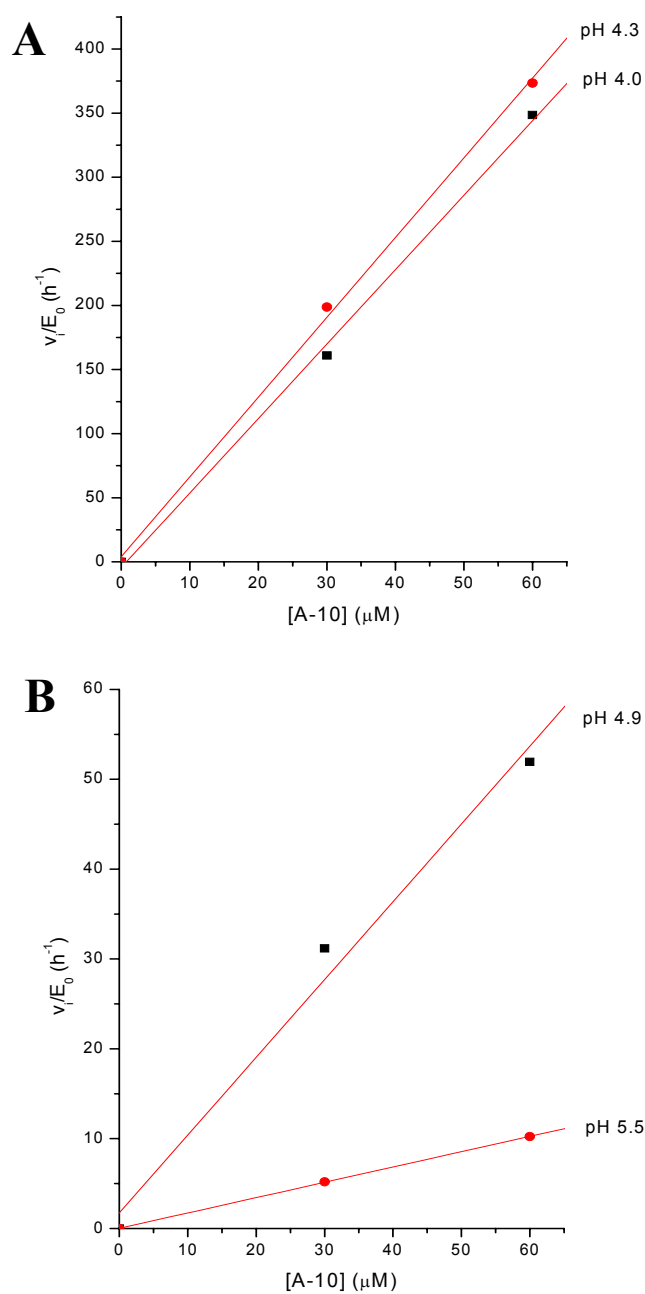


Figure 7-11. Linear fitting to high A-10 concentration A-10/ricin A-chain initial velocity experiments. The experimental conditions were $[A-10] = 30$ and $60 \mu\text{M}$, and $[\text{ricin A-chain}] = 0.2 \mu\text{M}$. The fitting parameters are A and B, in the equation for the line $v_i/E_0 = A + B[A-10]$. **(A)** pH 4.0 (■): $A = -4. \pm 10.$, $B = 5.8 \pm 0.3$; pH 4.3 (●): $A = 4. \pm 9.$, $B = 6.2 \pm 0.2$. **(B)** pH 4.9 (■): $A = 2. \pm 4.$, $B = 0.87 \pm 0.10$; pH 5.5 (●): $A = 0.03 \pm 0.06$, $B = 0.17 \pm 0.$

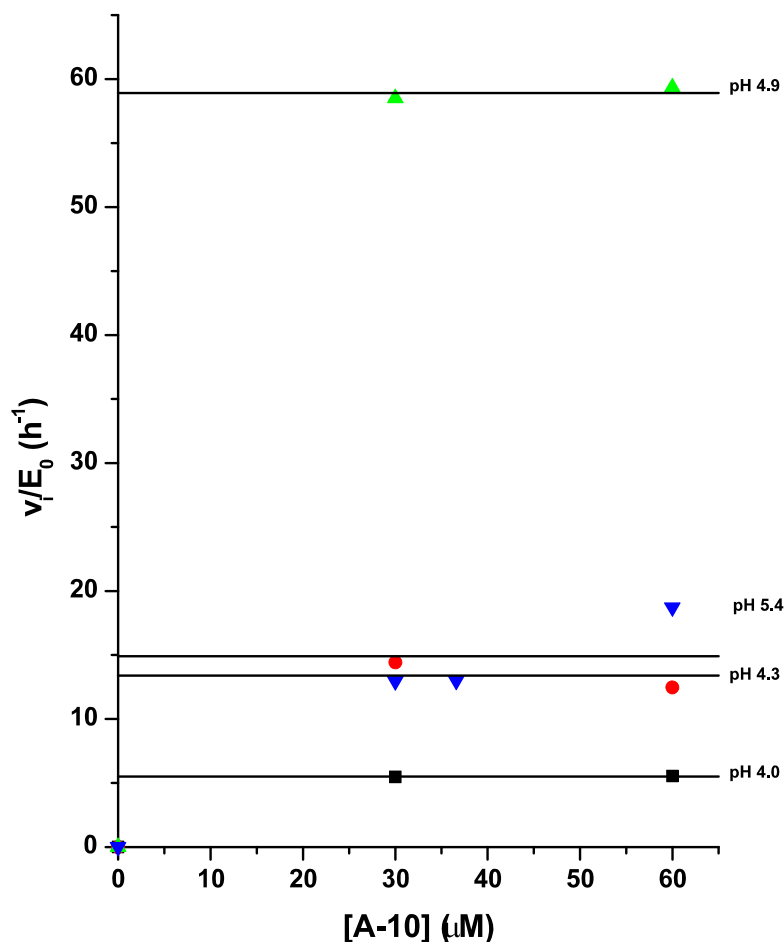


Figure 7-12. The results of high A-10 concentration A-10/maizeRIP1 initial velocity experiments at pH 4.0 (■), pH 4.3 (●), pH 4.9 (▲), and pH 5.4 (▼). The experimental conditions were: at pH 4.0 and 4.3, [A-10] = 30 and 60 μM, and [maizeRIP1] = 1.0 μM; at pH 4.9, [A-10] = 30 and 60 μM, and [maizeRIP1] = 0.8 μM; and at pH 5.4, [A-10] = 30 and 60 μM, and [maizeRIP1] = 0.8 μM, and for a third data point [A-10] = 36 μM, and [maizeRIP1] = 0.98 μM.

Lines of constant v_i/E_0 representing the average for each pH, are shown superimposed on the results of the high substrate concentration A-10/maizeRIP1 initial velocity experiments to estimate corresponding values of k_{cat} . The values obtained for v_i/E_0 were 5.5, 13.4, 58.9, and 14.9 for pH 4.0, 4.3, 4.9, and 5.4, respectively.

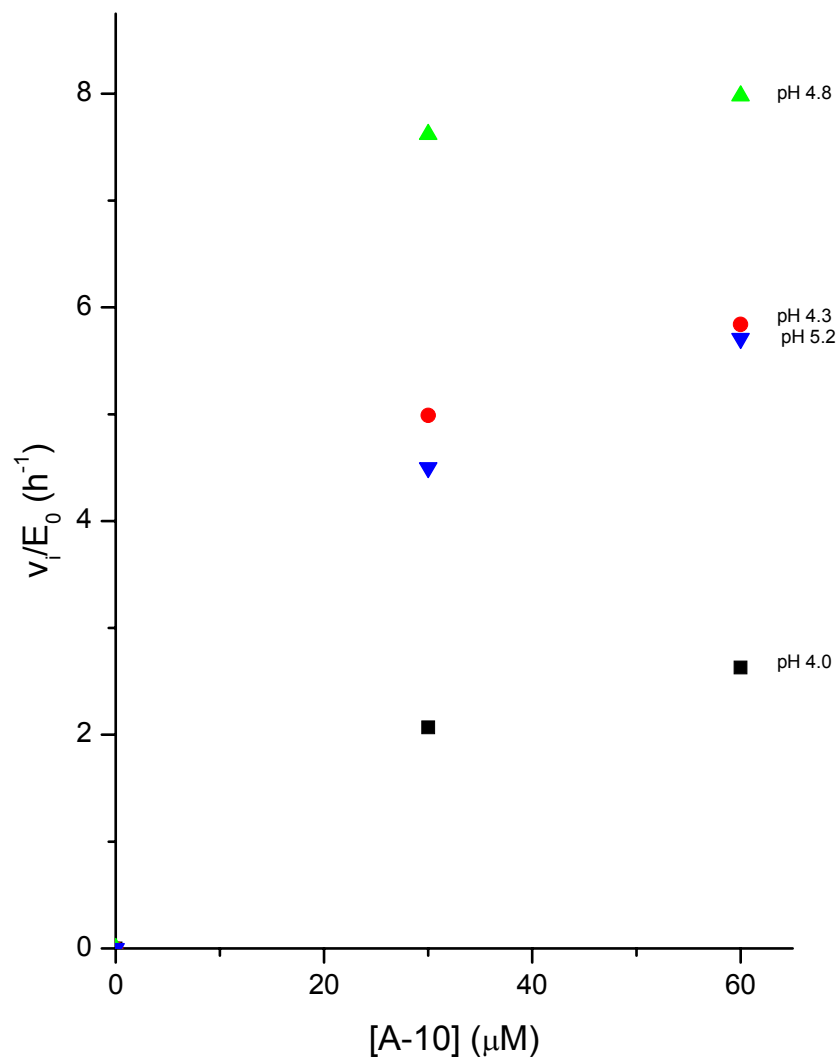


Figure 7-13. The results of high A-10 concentration A-10/MOD1 initial velocity experiments at pH 4.0 (\blacksquare), pH 4.3 (\bullet), pH 4.8 (\blacktriangle), and pH 5.2 (\blacktriangledown). The experimental conditions were $[\text{A-10}] = 30$ and $60 \mu\text{M}$, and $[\text{MOD1}] = 2.0 \mu\text{M}$. Note that v_i/E_0 as a function of $[\text{A-10}]$ is neither linear, as in Figure 7-10, allowing an estimate of k_{cat}/K_M at each pH, nor constant, as in Figure 7-11, allowing an estimate of k_{cat} at each pH.

CHAPTER 8. ANALYSIS, DISCUSSION, AND CONCLUSIONS

Attempts to obtain Michaelis-Menten parameters K_M and k_{cat} by double reciprocal plots, or direct curve fitting of the Michaelis-Menten equation to initial velocity versus substrate concentration data, or by curve fitting the integrated Michaelis-Menten equation to timecourse data, were unsuccessful. The initial velocity double reciprocal plots typically yielded negative values for V_{max} (and hence k_{cat}). The attempts to determine the Michaelis-Menten parameters K_M and k_{cat} by curve fitting the integrated Michaelis-Menten equation to timecourse data were not credible. A very close fit to the data could be obtained ($R > 0.99$), but the parameter values given by the fit were not unique. The error ranges reported by the fitting program were large relative to the fitted parameter values, and different initial values assigned to the variables (K_M , V_{max} , and sometimes S_0) would give different values for the parameters.

Although credible values of the Michaelis-Menten parameters K_M and k_{cat} for any of the five enzymes could not be obtained directly from the experimental timecourse data, it was possible to extract several kinds of useful comparisons among the enzymes from the timecourse data and the high substrate concentration experiments. Firstly, a meaningful comparison of the enzymatic activities of the five enzymes was obtained from initial velocity calculations using the first measurements (at 30 minutes after initiation of the reaction) made during timecourse experiments. Secondly, some of the results of the high substrate concentration experiments could be used to obtain quantitative estimates of k_{cat}/K_M for ricin A-chain, and of k_{cat} (or V_{max}) for maizeRIP1. Thirdly, where values of V_{max} were obtained from high substrate concentration experiments, they could then be used as

fixed parameters during curve fitting calculations, making it possible to get corresponding values of K_M by curve fitting the integrated Michaelis-Menten equation to the corresponding timecourse data.

In what follows in this Section, estimates of Michaelis-Menten parameters are referred to as pseudo K_M and k_{cat} to emphasize that these parameters could not be obtained from the experimental data by the usual analytic methods (double reciprocal plots of initial velocity data, or curve fitting of the integrated Michaelis-Menten equation to timecourse data). However, the simple Michaelis-Menten equation, even if not rigorously applicable, is probably a reasonable approximation to the actual description of both the high substrate concentration initial velocity and the timecourse data. The parameter values estimated on this basis can serve as comparative values among the five enzymes in the experiments, as well as for comparison to relevant results in the literature.

Comparison of enzyme activities [$\log(v_i/E_0)$ versus pH] at 30 °C using initial velocities from the timecourse experiments.

The initial velocities v_i and the scaled quantities v_i/E_0 measured in the timecourse experiments (at 30 °C) presented in Chap. 7 are listed in Table 8-1. In addition to the individual values of v_i/E_0 for each experiment, the average, $\text{avg } v_i/E_0$, for each enzyme-pH combination is given. Since the values of $\text{avg } v_i/E_0$ range over a factor of 400, it is more convenient to plot $\log(\text{avg } v_i/E_0)$, also listed in the Table.

A line plot comparison of ricin A-chain, maizeRIP1, MOD1, MOD1X, and rproRIP1 reactivities with respect to A-10 as a function of pH, based on the initial velocities and

means listed in Table 8-1, is shown in Fig. 8-1. The reactivities are given in terms of $\log(v_i/E_0)$, which involves scaling with respect to enzyme concentrations. As seen in the Figure:

i) Ricin A-chain is considerably more active than any of the group of maizeRIP1 related enzymes. This is consistent with the literature on ricin A-chain and maizeRIP1 reactions with ribosomes (Walsh *et al.*, 1991; Hey *et al.*, 1995; Krawetz, 1998).

ii) MOD1X and maizeRIP1 are equally reactive.

iii) MOD1X is more reactive than MOD1, which has both the amino and carboxy terminal sequences that are removed during full activation. This is consistent with the results in the literature on the effects of the presence of these terminal sequences on the reactivity of maizeRIP1 mutants with ribosomes (Hey *et al.*, 1995; Krawetz, 1998).

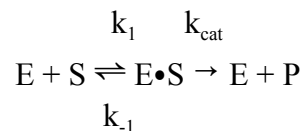
iv) rproRIP1 was expected to be either nonreactive (Bass *et al.*, 1992; Krawetz and Boston, 2000) or at most only very slightly reactive. Walsh *et al.*, (1991) found maize proRIP to be 10,000-fold less reactive than maizeRIP when reacting with ribosomes. Although the measured apparent rproRIP1 activity is less than any of the maizeRIP1-related enzymes in the experiments reported herein, it is no more than an order of magnitude less reactive than maizeRIP1 when reacting with A-10, as compared to the four orders of magnitude difference between rproRIP1 and maizeRIP1 when reacting with ribosomes found by Walsh *et al.* (1991).

Catalytic activity of rproRIP1 is consistent with the suggestion that the active site in rproRIP1 is well formed, and that, as proposed by Hey *et al.* (1995) the internal 25-residue segment removed during proRIP activation is a surface loop accessible to activating

proteases, but is not in the immediate vicinity of the active site cleft. The MOD1 construct, in which the internal 25-residue section is deleted and the adjacent residues are covalently bound, is enzymatically active, which indicates that extensive conformational change during rproRIP1 activation does not occur. Activation may consist mainly of removal of a surface loop with very little accompanying change in conformation. The catalytic active site of the resulting heterodimer is initially well-formed (although not covalently bound, as in MOD1) and very little dissociation and reassociation occurs during activation. Then the explanation for why the rproRIP1 is barely, if at all, active with respect to ribosomes, but may be significantly active with respect to A-10, could be that steric interference occurs between the internal 25-residue segment and some part of the ribosome, not necessarily in the α -sarcin loop-proRIP1 binding region, but the very small A-10 oligo tetraloop substrate might be able to bind to the active site with less steric interference from the internal 25-residue segment.

Estimates of pseudo k_{cat} and k_{cat}/K_M from initial velocity experiments with $S_0 \gg 10 \mu\text{M}$.

Asymptotic forms of the Michaelis-Menten equation when $K_M \ll S_0$ and when $K_M \gg S_0$. From the simple Michaelis-Menten enzyme catalysis model, eq. A1-1, using the notation k_{cat} in place of k_2 ,



and using the Briggs-Haldane steady-state assumptions, we obtain the Michaelis-Menten

equation

$$v = V_{\max} S/(K_M + S) \quad \text{or} \quad v = V_{\max}/(K_M/S + 1) \quad (8-1)$$

relating the reaction velocity $v = -dS/dt = dP/dt$ and the substrate concentration S for any S . In eq. 8-1, $K_M = (k_{-1} + k_{\text{cat}})/k_1$ and $V_{\max} = E_0 k_{\text{cat}}$. If v is measured early in the reaction, before a significant amount of substrate has been consumed (less than 10-15%), eqs 8-1 become

$$v_i = V_{\max} S_0/(K_M + S_0) \quad \text{or} \quad v_i = V_{\max}/(K_M/S_0 + 1) \quad (8-2)$$

where v_i is the initial velocity, and S_0 is the known initial substrate concentration.

Case I. If $K_M \ll S_0$, then $v_i = V_{\max}$ and $k_{\text{cat}} = v_i/E_0$. Thus, when analyzing the data, if v_i is essentially constant over a range of substrate concentrations, we can estimate

$$v_i = V_{\max}, \quad K_M \ll S_0, \quad \text{and} \quad k_{\text{cat}} = v_i/E_0. \quad (8-3)$$

Case II. If $K_M \gg S_0$, then $v_i/E_0 = (k_{\text{cat}}/K_M) S_0$, the slope $\alpha = d(v_i/E_0)/dS_0 = k_{\text{cat}}/K_M$, and we can estimate

$$K_M \gg S_0, \quad \text{and} \quad k_{\text{cat}} = \alpha K_M \gg \alpha S_0. \quad (8-4)$$

Estimating pseudo k_{cat}/K_M for ricin A-chain at four pH values. The results of the high A-10 concentration A-10/ricin A-chain initial velocity experiments at pH 4.0, 4.3, 4.9, and 5.5, were shown in Fig. 7-11 to be fit quite closely, at all the pH values, by linear expressions. The linear relation between v_i/E_0 and S_0 corresponds to Case II (eq. 8-4) above, and permits calculation for each pH of $k_{\text{cat}}/K_M = \alpha$, the slope given by the linear fitting procedure for that pH. The numerical results are listed in Table 8-2, and are also included in the overall summary of parameter estimates given in Table 8-5.

Estimating pseudo k_{cat} for maizeRIP1 at four pH values. Inspection of the results of the high A-10 concentration A-10/maizeRIP1 initial velocity experiments in Fig. 7-12 shows that over a substrate concentration range of 30-60 μ M, the initial velocities at each pH were effectively independent of substrate concentration. The average for each pH is shown as a line of constant v_i/E_0 superimposed on the data shown in Fig. 7-12. This corresponds to Case I (eq. 8-3) above, and permits estimation of k_{cat} from the relation $k_{cat} = v_i/E_0$. The numerical values are listed in Table 8-3, and are also included in the summary Table 8-5.

Estimates of pseudo K_M from A-10/maizeRIP1 timecourse data using nonlinear curve fitting to the integrated Michaelis-Menten rate equation with V_{max} held constant at values in the neighborhood of estimates from initial value experiments in which $S_0 \gg K_M$.

An integrated form of the Michaelis-Menten equation,

$$t = P/V_{max} - (K_M/V_{max}) \ln(1 - P/S_0) \quad (8-5)$$

is derived in Appendix A2. Eq. (8-5) is referred to herein as the t-dep form of the integrated Michaelis-Menten equation, where t-dep is an abbreviation for “time-as-dependent-variable”. In actuality, the extent of reaction is a function of time. The substrate (or product) concentration is the dependent variable and time is the independent variable. However, eq. (8-5) cannot be expressed in the intuitive form in which substrate or product concentration is an explicit function of time. The form of eq. (8-5) in which time seems to be a function of product is somewhat nonintuitive, but it is expedient because the curve fitting program used herein (Origin, Microcal Software, Inc.) requires an explicit expression for the dependent variable in the fitting equation.

Estimates of pseudo K_M for the A-10/maizeRIP1 reaction using nonlinear curve fitting with a constant V_{max} constraint. As mentioned at the beginning of this Section, it was not possible to obtain credible values for the parameters V_{max} and K_M through direct nonlinear curve fitting of the integrated Michaelis-Menten equation to any of the timecourse data. Possible reasons for this were discussed, ranging from the inherent nature of the enzymatic reaction possibly not conforming to the simple Michaelis-Menten model, to lack of satisfaction of the Briggs and Haldane steady-state hypotheses on which the Michaelis-Menten equation is based. In addition to these reasons, another source of difficulty might be the fitting algorithm itself. Attempts to fit timecourse data to the time-as-dependent-variable equation with S_0 held constant at the known (intended) initial substrate concentration, and with the parameters V_{max} and K_M as fitting variables, were not successful. The fitting procedure (using the program Origin from Microcal Software, Inc.) usually failed entirely, or, when neighboring values of S_0 were tried, it was sometimes possible to get fitting results, but the results were not credible because the error magnitudes were greater than the values of the corresponding parameters. The sensitivity of the fitting algorithm to the choice of S_0 is not surprising in view of its context in the integrated Michaelis-Menten equation, where the term $\ln(1 - P/S_0)$ approaches negative infinity as P approaches S_0 , expressing the fact that P approaches S_0 asymptotically as t tends to infinity. Some calculations were performed in which S_0 was included among the fitting variables, rather than treated as a constant, to give the fitting algorithm more flexibility to adjust for discrepancies between the intended and the actual S_0 . This approach was an improvement in that the fitting procedure usually did not fail entirely, but

the results were still not credible because of the large error magnitudes.

Having independently obtained values for V_{\max} for the A-10/maizeRIP1 reaction, nonlinear curve fitting of the integrated Michaelis-Menten equation to the A-10/maizeRIP1 timecourse data was again attempted, but this time, with V_{\max} held constant, and K_M and S_0 as fitting variables. The fitting procedure gave credible results when the independently obtained values for V_{\max} were used as fixed parameters. At two of the timecourse pHs, 4.7 and 5.3, the corresponding measured V_{\max} were obtained from high A-10 concentration A-10/maizeRIP1 initial velocity experiments at somewhat different pHs, namely, 4.9 and 5.4, respectively. In these cases, small manual adjustments to the constant V_{\max} were made to improve the fits. These fits are shown graphically for pH 4.0, 4.3, 4.7, and 5.3 in Fig. 8-2. The numerical results are listed in Table 8-4, including both the measured values for V_{\max} and the adjusted values used in the fitting.

Estimated pseudo K_M , k_{cat} , and k_{cat}/K_M values and bounds for ricin A-chain and maizeRIP1, including comparative values from the literature for ricin A-chain.

A summary of the measured estimates of pseudo k_{cat}/K_M for ricin A-chain at four pH values, of the measured estimates of pseudo k_{cat} for maizeRIP1 at four pH values, and of values of pseudo K_M for the A-10/maizeRIP1 reaction obtained using nonlinear curve fitting with a constant V_{\max} constraint, is shown in Table 8-5. In addition to the specific estimates of some parameters, Table 8-5 contains bounds for other parameters which can be estimated when the high A-10 concentration initial velocity experiments results in Case I or Case II behavior. For comparison, Table 8-5 also lists some parameter values for ricin

A-chain from the literature.

Comparison of A-10/MOD1 activity at 20 °C and 30 °C. Timecourse experiments were carried out at 20 °C to compare with those at 30 °C in order to estimate the extent to which A-10 substrate instability at low pH at the experimental temperature of 30 °C might contribute to the observed decrease in enzyme activity at low pH for all of the enzymes studied here.

The experiments were performed with MOD1 because more MOD1 enzyme was available than maizeRIP1 stock. But even with MOD1, there was not enough enzyme to carry out repeated experiments over the pH range (3.0 to 6.0) covered in the main experiments. Faced with a choice of either repeated experiments restricted to pH values in the range where the substrate T_m was decreasing with decreasing pH, or single experiments over a wider range of pH values which would include a pH range in which the T_m was no longer pH-dependent, the wider range was chosen for the following reasons:

i) All of the previous experiments were conducted at 30 °C. The new experiments at 20 °C would introduce a new variable and might thereby make it difficult to separate the temperature and pH effects if the experiments were restricted to a range in which both the pH and T_m were varying. Including in the 20 °C experiments a range of pH values in which the T_m was constant, would provide data to help separate the temperature and pH effects at low pH where the T_m is pH-dependent.

ii) It had been established in the main experiments that the relative errors in measured enzyme activity associated with a single timecourse experiment were much smaller than the measured pH-dependent changes in enzyme activities.

iii) In addition to the new experimental timecourses at 20 °C, one timecourse experiment at 30 °C and pH 4.0 was carried out as a repeat experiment to verify that the current experimental conditions gave repeatable results relative to previous experiments.

The adenine released as a function of time for A-10/MOD1 reactions at 20 °C and pH values ranging from 3.4 to 5.8 is shown in Fig. 7.10. The experimental substrate and enzyme concentrations were the same as those used in the main experiments at 30 °C: [A-10] = 10.0 μ M and [MOD1] = 1.0 μ M. Smaller pH steps were used in the neighborhood of the expected activity maximum than at the higher and lower pH ranges in order to more closely ascertain the optimum pH. The enzyme activities at the various pHs at 20 °C are around 40 to 60% of those at the corresponding pHs at 30 °C. The relatively small apparent scatter along each timecourse, and the systematic patterning of the timecourses with respect to pH supports the credibility of these experimental results.

The initial velocities calculated using the concentrations of the released adenine at the first measured time point (30 min) for the timecourses at 20 °C and the corresponding timecourses at 30 °C are shown in Fig. 8-3. An additional curve representing the values from the 20 °C timecourses multiplied by a factor of two is shown for comparison with the 30 °C values to evaluate the extent to which the reactions at 20 °C and 30 °C satisfy the Q_{10} rule (derived from the Arrhenius equation) on the effect of a 10 °C change of temperature on the rate of a reaction (Segel, 1975, p. 993)). To the extent that the experimentally observed rate of decrease of enzyme activity at 30 °C as a function of pH at low pH might be, at least partially, due to temperature-dependent substrate hairpin instability, a noticeably slower rate of decrease of enzyme activity would be expected as a function of

pH at low pH at 20 °C than at 30 °C. Inspection of Fig. 8-3, reveals no evidence that the rate of decrease of enzyme activity as a function of pH at low pH is slower at 20 °C than at 30 °C. These results demonstrate that the decrease of enzyme activity as a function of pH at low pH is due predominantly, if not almost completely, to effects other than substrate hairpin instability. The agreement between the values obtained from the 20 ° timecourses values multiplied by two, and the 30 °C timecourse values is consistent with the Q_{10} rule, and the corresponding activation energy for the reaction is (Segel, 1975, p. 993)

$$E_a = 2.3RT_1T_2\log Q_{10}/10 \cong 12 \text{ kcal/mole}$$

Requirements for obtaining credible Michaelis-Menten parameters from experimental data.

There are three classes of reasons that might, separately or in combination, account for failure to obtain credible Michaelis-Menten parameters from initial velocity or timecourse experiments: i) the reaction intrinsically departs significantly from the simple Michaelis-Menten model, ii) the reaction does in fact conform to the simple Michaelis-Menten model, but the experimental conditions did not satisfy all the assumptions used to derive the Michaelis-Menten equation defining the Michaelis-Menten parameters K_M and k_{cat} from the simple Michaelis-Menten model, or, the experimental conditions were not appropriate ($S_0 \sim K_M$) to simultaneously show the effects of both substrate-enzyme binding rate constants and the substrate-enzyme complex turnover rate, and iii) normal experimental inaccuracies, ranging from inconsistencies in pipeting when preparing

reaction mixtures to spectrophotometer drift during a series of measurements when determining substrate or enzyme concentrations.

Some possible contributors to the first class are:

Substrate inhibition. The curves of initial velocity versus substrate concentration did not rise and then fall with increasing substrate concentration as would be expected with substrate inhibition (Cleland, 1979). See, for example, Fig. 7-1(A). Thus, there are no signs of significant substrate inhibition.

Product inhibition. In exploratory (scouting) initial velocity Michaelis-Menten experiments in which the enzyme concentration was too high to keep the extent of reaction less than 10-15%, the extent of reaction would approach 100%. Also, as described above (Watanabe *et al.*, 1992; Pallanca *et al.*, 1998), experiments on adenine inhibition of ricin A-chain enzymatic activity with respect to ribosomes showed that it was negligible at the substrate/enzyme concentrations in our initial velocity experiments. The ratio of adenine to substrate concentration in these product inhibition experiments ranged from 100 to 50,000 and resulted in ~50 % reduction in ricin toxicity. However, in initial velocity experiments, since the free adenine is generated by cleavage of the substrate, the ratio of adenine to substrate concentration ranges from zero at the start of the reaction to ~0.15 at 15% extent of reaction (or ~0.18 if only unreacted substrate is considered). In summary, the effects, if any, of product inhibition were at most insignificant under our experimental conditions.

Enzyme inactivation during the experiment. Spiking experiments in which A-10 was added to a reaction which had reached ~100% extent of reaction yielded the usually

observed level of substrate/enzyme reactivity.

Some possible contributors to the second class are outlined below and analysed in detail in Appendices A1 and A3.

The substrate concentration is not far in excess of enzyme concentration. This would invalidate the Briggs and Haldane assumption used in the derivation of the Michaelis-Menten equation that the substrate concentration is effectively the same at the beginning of the steady-state phase as it was at the beginning of the reaction. In other words, it is assumed that the amount of substrate bound in the steady-state substrate-enzyme complex is not significant. The replacement of the standard Michaelis-Menten conservation assumption $S + P = S_0$ by the substrate conservation equation $S + P + C_{ES} = S_0$ leads to a very different form of the initial velocity versus substrate concentration equation. This equation is derived in Reiner (1969, Chap. 4), but no quantitative comparison of the two equations, showing the conditions under which the difference is significant, is given by Reiner (or was found in a literature search). Derivations of the initial velocity equation with and without inclusion of the substrate conservation equation, and a quantitative comparison of the predictions of the two forms of initial velocity versus substrate concentration equations are given in Appendix A1.

The change in the substrate concentration S during the reaction period (the time between the initiation of the reaction and the measurement) may be ignored. It is usually assumed (Reiner, 1971; Segel, 1975; Chen, 1998) that the error introduced by measuring the initial velocity of product formation (or substrate depletion) after an extent of reaction

~10 to 15% is not significant. However, there is a dearth of quantitative analysis of this assumption in the literature. Lee and Wilson (1971) analyzed this assumption quantitatively. However, they did not focus directly on the initial velocity, but rather, on the error, as a function of the extent of reaction, of the slope coefficient in the Lineweaver-Burk double reciprocal form of the Michaelis-Menten equation. A direct expression for the percent error in initial velocity measurement, relative to the true initial velocity, as a function of the extent of reaction at the instant of measurement, is derived in Appendix A3. The error at any given extent of reaction is dependent on the ratio $\alpha = K_M/S_0$. Quantitative results are shown graphically in Appendix A3.

Invalidity of the hypothesis regarding the onset and duration of a steady state. Briggs and Haldane (1925), on the basis of theoretical considerations, not experimental data, hypothesized that a steady state of the substrate-enzyme complex concentration is established very quickly relative to the initial velocity measurement time, and that it persists through the total duration of the experiment. They argued that since the enzyme and enzyme-substrate complex concentrations in Michaelis-Menten type experiments are assumed to be much less than the concentrations of substrate and product, the rate of change of the complex (“... except during the first instant of the reaction . . .”) must be negligible compared to the rate of change of substrate and product. Otherwise, the complex concentration would quickly become zero, and the reaction would come to an end. This was the justification for proposing that the rate of change of the enzyme-substrate complex be approximated by zero, thereby permitting derivation of the Michaelis-Menten equation.

Note that with regard to the rapid onset component of their theory, Briggs and Haldane simply asserted, with no discussion, that a substrate-enzyme complex was established “ . . . during the first instant . . . ” of the reaction. They also restricted their analysis to situations in which the enzyme and the enzyme-substrate complex concentrations were negligibly small compared not only with the substrate concentration, but also with the product concentration. Initially, when the product concentration is zero, the enzyme/product ratio is infinite, then falls as the reaction proceeds and product accumulates, until, when the extent of reaction reaches 1.0, the enzyme/product ratio is equal to the initial enzyme/substrate ratio. Algebraically,

$$E_0/P = E_0/\xi_f S_0$$

where E_0 , S_0 and P represent enzyme, substrate, and product concentration, respectively, and ξ_f represents the fractional extent of reaction. A typical Michaelis-Menten experiment ends with $\xi_f = 0.10$. In the middle of the experiment, $\xi_f = 0.05$, and

$$E_0/P = 20 (E_0/S_0)$$

If, as is desirable in Michaelis-Menten experiments, $E_0/S_0 < 0.001$, then $E_0/P < 0.02$ at 5% extent of reaction, which is probably negligible. However, in the A-10/ricin A-chain experiments reported herein, the initial enzyme/substrate ratio was 0.005, so that $E_0/P = 0.1$ at 5% extent of reaction, which is not clearly negligible. In subsequent experiments with maize related enzymes, E_0/S_0 ranged from 0.01 to 0.1, with a corresponding range of E_0/P from 0.2 to 2.0 at 5% extent of reaction, which is clearly not negligible.

The Briggs and Haldane steady-state theory has been universally accepted as a standard treatment of the simple Michaelis-Menten model of enzyme catalysis. However, there has

been very little direct experimental validation of either of the two assumptions (rapid onset and constancy of the enzyme-substrate complex concentration) underlying the steady-state theory. This is not surprising, since it would require the development of an assay for the transitory enzyme-substrate complex which could be applied during the enzymatic catalytic reaction without affecting the reaction. Chance (1943) carried out a combined experimental and theoretical study in which the enzyme-substrate complex horseradish peroxidase-hydrogen peroxide was measured during Michaelis-Menten type experiments, and the measured values were compared with numerical solutions of the rigorous set of kinetic equations (equations A1-2 - A1-5 in Appendix A1) obtained using the values of the rate constants determined experimentally. The experiments were carried out using rapid reaction measurement techniques. Chance obtained credible Michaelis-Menten parameters, but the data presented show that the concentration of the enzyme-substrate complex over the duration of the experiments was quite far from steady-state.

It is difficult, except in some special cases, to capture the characteristics and kinetics of the enzyme-substrate complex experimentally. However, it is possible to carry out mathematical analyses to find specific conditions in which the steady-state hypotheses are valid, and to carry out theoretical computer-based mathematical comparisons of the timecourse predictions of the rigorous set of equations A1-2 - A1-5 and the predictions of the integrated Michaelis-Menten equation (derived in Appendix A2), trying various realistic sets of values for the rate constants k_1 , k_{-1} , and k_2 in the simple Michaelis-Menten model (eq. A1-1). This would focus attention not on some abstract criteria for evaluating how well the calculated kinetics of the enzyme-substrate complex concentration satisfied

the steady-state hypotheses, but rather, directly on the validity of the Michaelis-Menten equation as an approximation of the rigorous set of equations A1-2 - A1-5.

Hommes (1962) showed theoretically that for the special case where S_0 is of the same magnitude as K_M , an equation of the form of the integrated Michaelis-Menten equation to describe such a system can be derived without assuming a steady state of the intermediate enzyme-substrate complex.

Stayton and Fromm (1979) generated timecourses by numerical integration of the rigorous equations (eqs A1-2-- A1-5) describing the simple Michaelis-Menten model with various rate constants k_1 , k_{-1} , and k_2 , and compared them with timecourses generated by the integrated Michaelis-Menten equation using the same rate constants k_1 , k_{-1} , and k_2 . They found that the differences between the curves were less than had been estimated theoretically. However, they also found that the enzyme-substrate complex concentration was not constant, so that dC_{ES}/dt was not essentially equal to zero. Their explanation for the good timecourse agreement despite C_{ES} not being constant was that except for the early transient phase of the reaction, $C_{ES} \ll P$ and $dC_{ES}/dt \ll dP/dt$. As a result, changes in dC_{ES}/dt will not affect dP/dt except where C_{ES} approaches the same order of magnitude as P , which only happens very early in the simulated reactions.

Segel (1988) showed in an analytic study that the requirements that the transient presteady-state of the substrate-enzyme complex concentration be very short relative to the initial velocity measurement time, and that there be only a negligible decrease in substrate concentration during the presteady state are satisfied if

$$E_0/(K_M + S_0) \ll 1,$$

which implies that the condition $E_0/S_0 \ll 1$ is sufficient but not necessary to satisfy these requirements when $E_0/K_M \ll 1$.

In summary regarding the steady-state hypotheses, it appears that the Michaelis-Menten equation can be a valid approximation to the rigorous kinetic equations without requiring stringent satisfaction of the Briggs-Haldane steady state assumptions, as long as the conditions on the enzyme-substrate ratio are appropriately satisfied.

A literature search to determine the prevalence of non-Michaelian kinetics was reported in a paper by Hill *et al.* (1977) titled, “Does Any Enzyme Follow the Michaelis-Menten Equation?”. Their criteria for non-Michaelian kinetics were non-hyperbolic initial velocity versus substrate concentration curves, and nonlinear double reciprocal plots. They concluded that, “In the light of these facts, we suggest the possibility that few enzymes really do obey Michaelis-Menten kinetics and the assumption that K_m and V values exist and can be obtained in most cases to an allowed degree of confidence by statistical procedures, should not any longer be uncritically accepted.”. However, it should be noted that they believed that Michaelis-Menten experiments should be carried out over a substrate concentration range of at least 1000, and that they considered experiments in which the substrate concentration varied by “ . . . a mere ten-fold range . . . ” to be insufficiently rigorous.

Conclusions

The profiles of catalytic activity versus pH for all the enzymes studied here suggests a catalytic mechanism involving active site residues with apparent pKas of ~4.2 and ~5.7. Glu177 with a pKa of 4.1 can account for the decreased activity at pH values below the

optimal pH of ~4.5. However, Arg180 with a pKa of 12.5 cannot account for the strong decrease of catalytic activity within a unit of pH above the optimal pH of ~4.5. Thus, the generally accepted mechanism of RIP N-glycosidase activity discussed in Chapter 1, which is consistent with observations of ribosome/RIP reactions at pH ~7, requires modification to account for the pH dependence of the activity of RIPs interacting with small RNA oligoribonucleotide substrates.

The observation that there is no shift in the profile of enzymatic activity versus pH between experiments at 20 ° and 30 ° indicates that the effect of pH on activity is due to ionization of side chains rather than to changes in the conformation of the substrate.

Ricin A-chain is an order of magnitude more active catalytically than maizeRIP1 with respect to A-10.

MaizeRIP1 and MOD1X are about equal in catalytic activity with respect to A-10, and are about four times as active as MOD1.

rproRIP1 conformation: it is very likely that the active site is structurally competent before activation and, as suggested by Hey *et al.* (1995) is not obstructed by the internal 25-residue segment deleted during activation. This conclusion is based on: i) the monomer MOD1X is as catalytically active as the dimer maizeRIP1 with respect to A-10, ii) the monomer MOD1, which still has the amino and carboxy terminal segments that are deleted during full activation of the rproRIP1, is catalytically active with respect to both ribosomes and A-10, although at a lower level than maizeRIP1. Krawetz (1988) found the catalytic activity of MOD1 to be about one-seventh that of maizeRIP1 with respect to ribosomes, and it was found herein to be about one-fourth that of maizeRIP1 with respect to A-10, and

iii) with the qualification that the source of the faint bands at ~30 kDa seen in the rproRIP1 lanes in Fig. 5-1 is unknown at present, rproRIP1 may have a small but significant level of catalytic activity with respect to the A-10 oligo.

Table 8-1. Enzyme activities at 30 °C using initial velocities from timecourse experiments.^a

Enzyme	Ext Reac (%ξ)	pH	E ₀ (μM)	v _i (μM/h)	v _i /E ₀ (h ⁻¹)	avg v _i /E ₀ (h ⁻¹)	log(v _i /E ₀)
ricin A-chain	30.4	4.00	0.05	6.09	122.	61. ± 46.	1.8 ± 0.8
	3.4	4.00	0.05	0.66	13.2		
	10.7	4.00	0.05	2.14	42.8		
	36.3	4.50	0.05	7.56	146.	129. ± 23.	2.1 ± 0.2
	28.3	4.50	0.05	5.67	113.		
maizeRIP1	1.5	2.90	1.00	0.31	0.31	0.3	- 0.51
	5.5	3.40	1.00	1.10	1.10	1.10	.04
	12.5	4.00	0.50	2.50	5.00	4.9 ± 0.5	0.69 ± .09
	13.1	4.00	0.50	2.62	5.24		
	11.4	4.00	0.50	2.27	4.54		
	11.1	4.00	0.50	2.22	4.44		
	12.4	4.00	0.50	2.48	4.96		
	14.1	4.00	0.50	2.83	5.66		
	24.2	4.00	1.00	4.85	4.85		
	21.1	4.00	1.00	4.22	4.22		
	23.0	4.30	0.10	4.60	46.0	46.0	1.66
	20.3	4.70	0.20	12.20	61.0	49. ± 20.	1.69 ± 0.38
	9.5	4.70	0.10	1.90	19.0		
	29.4	4.70	0.10	5.90	59.0		
	27.3	4.70	0.10	5.50	55.0		
	7.1	5.30	0.10	1.42	14.2	14.2	1.15

(continued)

Table 8-1 (continued)

Enzyme	Ext Reac (% ξ)	pH	E_0 (μ M)	v_i (μ M/h)	v_i/E_0 (h ⁻¹)	avg v_i/E_0 (h ⁻¹)	log(v_i/E_0)
MOD1	0.7	2.90	1.00	0.13	0.13	0.13	- 0.89
	3.5	3.40	1.00	0.71	0.71	0.71	- 0.15
	9.8	4.00	1.00	1.96	1.96	1.9 \pm 0.1	0.28 \pm 0.04
	9.4	4.00	1.00	1.88	1.88		
	9.9	4.00	1.00	1.98	1.98		
	9.0	4.00	1.00	1.80	1.80		
	4.5	4.40	0.20	0.90	4.52	5. \pm 1.	0.72 \pm 0.18
	29.7	4.40	1.00	5.95	5.95		
	51.5	4.90	1.00	10.3	10.3	10.30	1.01
	23.2	5.3	1.00	4.64	4.64	4.1 \pm 0.8	0.61 \pm 0.17
	17.7	5.3	1.00	3.54	3.54		
	3.7	5.8	1.00	0.75	0.75	0.8 \pm 0.1	0.08
	4.6	5.8	1.00	0.91	0.91		
MOD1X	18.6	4.70	0.20	11.2	56.0	46. \pm 13.	1.67 \pm 0.25
	19.2	4.70	0.10	3.75	37.5		
	7.4	4.90	0.10	4.41	44.1	36. \pm 11.	1.56 \pm 0.27
	11.9	4.90	0.10	2.38	23.8		
	13.4	4.90	0.20	8.04	40.2		
rproRIP1	4.0	3.90	1.00	0.81	0.81	0.81	- 0.09
	10.8	4.40	1.00	2.17	2.17	2.17	0.34
	14.0	4.85	1.00	2.80	2.80	2.80	0.45
	5.3	5.30	1.00	1.05	1.05	1.05	0.02
	1.8	5.80	1.00	0.36	0.36	0.36	- 0.44

^a Where there is more than one experiment for a given enzyme and pH, the average values (direct and log) are shown in the first row for that enzyme and pH combination.

Table 8-2. Estimates of pseudo k_{cat}/K_M for A-10/ricin A-chain at four pH values.^a

pH	Slope ($\mu\text{M}^{-1}\text{h}^{-1}$)	R	k_{cat}/K_M ($\mu\text{M}^{-1}\text{h}^{-1}$)
4.0	5.81	0.999	5.8
4.3	6.23	0.999	6.2
4.9	0.87	0.993	0.87
5.5	0.17	0.999	0.17

^a see p. 87

Table 8-3. Estimates of pseudo k_{cat} for A-10/maizeRIP1 at four pH values.^a

pH	k_{cat}
4.0	5.5
4.3	13.4
4.9	58.9
5.4	14.9

^a see p. 88

Table 8-4. Estimates of pseudo K_M for the A-10/maizeRIP1 reaction using nonlinear curve fitting with a constant V_{max} constraint.^a

pH	V_{max} meas.	V_{max} adjusted	K_M	S_0
4.0	0.092	0.092	$7.4 \pm 1.$	5.6 ± 0.3
4.3	0.22	0.22	11.1 ± 0.3	6.4 ± 0.04
4.7	0.98^b	0.79	$90. \pm 10.$	11.1 ± 0.7
5.3	0.25^c	0.20	$80. \pm 30.$	$10. \pm 4.$

^a see p. 87

^b Measured at pH 4.9

^c Measured at pH 5.4

Table 8-5. Estimated pseudo K_M , k_{cat} , and k_{cat}/K_M values and bounds for A-10/ricin A-chain and A-10/maizeRIP1, including comparative values from the literature for ricin A-chain.

Source	pH	ricin A-chain			MaizeRIP1	
		k_{cat} (m^{-1})	K_M (μM)	k_{cat}/K_M ($\mu M^{-1}h^{-1}$)	k_{cat} (m^{-1})	K_M (μM)
High substrate concentration experiments ^a	4.0	> 5.8	> 60	5.8	0.092	< 30
	4.3	> 6.2	> 60	6.2	0.22	< 30
	4.9	> 0.87	> 60	0.87	0.98	< 30
	5.5	> 0.17	> 60	0.17	0.25	< 30
Timecourse fitting with specified V_{max} from high substrate experiments	4.0				0.092	7.4
	4.3				0.22	11.1
	4.7				0.79	88.3
	5.3				0.20	76.1
Gluck (1992) ^b	7.5	0.01	5.7	0.0018		
Link (1996) ^c	7.5	0.00033				
Chen (1998) ^d	4.0	4.1	4.1	1.0		
	4.5	1.6	18.0	0.089		
	5.0	0.5	75.0	0.0067		

^a [A-10] = 30 and 60 μM

^b substrate 19-mer tetraloop

^c substrate A-10

^d substrate A-10

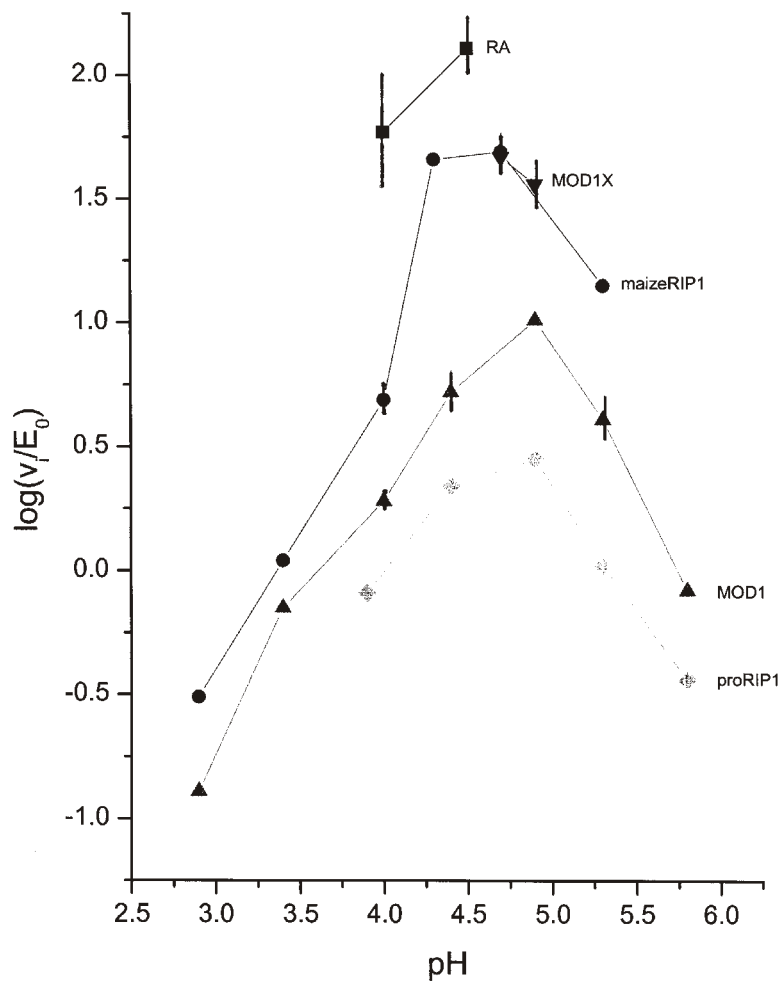


Figure 8-1. A line plot comparison of ricin A-chain, maizeRIP1, MOD1, MOD1X, and rproRIP1 reactivities with A-10 as a function of pH, based on initial velocities. The reactivities are given in terms of $\log(v_i/E_0)$, which involves scaling with respect to enzyme concentrations. The v_i values were obtained from timecourse experiments using the first measured point. The data underlying this graphical presentation are listed in Table 8-1. The symbols for the data points of the various enzymes are ricin A-chain (■), maizeRIP1 (●), MOD1 (▲), MOD1X (▼), and rproRIP1 (◆).

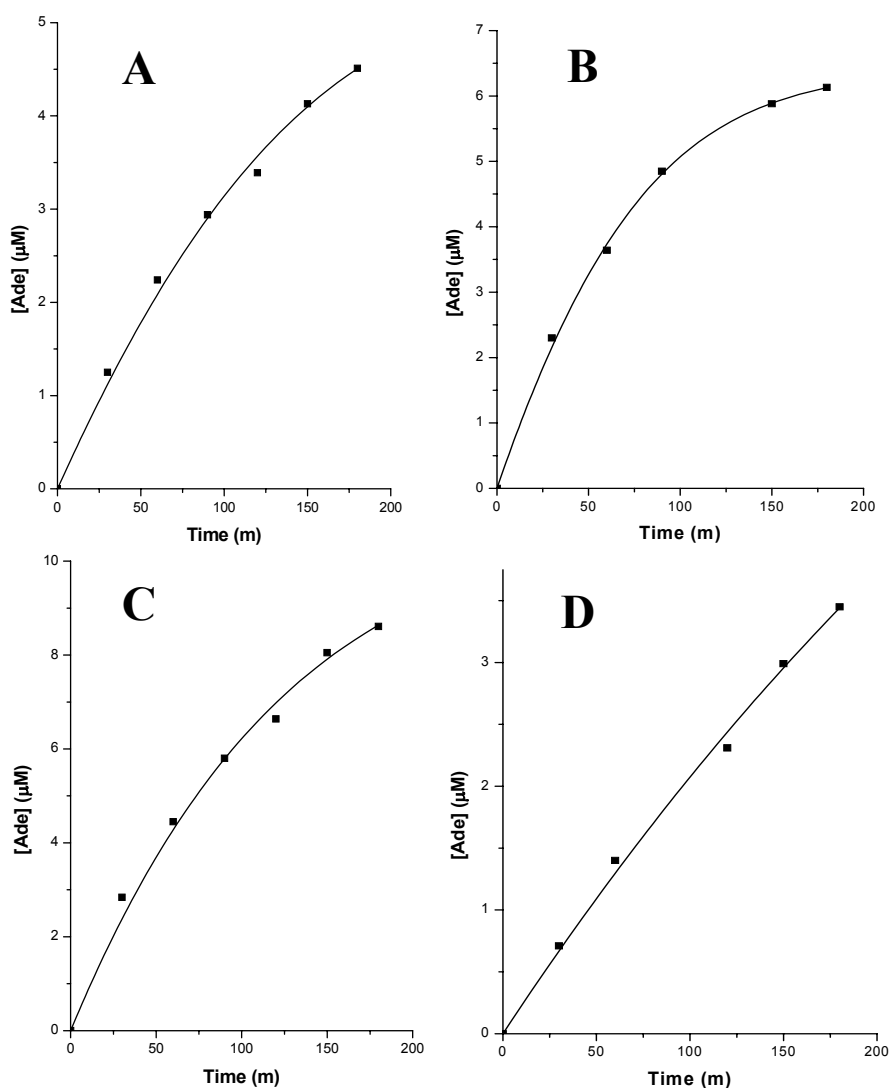


Figure 8-2. Results obtained from nonlinear curve fitting of the integrated Michaelis-Menten equation (eq. A2-5, in which the explicit dependent variable is the time t) to A-10/maizeRIP1 reaction timecourses with V_{\max} held constant at values given by the high substrate concentration experiments (Figure 7-12), and with K_M and S_0 as fitting variables. The experimental conditions were $[A-10] = 10 \mu\text{M}$ and $[\text{maizeRIP1}] = 0.1 \mu\text{M}$.

(A) pH 4.0, $V_{\max} = 0.092 \mu\text{M/m}$. The fitting results are: $R^2 = 0.995$, $K_M = 7.4 \pm 1. \mu\text{M}$, $S_0 = 5.6 \pm 0.3 \mu\text{M}$.

(B) pH 4.3, $V_{\max} = 0.22 \mu\text{M/m}$. The fitting results are: $R^2 = 0.999$, $K_M = 11.1 \pm 0.3 \mu\text{M}$, $S_0 = 6.4 \pm 0.04 \mu\text{M}$.

(C) pH 4.7, $V_{\max} = 0.79 \mu\text{M/m}$. The fitting results are: $R^2 = 0.993$, $K_M = 90. \pm 10. \mu\text{M}$, $S_0 = 11.1 \pm 0.7 \mu\text{M}$.

(D) pH 5.3, $V_{\max} = 0.20 \mu\text{M/m}$. The fitting results are: $R^2 = 0.997$, $K_M = 80. \pm 30. \mu\text{M}$, $S_0 = 10. \mu\text{M} \pm 4.$

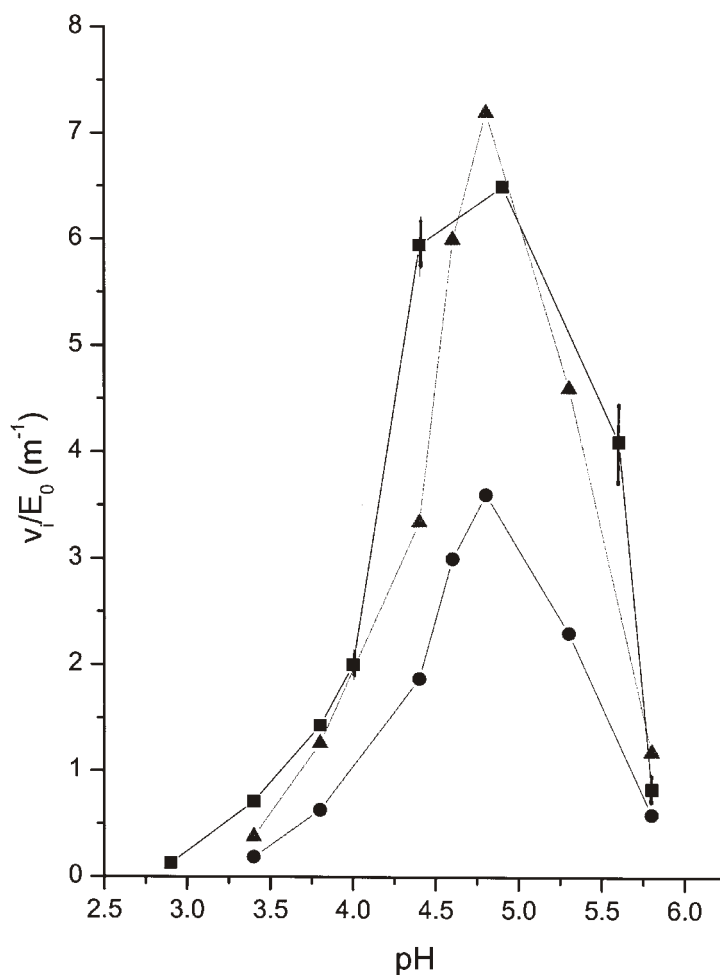


Figure 8-3. A line plot comparison of MOD1 reactivity with A-10 at 20 °C (●) and 30 °C (■) as a function of pH, based on initial velocities. An additional curve (▲) representing the values from the 20 °C timecourses multiplied by a factor of two is shown for comparison with the 30 °C values to evaluate the extent to which the reactions at 20 °C and 30 °C satisfy the Q_{10} rule (see p. 93). The reactivities are given in terms of v_i/E_0 . v_i was obtained from timecourse experiments using the first measured data point.

REFERENCES

Ago, Hideo, Kataoka, Jiro, Tsuge, Hideaki, Nabuka, Noriyuki, Inagaki, Eiji, Noma, Masana, and Miyano, Masashi (1994) X-ray structure of a pokeweed antiviral protein, coded by a new genomic clone, at 0.23 nm resolution. *Eur. J. Biochem.* **225**, 369-374.

Allison, R. Donald and Purich, Daniel L. (1979) Practical considerations in the design of initial velocity enzyme rate assays. *Methods in Enzymology* **63**, 3-22.

Atkins, Gordon L. and Nimmo, Ian A. (1973) The reliability of Michaelis constants and maximum velocities estimated by using the integrated Michaelis-Menten equation. *Biochem. J.* **135**, 779-784.

Barbieri, Luigi, Battelli, Maria Giulia, and Stirpe, Fiorenzo (1993) Ribosome-inactivating proteins from plants. *Biochim. Biophys. Acta* **1154**, 237-282.

Barbieri, Luigi, Valbonesi, Paola, Gorini, Paola, Pession, Annalisa, and Stirpe, Fiorenzo (1996) Polynucleotide:adenosine glycosidase activity of saporin-L1: effect on DNA, RNA and poly(A). *Biochem. J.* **319**, 507-513.

Barbieri, Luigi, Valbonesi, Paola, Bonora, Elena, Gorini, Paola, Bolognesi, Andrea, and Stirpe, Fiorenzo (1997) Polynucleotide:adenosine glycosidase activity of ribosome-inactivating proteins: effect on DNA, RNA and poly(A). *Nucleic Acids Research* **25**(3), 518-522.

Bartha, F. (1980) Effect of error of the quasi-steady-state approximation on the estimation of K_M and V_m from a single time curve. *J. Theor. Biol.* **86**, 105-115.

Bass, Hank W., Webster, Cecilia, O'Brien, Gregory R., Roberts, Justin K. M., and Boston, Rebecca S. (1992) A maize ribosome-inactivating protein is controlled by the transcriptional activator *Opaque-2*. *The Plant Cell* **4**, 225-234.

Briggs, George Edward and Haldane, John Burdon Sanderson (1925) A note on the kinetics of enzyme action. *Biochemical Journal* **19**, 338-339.

Cameselle, Jose C., Ribeiro, Joao Meireles, and Sillero, Antonio (1986) Derivation and use of a formula to calculate the net charge of acid-base compounds. Its application to amino acids, proteins and nucleotides. *Biochemical Education* **14**(3), 131-136.

Carnicelli, Domenica, Brigotti, Maurizio, Montanaro, Lucio, and Sperti, Simonetta (1992) Differential requirement of ATP and extra-ribosomal proteins for ribosome inactivation by eight RNA *N*-glycosidases. *Biochem. Biophys. Res. Commun.* **182**(2),

579-582.

Chaddock, John A., Monzingo, Arthur F., Robertus, Jon D., Lord, J. Michael, and Roberts, Lynne M. (1996) Major structural differences between pokeweed antiviral protein and ricin A-chain do not account for their differing ribosome specificity. *Eur. J. Biochem.* **235**, 159-166.

Chance, Britton (1943) The kinetics of the enzyme-substrate compound of peroxidase. *J. Biol. Chem.* **151**, 553-577.

Chen, Xiang-Yang, Link, Todd M., and Schramm, Vern L. (1996) Inhibition of ricin by an RNA stem-loop containing a ribo-oxocarbenium mimic. *J. Am. Chem. Soc.* **118**, 3067-3068.

Chen, Xiang-Yang, Link, Todd M., and Schramm, Vern L. (1998) Ricin A-chain: kinetics, mechanism, and RNA stem-loop inhibitors. *Biochemistry* **37**, 11605-11613.

Cleland, W. Wallace (1979) Substrate Inhibition. *Methods in Enzymology* **63**, 500-513.

Collins, Edward J., Robertus, Jon D., LoPresti, Mary, Stone, Kathy L., Williams, Kenneth R., Wu, Paul, Hwang, Kou, and Piatak, Michael (1990) Primary amino acid sequence of α -trichosanthin and molecular models for abrin A-chain and α -Trichosanthin. *J. Biol. Chem.* **265**(15), 8665-8669.

Cornish-Bowden, Athel (1975) The use of the direct linear plot for determining initial velocities. *Biochem. J.* **149**, 305-312.

Day, Philip J., Ernst, Stephen R., Frankel, Arthur E., Monzingo, Arthur F., Pascal, John M., Molina-Svinth, Maria C., and Robertus, Jon D. (1996) Structure and activity of an active site substitution of ricin A chain. *Biochemistry* **35**, 11098-11103.

Di Fonzo, N., Manzocchi, L., Salamini, F., and Soave, C. (1986) Purification and properties of an endospermic protein of maize associated with the *Opaque-2* and *Opaque-6* genes. *Planta* **167**, 587-594.

Di Fonzo, N., Hartings, H., Brembilla, M., Motto, M., Soave, C., Navarro, E., Palau, J., Rhode, W., and Salamini, F. (1988) The b-32 protein from maize endosperm, an albumin regulated by the *O2* locus: Nucleic acid (cDNA) and amino acid sequences. *Mol. Gen. Genet.* **212**, 481-487.

Duggleby, Ronald G. and Clarke, Robyn B. (1991) Experimental designs for estimating the parameters of the Michaelis-Menten equation from progress curves of enzyme-catalyzed reactions. *Biochimica et Biophysica Acta* **1080**, 231-236.

Duggleby, Ronald G. (1995) Analysis of progress curves by nonlinear regression. *Methods in Enzymology* **249**, 61-90.

Endo, Yaeto, Mitsui, Kazuhiro, Motizuki, Mitsuyoshi, and Tsurugi, Kunio (1987) The mechanism of action of ricin and related toxic lectins on eukaryotic ribosomes. *J. Biol. Chem.* **262**(12), 5908-5912.

Endo, Yaeto. and Tsurugi, Kunio (1988a) The RNA *N*-glycosidase activity of ricin A-chain. *J. Biol. Chem.* **263**(18), 8735-8739.

Endo, Yaeto, Tsurugi, Kunio, and Lambert, John M. (1988b) The site of action of six different ribosome-inactivating proteins from plants on eukaryotic ribosomes: The RNA *N*-glycosidase activity of the proteins. *Biochemical and Biophysical Research Communications* **150**(3), 1032-1036.

Endo, Yaeto, Chan, Yuen-Ling, Lin, Alan, Tsurugi, Kunio, and Wool, Ira G. (1988c) The cytotoxins α -sarcin and ricin retain their specificity when tested on a synthetic oligoribonucleotide (35-mer) that mimics a region of 28S ribosomal ribonucleic acid. *J. Biol. Chem.* **263**(17), 7917-7920.

Endo, Yaeto, Gluck, Anton, and Wool, Ira G. (1991) Ribosomal RNA identity elements for ricin A-chain recognition and catalysis. *J. Mol. Biol.* **221**, 193-207.

Fasman, G. D. (1975) *Handbook of Biochemistry and Molecular Biology, Nucleic Acids, I*, CRC Press, 3rd ed., Boston, MA.

Funatsu, G., Islam, M. R., Minami, Y., Sung-Sil, K., and Kimura, M. (1991) Conserved amino acid residues in ribosome-inactivating proteins from plants. *Biochimie* **73**, 1157-1161.

Gill, Stanley. C and von Hippel, Peter H. (1989) Calculation of protein extinction coefficients from amino acid sequence data. *Analytical Biochemistry* **182**, 319-326.

Gluck, Anton, Endo, Yaeto, and Wool, Ira G. (1992) Ribosomal RNA identity elements for ricin A-chain. Recognition and catalysis. Analysis with tetraloop Mutants. *J. Mol. Biol.* **226**, 411-424.

Gluck, Anton, Endo, Yaeto, and Wool, Ira G. (1994) The ribosomal RNA identity elements for ricin and for α -sarcin: mutations in the putative CG pair that closes a GAGA tetraloop. *Nucleic Acids Research* **22**(3), 321-324.

Gluck, Anton and Wool, Ira G. (1996a) Dependence of depurination of oligoribonucleotides by ricin A-chain on divalent cations and chelating agents. *Biochemistry and Molecular Biology International* **39**(2), 285-291.

Gluck, Anton and Wool, Ira G. (1996b) Determination of the 28S ribosomal RNA identity element (G4319) for alpha-sarcin and the relationship of recognition to the selection of the catalytic site. *J. Mol. Biol.* **256**, 838-848.

Gu, Yi-Jun and Xia, Zong-Xiang (2000) Crystal structures of the complexes of trichosanthin with four substrate analogs and catalytic mechanism of RNA N-glycosidase. *Proteins* **39**, 37-46.

Habuka, Noriyuki, Aakiyama, Kiyotaka, Tsuge, Hideaki, Miyano, Masashi, Matsumoto, Takashi, and Noma, Masana (1990) Expression and secretion of *Mirabilis* antiviral protein in *Escherichia coli* and its inhibition of *in vitro* eukaryotic and prokaryotic protein synthesis. *J. Biol. Chem.* **265**(19), 10988-10922.

Hartings, Hans, Lazzaroni, Nadia, Marsan, Paolo Ajmone, Aragay, Anna, Thompson, Richard, Salamini, Francesco, Di Fonzo, Natale, Palau, Jaume, and Motto, Mario (1990) The b-32 protein from maize endosperm: characterization of genomic sequences encoding two alternative central domains. *Plant Molecular Biology* **14**, 1031-1040.

Hartley, Martin R., Chaddock, John A., and Bonness, Maureen S. (1996) The structure and function of ribosome-inactivating proteins. *Trends in Plant Science* **1**(8), 254-260.

Heus, Hans A. and Pardi, Arthur (1991) Structural features that give rise to the unusual stability of RNA hairpins containing GNRA loops. *Science* **253**, 191-194.

Hey, Timothy D., Hartley, Martin, and Walsh, Terence A. (1995) Maize ribosome-inactivating protein (b-32): Homologs in related species, effects on maize ribosomes, and modulation of activity by pro-peptide deletions. *Plant Physiol.* **107**, 1323-1332.

Hill, Charles M., Waight, Roy D., and Bardsley, William G. (1977) Does any enzyme follow the Michaelis-Menten equation? *Molecular and Cellular Biochemistry* **15**(3), 173-178.

Hommes, F. A. (1962) The integrated Michaelis-Menten equation. *Archives of Biochemistry and Biophysics* **96**, 28-31.

Hosur, M. V., Nair, Bindu, Satyamurthy, P., Misquith, S., Surolia, A., and Kannan, K. K. (1995) X-ray structure of gelonin at 1.8 Å resolution. *J. Mol. Biol.* **250**, 368-380.

Huang, Qichen, Liu, Shenping, Tang, Youqi, Jin, Shanwei, and Wang, Yu (1995) Studies on crystal structures, active-centre geometry and depurinating mechanism of

two ribosome-inactivating proteins. *Biochem J.* **309**, 285-298.

Kajava, Andrey and Ruterjans, Heinz (1993) Molecular modelling of the 3-D structure of RNA tetraloops with different nucleotide sequences. *Nucleic Acids Research* **21**(19), 4556-4562.

Katzin, Betsy J., Collins, Edward J., and Robertus, Jon D. (1991) Structure of ricin A-chain at 2.5 Å. *Proteins* **10**, 251-259.

Kim, Youngsoo, Mlsna, Debra, Monzingo, Arthur F., Ready, Michael P., Frankel, Art, and Robertus, Jon D. (1992) Structure of a ricin mutant showing rescue of activity by a noncatalytic residue. *Biochemistry* **31**, 3294-3296.

Krawetz, Julie E. (1998) *Functional and Biochemical Characterization of a Maize Ribosome-Inactivating Protein (RIP) Zymogen*. Thesis (Ph.D.) - North Carolina State University, NC.

Krawetz, Julie E. and Boston, Rebecca S. (2000) Substrate specificity of a maize ribosome-inactivating protein differs across diverse taxa. *Eur. J. Biochem.* **267**, 1966-1974.

Lee, Hyun-Jae and Wilson, Irwin B. (1971) Enzymic parameters: Measurement of V and K_m. *Biochimica et Biophysica Acta* **242**, 519-522.

Lin, Jung-Yaw, Kao, Whei-Yang, Tserng, Kou-Yi, Chen, Chi-Ching, and Tung, Ta-Cheng (1970) Effect of crystalline abrin on the biosynthesis of protein, RNA, and DNA in experimental tumors. *Cancer Research* **30**, 2431-2433.

Lin, Jung-Yaw, Liu, Kang, Chen, Chi-Ching, and Tung, Ta-Cheng (1971) Effect of crystalline ricin on the biosynthesis of protein, RNA, and DNA in experimental tumor cells. *Cancer Research* **31**(7), 921-924.

Link, Todd, Chen, Xiang Yang, Niu, Lin Hao, and Schramm, Vern L. (1996) A hypothesis to explain the substrate reactivity of ribosomal and stem-loop RNA with ricin A-chain. *Toxicon* **34**(11/12), 1317-1324.

Marchant, Alan and Hartley, Martin R. (1995) The Action of pokeweed antiviral protein and ricin A-chain on mutants in the α-sarcin loop of *Escherichia coli* 23S ribosomal RNA. *J. Mol. Biol.* **254**, 848-855.

Mehta, Ashwin D. and Boston, Rebecca S. (1998) Ribosome-inactivating proteins, in *A Look Beyond Transcription: Mechanisms Determining mRNA Stability and Translation in Plants*, Julia Bailey-Serres, Daniel R Gallie, eds., American Society of Plant Physiologists, 145-152.

Montfort, William, Villafranca, Jesus E., Monzingo, Arthur F., Ernst, Stephen R., Katzin, Betsy, Rutenber, Earl, Xuong, Nuyhen H., Hamlin, Ron, and Robertus, Jon D. (1987) The three-dimensional structure of ricin at 2.8 Å. *J. Biol. Chem.* **262**(11), 5398-5403.

Monzingo, Arthur F. and Robertus, John D. (1992) X-ray analysis of substrate analogs in the ricin A-chain active site. *J. Mol. Biol.* **227**, 1136-1145.

Monzingo, Arthur F., Collins, Edward J., Ernst, Stephen R., Irvin, James D. and Robertus, Jon D. (1993) The 2.5 Å structure of pokeweed antiviral protein. *J. Mol. Biol.* **233**, 705-715.

Moore, Dexter S. (1985) Amino acid and peptide net charges: A simple calculational procedure. *Biochemical Education* **13**(1), 10-11.

Morris, Kevin N. and Wool, Ira G. (1994) Analysis of the contribution of an amphiphilic α -helix to the structure and to the function of ricin A chain. *Proc. Natl. Acad. Sci.* **91**, 7530-7533.

Nielsen, Kirsten and Boston, Rebecca S. (2001) Ribosome-inactivating proteins: A plant perspective. *Annu. Rev. Plant Physiol. Plant Mol. Biol.* **52**, 785-816.

Nicolas, Emmanuelle, Beggs, Joseph M., Haltiwanger, Brett M., and Taraschi, Theodore F. (1998) A new class of DNA glycoylase/apurinic/apyrimidinic lyases that act on specific adenines in single-stranded DNA. *J. of Biol. Chem.* **273**(27), 17216-17220.

Nicolas, Emmanuelle, Beggs, Joseph M., and Taraschi, Theodore F. (2000) Gelonin is an unusual DNA glycosylase that removes adenine from single-stranded, normal base pairs and mismatches. *J. of Biol. Chem.* **275**(40), 31399-31406.

Olsnes, S. and Pihl, A. (1972) Ricin - a potent inhibitor of protein synthesis. *FEBS Letters* **20**(3), 327-329.

Olsnes, Sjur, Fernandez-Puentes, Carmen, Carrasco, Luis, and Vazquez, David (1975) Ribosome inactivation by the toxic lectins abrin and ricin. *Eur. J. Biochem.* **60**, 281-288.

Orita, Masaya, Nishikawa, Fumiko, Shimayama, Takashi, Taira, Kazunari, Endo, Yaeta, and Nishikawa, Satoshi (1993) High-resolution NMR study of a synthetic oligoribonucleotide with a tetranucleotide GAGA loop that is a substrate for the cytotoxic protein, ricin. *Nucleic Acids Research* **21**(24), 5670-5678.

Orita, Masaya, Nishikawa, Fumiko, Kohno, Tetsuya, Senda, Toshiya, Mitsui,

Yukio, Endo, Yaeta, Taira, Kazunari, and Nishikawa, Satoshi (1996) High-resolution NMR study of a GdAGA tetranucleotide loop that is an improved substrate for ricin, a cytotoxic plant protein. *Nucleic Acids Research* **24**(4), 611-618.

Orsi, Bruno A. and Tipton, Keith F. (1979) Kinetic analysis of progress curves. *Methods in Enzymology* **63**, 159-183.

Pallanca, Alessandra, Mazzaracchio, Raffaella, Brigotti, Maurizio, Carnicelli, Domenica, Alvergnà, Paola, Sperti, Simonetta, and Montanaro, Lucio (1998) Uncompetitive inhibition by adenine of the RNA-*N*-glycosidase activity of ribosome-inactivating proteins. *Biochim. Biophys. Acta* **1384**, 277-284.

Putnam, Christopher D. and Tainer, John A. (2000) The food of sweet and bitter fancy. *Nature Structural Biology* **7**(1), 17-18.

Ready, Michael P., Kim, Youngsoo, and Robertus, Jon D. (1991) Site-directed mutagenesis of ricin A-chain and implications for the mechanism of action. *Proteins* **10**, 270-278.

Reiner, John M., (1969) *Behavior of Enzyme Systems*, 2nd ed. Van Nostrand Reinhold Company, New York.

Ries-Kautt, Madeleine and Ducruix, Arnaud (1997) Inferences drawn from physicochemical studies of crystallogenes and precrystalline state. *Meth. Enzymol.* **276**, 23-59.

Sambrook, J., Fritsch, E. F., and Maniatis, T. (1987) *Molecular Cloning: a laboratory manual* 2nd ed., Cold Spring Harbor, N. Y. : Cold Spring Harbor Laboratory.

Segel, Irwin H. (1975) *Enzyme Kinetics, Behavior and Analysis of Rapid Equilibrium and Steady-State Enzyme Systems*. New York, John Wiley & Sons.

Segel, Lee A. (1988) On the validity of the steady state assumption of enzyme kinetics. *Bulletin of Mathematical Biology* **50**(6), 579-593.

Sillero, Antonio and Ribeiro, Joao Meireles (1989) Isoelectric points of proteins: Theoretical determination. *Analytical Biochemistry* **179**, 319-325.

Soave, Carlo, Tardani, Laura, Di Fonzo, Natale, Salamini, Francesco (1981) Zein level in maize endosperm depends on a protein under control of the *Opaque-2* and *Opaque-6* Loci. *Cell* **27**, 403-410.

Sperti, Simonetta, Brigotti, Maurizio, Zamboni, Mariacristina, Carnicelli,

Domenica, and Montanaro, Lucio (1991) Requirements for the inactivation of ribosomes by gelonin. *Biochem. J.* **277**, 281-284.

Stayton, Mark M. and Fromm, Herbert J. (1979) A computer analysis of the validity of the integrated Michaelis-Menten equation. *J. Theor. Biol.* **78**, 309-323.

Stirpe, Fiorenzo, Barbieri, Luigi, Battelli, Maria Giulia, Soria, Marco, and Lappi, Douglas A. (1992) Ribosome-inactivating proteins from plants: Present status and future prospects. *Bio/Technology* **10**, 405-412.

Szewczak, Alexander A., Moore, Peter B., Chan, Yuen-Ling, and Wool, Ira G. (1993) The conformation of the sarcin/ricin loop from 28S ribosomal RNA. *Biochemistry* **90**, 9581-9585.

Thompson, Julie D., Higgins, Desmond G., and Gibson, Toby J. (1994) CLUSTAL W: improving the sensitivity of progressive multiple sequence alignment through sequence weighting, position-specific gap penalties and weight matrix choice. *Nucleic Acids Research* **22**(22), 4673-4680.

Tumer, Nilgun E., Hwang, Duk-Ju, and Bonness, Maureen (1977) C-terminal deletion mutant of pokeweed antiviral protein inhibits viral infection but does not depurinate host ribosomes. *Proc. Natl. Acad. Sci.* **94**, 3866-3871.

Vandenberg, Jamie I., Kuchel, Philip W., and King, Glenn F. (1986) Application of progress curve analysis to *in situ* enzyme kinetics using ¹H NMR spectroscopy. *Analytical Biochemistry* **155**, 38-44.

Walsh, Terrence A., Morgen, Alice E., and Hey, Timothy D. (1991) Characterization and molecular cloning of a proenzyme form of a ribosome-inactivating protein from maize. *J. Biol. Chem.* **266**(34), 23422-23427.

Wang, Yun-Xing, Neamati, Nouri, Jacob, Jaison, Palmer, Ira, Stahl, Stephen J., Kaufman, Joshua D., Huang, Philip Lin, Huang, Paul Lee, Winslow, Heather E., Pommier, Yves, Wingfield, Paul T., Lee-Huang, Sylvia, Bax, Ad, and Torchia, Dennis A. (1999) Solution structure of anti-HIV-1 and anti-tumor protein MAP30: Structural Insights into its multiple functions. *Cell* **99**, 433-442.

Wang, Yun-Xing, Jacob, Jaison, Wingfield, Paul T., Palmer, Ira, Stahl, Stephen J., Kaufman, Joshua D., Huang, Philip Lin, Huang, Paul Lee, Lee-Huang, Sylvia, and Torchia, Dennis A. (2000) Anti-HIV and anti tumor protein MAP30, a 30 kDa single-strand type-I RIP, shares similar secondary structure and β -sheet topology with the A chain of ricin, a type-II RIP. *Protein Science* **9**, 138-144.

Watanabe, Keiichi, Honjo, Eijiro, Tsukamoto, Takuji, and Funatsu, Gunki (1992)

Fluorescence studies on the interaction of adenine with ricin A-chain. *FEBS Letters* **304**(2,3), 249-251.

APPENDICES

A1. Derivation of the Initial Velocity Equation When the Briggs and Haldane Assumption That the Substrate Concentration is Very Much Greater Than the Enzyme Concentration is Not Satisfied.

First, the usual derivation of the Michaelis-Menten initial velocity equation, where the substrate concentration is very much greater than the enzyme concentration will be given as a reference. Then, the derivation of the corresponding equation when the substrate concentration is not very much greater than the enzyme concentration will be presented, and the differences with the usual derivation will be indicated.

Derivation of the initial velocity equation when the substrate concentration is very much greater than the enzyme concentration.

The chemical stoichiometric form of the simple Michaelis-Menten model of enzyme catalysis is



where E, S, C_{ES} , and P denote free enzyme, substrate, enzyme-substrate complex, and product, respectively, and the k_i s are rate constants. Note that the rate constant k_2 is often denoted by k_{cat} . Also note the use of C_{ES} rather than the frequently used $E \cdot S$ to denote the enzyme-substrate complex.

Applying the law of mass action, we obtain the following set of kinetic equations:

$$dS/dt = -k_1ES + k_{-1}C_{ES} \quad (A1-2)$$

$$dC_{ES}/dt = k_1ES - k_{-1}C_{ES} - k_2C_{ES} \quad (A1-3)$$

$$dE/dt = -k_1ES + k_{-1}C_{ES} + k_2C_{ES} \quad (A1-4)$$

$$dP/dt = k_2C_{ES} \quad (A1-5)$$

Note that in the expression for the reaction model (A1-1), the symbols represent

substances, but in equations (A1-2) - (A1-5), and the mathematical expressions below, the same symbols, though unbracketed, represent time-dependent concentrations of the substances represented by the corresponding symbols in (A1-1).

The set of kinetic equations (A1-2) - (A1-5) represents a complete and rigorous description of the dynamics of an enzymatic reaction conforming to the simple Michaelis-Menten model (A1-1). However, the set of equations are nonlinear, and as a result, cannot be solved so as to give the individual variables E, S, C_{ES} , and P as explicit functions of time. Thus, these equations, although correct representations of the theoretical model, cannot be easily used for comparison of experimental results with theoretical models. However, we can reduce the full set of kinetic equations to a single equation in a form permitting comparison with experiments by introducing the Briggs and Haldane steady-state assumptions, namely, that a steady state, in which substrate is converted to product while the concentration of the enzyme-substrate complex remains constant, is established very quickly (relative to the time scale of the experiment), and persists over the duration of the experiment.

The condition that the enzyme-substrate complex remains constant ($dC_{ES}/dt = 0$) reduces the rate equation (A1-3) to the algebraic equation

$$k_1ES - k_{-1}C_{ES} - k_2C_{ES} = 0 \quad (A1-6)$$

giving C_{ES} in terms of E and S. Using the enzyme conservation equation

$$E_0 = E + C_{ES} \quad (A1-7)$$

in (A1-6) and defining $K_M = (k_{-1} + k_2)/k_1$, we obtain

$$C_{ES} = E_0S/(K_M + S) \quad (A1-8)$$

Under steady-state conditions, the rate of disappearance of substrate ($-dS/dt$) and the rate of formation of product (dP/dt) are the same. Denoting this rate, or velocity, by v , and using eq (A1-5),

$$v = k_2 C_{ES} = k_2 E_0 S / (K_M + S) \quad (A1-9)$$

and, using the standard terminology $V_{\max} = k_2 E_0$ in eq (A1-9), we get the Michaelis-Menten equation

$$v = V_{\max} S / (K_M + S)$$

Finally, under conditions in which the amount of substrate sequestered in the enzyme-substrate complex is negligibly small compared to the total amount of substrate during the course of the experiment, we can assume that the substrate concentration at the start of the steady-state regime is effectively equal to the total substrate concentration at the start of the reaction, S_0 , and obtain the expression for the initial velocity v_i

$$v_i = V_{\max} S_0 / (K_M + S_0) \quad (A1-10)$$

Derivation of the initial velocity equation when the substrate concentration is not very much greater than the enzyme concentration.

In this case, the derivation is the same through eq (A1-6). Then, in addition to the enzyme conservation condition expressed in eq (A1-7), we take into account the amount of substrate sequestered in the enzyme-substrate complex by use of a substrate conservation expression

$$S_0 = S + C_{ES} \quad (A1-11)$$

Replacing E and S in eq (A1-6) by eqs (A1-7) and (A1-11) gives

$$k_1(E_0 - C_{ES})(S_0 - C_{ES}) - k_{-1}C_{ES} - k_2C_{ES} = 0$$

or,

$$C_{ES}^2 - (E_0 + S_0 + K_M)C_{ES} + E_0S_0 = 0$$

from which

$$C_{ES} = (1/2)\{E_0 + S_0 + K_M - [(E_0 + S_0 + K_M)^2 - 4 E_0S_0]^{1/2}\}$$

where only the negative square root is meaningful because, as noted by Reiner, if either E_0 or S_0 is zero, then C_{ES} must be zero. Finally, denoting the velocity in this case by $v_{isc} = k_2C_{ES}$

$$v_{isc} = (1/2) k_2 \{E_0 + S_0 + K_M - [(E_0 + S_0 + K_M)^2 - 4 E_0S_0]^{1/2}\} \quad (A1-12)$$

The form of eq (A1-12) is very different from that of the initial velocity Michaelis-Menten equation (A1-10). However, in the limit $E_0 \ll S_0$ and K_M , eq (A1-12) approaches the form of eq (A1-10).

The percent error in using v_i (eq A1-10) rather than v_{isc} (eq A1-12) is

$$\%err = 100 (v_i - v_{isc})/v_i \quad (A1-13)$$

Dividing top and bottom of eq A1-10 by S_0 , using $V_{max} = k_2E_0$, and letting $\alpha = K_M/S_0$ gives

$$v_i = k_{cat} E_0/(1 + \alpha) \quad (A1-14)$$

Multiplying and dividing eq (A1-12) by S_0 , and letting $\beta = E_0/S_0$ gives

$$v_{isc} = (1/2) k_{cat} S_0 \{1 + \alpha + \beta - [(1 + \alpha + \beta)^2 - 4 \beta]^{1/2}\} \quad (A1-15)$$

where we have replaced the symbol k_2 by its equivalent k_{cat} .

Substituting eqs (A1-14) and (A1-15) into eq (A1-13), we obtain

$$\%err = 100 (1 - [(1 + \alpha)/2 \beta] \{1 + \alpha + \beta - [(1 + \alpha + \beta)^2 - 4 \beta]^{1/2}\}) \quad (A1-16)$$

A graph of %err versus β is shown in Fig. A1-1 for $\alpha = 0.2, 1.0$, and 5.0 . Note that

the %error as a function of α is greatest when $\alpha = 1.0$, which unfortunately is the optimum value for Michaelis-Menten experiments.

A2. Derivation of the integrated form of the Michaelis-Menten equation

Starting with the Michaelis-Menten equation

$$v = -dS/dt = V_{\max} S/(K_M + S) \quad (\text{A2-1})$$

and rearranging terms gives

$$- [(K_M + S)/S]dS = V_{\max} dt \quad (\text{A2-2})$$

Integrating both sides of eq. A2-2 we get

$$- K_M \int (1/S) dS - \int dS = V_{\max} \int dt \quad (\text{A2-3})$$

where the integration limits are S_0 to S for the two integrals on the left side of the equation, and 0 to t for the integral on the right side. Carrying out the integration gives the following implicit equation for the substrate concentration S as a function of the time t ,

$$- K_M \ln(S/S_0) - S + S_0 = V_{\max} t \quad (\text{A2-4})$$

or, in terms of product $P = S_0 - S$,

$$t = P/V_{\max} - (K_M/V_{\max}) \ln(1 - P/S_0) \quad (\text{A2-5})$$

A3. Calculation of the Difference Between the True and the Measured Initial Velocity as a Function of the Extent of Reaction

The integrated form of the Michaelis-Menten equation derived in Appendix A2 will be used to derive an expression comparing the true initial velocity at time $t = 0$ with the velocity obtained by measuring substrate (or product) concentration at some later time at which the extent of reaction (expressed as a percent) is $\xi\%$.

The initial velocity at the start of the reaction, v_{it} (true initial velocity) in the Michaelis-Menten model is

$$v_{it} = V_{\max} S_0 / (K_M + S_0) \quad (\text{A3-1})$$

If this velocity were maintained for time t , the substrate concentration S would be

$$S = S_0 - v_{it} t = S_0 - [V_{\max} S_0 / (K_M + S_0)] t$$

or

$$t = (S_0 - S) [(S_0 + K_M) / V_{\max} S_0]$$

But the actual relation between S and t is given by the integrated Michaelis-Menten equation (see Appendix A-2 eq. A2-4))

$$t = (S_0 - S) / V_{\max} - (K_M / V_{\max}) \ln(S / S_0) \quad (\text{A3-2})$$

The measured initial velocity is

$$v_{im} = (S_0 - S) / t \quad (\text{A3-3})$$

Substituting eq (A3-2) into eq (A3-3)

$$v_{im} = \frac{(S_0 - S)}{(S_0 - S) / V_{\max} - (K_M / V_{\max}) \ln(S / S_0)} \quad (\text{A3-4})$$

The percent extent of reaction is

$$\xi\% = 100(S_0 - S) / S_0 \quad (\text{A3-5})$$

and the percent error in the measured velocity is

$$\%err = 100(v_{im} - v_{it})/v_{im} \quad (A3-6)$$

Substituting eqs (A3-1) and (A3-4) into eq (A3-6), using eq (A3-5) in the equivalent form $S/S_0 = 1 - \xi_{\%}/100$, and letting $\alpha = K_M/S_0$ we obtain

$$\%err = 100\alpha[100 \ln(1 - \xi_{\%}/100) + \xi_{\%}]/\xi_{\%}(\alpha + 1) \quad (A3-7)$$

A graph of $\%err$ vs $\xi_{\%}$ is shown in Fig. A3-1 for $\alpha = 0.2, 1.0$, and 5.0 .

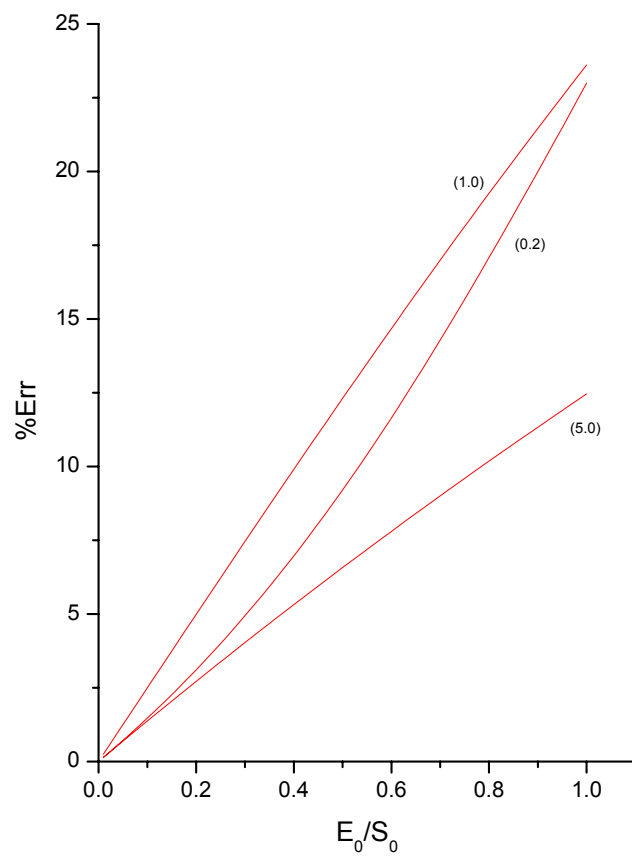


Figure A1-1. The percent error in the initial velocity, as a function of the substrate/enzyme ratio E_0/S_0 , incurred by using the Michaelis-Menten equation (eq. A1-10) rather than the equation for v_i derived using the conservation of substrate condition $S_0 = S + C_{ES}$ (eq. A1-15). Curves are shown for $K_M/S_0 = 0.2, 1.0$, and 5.0 .

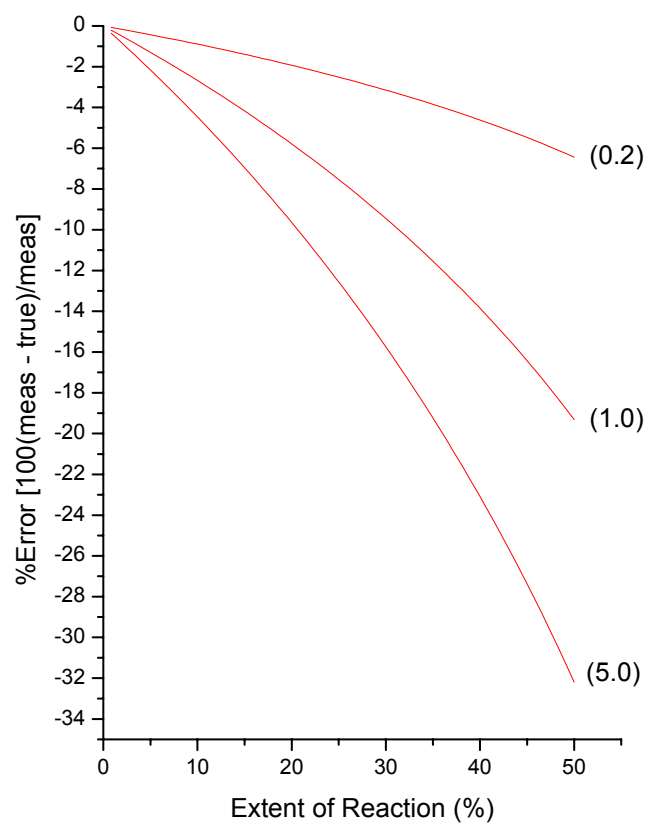


Figure A3-1. The percent error in measurements of the Michaelis-Menten initial velocity as a function of the extent of reaction, calculated using eq. A3-7. Curves are shown for $K_M/S_0 = 0.2, 1.0$, and 5.0 .